

FUNCTIONAL CHARACTERIZATION OF MICRORNA-125B
EXPRESSION IN MCF7 BREAST CANCER CELL LINE

A THESIS SUBMITTED TO
THE GRADUATE SCHOOL OF NATURAL AND APPLIED SCIENCES
OF
MIDDLE EAST TECHNICAL UNIVERSITY

BY
SERKAN TUNA

IN PARTIAL FULFILLMENT OF THE REQUIREMENTS
FOR
THE DEGREE OF MASTER OF SCIENCE
IN
BIOLOGY

SEPTEMBER 2010

Approval of the thesis

**FUNCTIONAL CHARACTERIZATION OF MICRORNA-125B
EXPRESSION IN MCF7 BREAST CANCER CELL LINE**

submitted by **SERKAN TUNA** in partial fulfillment of the requirements for the degree of **Master of Science in Biology Department, Middle East Technical University** by,

Prof. Dr. Canan Özgen
Dean, Graduate School of **Natural and Applied Sciences**

Prof. Dr. Musa Doğan
Head of the Department, **Biology**

Assist. Prof. Dr. A. Elif Erson Bensan
Supervisor, **Biology Dept., METU**

Examining Committee Members

Prof. Dr. Gülay Özcengiz
Biology Dept., METU

Assist. Prof. Dr. A. Elif Erson Bensan
Biology Dept., METU

Assist. Prof. Dr. Sreeparna Banerjee
Biology Dept., METU

Assist. Prof. Dr. Çağdaş D. Son
Biology Dept., METU

Assist. Prof. Dr. Özlen Konu
Molecular Biology and Genetics Dept.,
Bilkent University

Date: 14/09/2010

I hereby declare that all information in this document has been obtained and presented in accordance with academic rules and ethical conduct. I also declare that, as required by these rules and conduct, I have fully cited and referenced all material and results that are not original to this work

Name, Last name: Serkan TUNA

Signature :

ABSTRACT

FUNCTIONAL CHARACTERIZATION OF MICRORNA-125B EXPRESSION IN MCF7 BREAST CANCER CELL LINE

Serkan TUNA

M.Sc., Department of Biology

Supervisor: Assist. Prof. Dr. A. Elif ERSON BENSAN

September 2010, 104 pages

microRNA dependent gene expression regulation has roles in diverse processes such as differentiation, proliferation and apoptosis. Therefore, deregulated miRNA expression has functional importance for various diseases, including cancer. miR-125b is among the commonly downregulated miRNAs in breast cancer cells . Therefore we aimed to characterize the effects of miR-125b expression in MCF7 breast cancer cell line (BCCL) to better understand its roles in tumorigenesis. Here, we investigated mir-125 family members' expression levels in eleven BCCL and MCF10A, by semi-quantitative duplex RT-PCR. pre-miR-125b-1 levels were found to be low or absent in 7 of 11 BCCL. Among these, MCF7 cells were stably transfected with mir-125b-1 (MCF7-125b-1). MCF7-125b-1 cells demonstrated decreased proliferation and migration detected by MTT, *in vitro* wound closure and transwell migration assays compared to empty vector transfected cells (MCF7-EV). Putative miR-125b target, *ARID3B*, was bioinformatically analyzed for miR-125b binding sites. 3'UTR of *ARID3B* was cloned downstream of the luciferase gene in pMIR, a reporter vector. ~60% decrease in luciferase activity suggested the interaction between miR-125b and *ARID3B* 3'UTR. To further confirm this, a miR-125b binding site was deleted by site directed mutagenesis. Deletion of this predicted site in the *ARID3B* 3'UTR resulted with ~30% recovery in luciferase activity. Our

results further showed the tumor suppressor functions of miR-125b in MCF7 cells. Revealing the phenotypic effects of miR-125b expression and its mRNA targets may help us shed light on why miR-125b may act as a tumor suppressor in breast cancer cells.

Key words: Breast cancer, microRNAs, miR-125b, *ARID3B*

ÖZ

MİKRORNA-125B İFADESİNİN MCF7 MEME KANSERİ HÜCRELERİNDE FONKSİYONEL KARAKTERİZASYONU

Serkan TUNA

Yüksek Lisans, Biyoloji Bölümü

Tez Yöneticisi: Yrd. Doç. Dr. Ayşe Elif ERSON BENSAN

Eylül 2010, 104 sayfa

mikroRNA'lara bağlı gen ifadesinin kontrolü, farklılaşma, hücre büyümesi ve apoptoz gibi hücreSEL işlevlerde görev almaktadır. Önemli görevleri olan mikroRNA'ların kanser dahil hastalıklarda fonksiyonel önemi vardır. miRNA-125b, meme kanserinde gen ifadesi azalan önemli bir mikroRNA'dır. Bu sebeple, miRNA-125b geninin ifadesinin, MCF7 meme kanseri hücre hattında (MKHH) fonksiyonel karakterizasyonu yapılarak, bu mikroRNA'nın kanser oluşumunda görevlerinin bulunması amaçlanmıştır. mikroRNA-125 ailesinin gen ifadeleri, yarı nicel ikili RT-PCR metoduyla, 11 MKHH'da ve MCF10A hücrelerinde taranmıştır. Öncül-mikroRNA-125b-1 ifadesinin 11 MKHH'nın 7'sinde tamamem kaybolduğu ya da azaldığı gözlemlenmiştir. MCF7'ye, mikroRNA-125b-1 geni kalıcı olarak transfekte edilmiştir (MCF7-125b-1). Farklı teknikler kullanılarak, MCF7-125b-1 hücre hattında, boş vektör transfekte edilen hücrelere göre (MCF7-EV), hücre büyümesi ve hücre göçü özelliklerinde azalışlar tespit edilmiştir. Olası mikroRNA-125b hedef geni *ARID3B*, miRNA-125b'nin bağlanabileceği bölgeler açısından biyoinformatik yöntemlerle analiz edilmiştir. *ARID3B* geninin protein kodlamayan 3' bölgesi, lusiferaz geni içeren pMIR vektörüne klonlanmıştır. Lusiferaz aktivitesi deneyleri sonucunda %60'luk azalış görülmüş, miRNA-125b ve *ARID3B* arasındaki etkileşim kanıtlamıştır. Doğrudan etkileşimini onaylamak için, yönlendirilmiş mutageniz yöntemi kullanılarak, evrimsel açıdan korunmuş bir miRNA-125b bağlanma bölgesi

silinmiştir. Bu işlem, lusiferaz aktivitesinde %30'luk bir geri kazanıma sebep olmuştur. Artış oranı, silinen bölgenin dışındaki bağlanma bölgelerinin de miRNA-125b ve *ARID3B* etkileşiminde rol alabileceğini göstermiştir. Elde edilen bulgular, miRNA-125b geninin, MCF7 hücrelerinde tümör baskılayıcı özellik gösterdiğini kanıtlamıştır. mikroRNA-125b ifadesinin fenotipik etkilerini ve hedef mRNA'larını bulmak, miRNA-125b'nin kanser hücrelerinde nasıl tümör baskılayıcı özellik gösterdiğinin bulunmasına yardımcı olacaktır.

Anahtar kelimeler: meme kanseri, mikroRNA, miR-125b, *ARID3B*

To my family

ACKNOWLEDGEMENTS

Firstly, I would like to express my deepest gratitude to my supervisor. Assist. Prof. Dr. A. Elif Erson Bensan for her guidance, encouragement, support and comments throughout this study. It's hard to express my feelings about how lucky I am to be a part of her team.

I would like to thank all my jury members; Prof. Dr. Gülay Özcengiz, Assist. Prof. Dr. Sreeparna Banerjee, Assist. Prof. Dr. Çağdaş D. Son and Assist. Prof. Dr. Özlen Konu for their invaluable comments, advices and contributions to my thesis.

Many thanks to my lab mates Begüm Akman, Shiva Akhavan and Ayşegül Sapmaz. I feel great appreciation for Duygu Selçuklu, a former member of our lab, for her helpful advices, support and encouragement. Besides, she is the one who made me enter the microRNA world. I would like to express my grateful thanks to my lab buddy Cansaran Saygılı for always being around when a help is required. I am also thankful for her friendship, patience and motivation. I'm glad to work with her in the same group.

I am deeply thankful to my friends Aslı Aras Taşkın, Yaprak Dönmez and Duygu Yılmaz for their encouragement, moral support and suggestions throughout this study. I would like to thank Emre Kural, Mustafa Demir and Giray Bulut for their brotherhood.

I would like to revere my grandfather Orhan Tuna, my grandmother Naciye Tuna and my father Çağlar Tuna, who all passed away during this thesis study. I would like to express my endless gratitude to my mother Sibel Özer, my sister Çiğdem Aydoğan and my brother Aykut Aydoğan, for their love, care, endless support and trust throughout my life. I'm grateful to all my family for making everything possible for me.

Finally, my deepest thanks are extended to Burcu Can, who made life worth and easier with her endless trust, encouragement, understanding, moral support, care and patience at every stage of this thesis.

This project was funded by Scientific and Technological Research Council of Turkey (TUBITAK) (108S381), Turkish Academy of Sciences, GEBIP 2006.

TABLE OF CONTENTS

ABSTRACT	iv
ÖZ	vi
ACKNOWLEDGEMENTS	ix
TABLE OF CONTENTS	xi
LIST OF TABLES	xiv
LIST OF FIGURES	xv
LIST OF ABBREVIATIONS	xvii
CHAPTERS	
1 INTRODUCTION	1
1.1 microRNAs	1
1.1.1 miRNA Biogenesis	1
1.1.2 Gene Regulation by miRNAs	5
1.1.3 miRNAs and Cancer	8
1.1.4 miRNAs and Breast Cancer	15
1.2 miR-125 Family	17
1.2.1 Targets of miR-125 Family Members	20
1.3 Aim of the Study	24
2 MATERIALS AND METHODS	25
2.1 Cancer Cell Lines	25
2.2 Mammalian Cell Culture Conditions	25
2.3 Bacterial Culture Media and Culture Conditions	27
2.4 Expression Analysis of miRNAs in Breast Cancer Cell Lines	27
2.4.1 RNA Isolation by Trizol Reagent	27
2.4.2 RNA Isolation by High Pure RNA Isolation Kit	28
2.4.3 Determination of RNA Quantity and Quality	29
2.4.4 DNase I Treatment	29
2.4.5 cDNA Synthesis	30
2.4.6 Primer Design for Precursor miRNA (pre-miRNA)	31
2.4.7 Semi-quantitative Duplex RT-PCR	33
2.4.8 Densitometry Analysis of Semi-quantitative Duplex RT-PCR	34

2.5 Ectopic Expression of pre-miR-125b.....	34
2.5.1 Oligonucleotide Design.....	35
2.5.2 Oligonucleotide Cloning into pSUPER Vector.....	36
2.5.2.1 Preparation of Competent <i>E.coli</i> Cells.....	36
2.5.2.2 Oligo Annealing.....	37
2.5.2.3 Linearization of pSUPER Vector and Ligation Reaction.....	37
2.5.2.4 Transformation of Competent <i>E.coli</i> Cells.....	38
2.5.3 Stable Transfection of MCF7 Cells with pSUPER-125b.....	38
2.5.4 Confirmation of pSUPER Genomic Integration and Ectopic Expression	39
2.6 Functional Assays	40
2.6.1 Cellular Proliferation Assay	40
2.6.2 <i>In vitro</i> Wound Closure Assay	41
2.6.3 Transwell Migration Assay	42
2.7 Target Search for hsa-miR-125b.....	43
2.8 Analysis of Target 3'UTR and miRNA Interaction.....	45
2.8.1 <i>ARID3B</i> 3'UTR Cloning.....	45
2.8.2 Transient Transfections of Luciferase Constructs into MCF7 Cells.....	47
2.8.3 Dual Luciferase Assay	48
2.8.4 Site Directed Mutagenesis.....	49
3 RESULTS AND DISCUSSION	52
3.1 Expression Analysis of pre-miR-125a, pre-miR-125b-1 and pre-miR-125b-2 in Breast Cancer Cell Lines.....	52
3.2 Ectopic Expression of pre-miR-125b-1 in MCF7 Breast Cancer Cell Line	57
3.3 Functional Assays	59
3.3.1 Cellular Proliferation Assay.....	60
3.3.2 <i>In vitro</i> Wound Closure Assay.....	61
3.3.3 Transwell Migration Assay	63
3.4 Target Search for hsa-miR-125b.....	66
3.4.1 TargetScan.....	66
3.4.2 microRNA.org.....	67
3.4.3 PicTar	68
3.4.4 PITA.....	68
3.5 Analysis of <i>ARID3B</i> 3'UTR and miR-125b Interaction	70
4 CONCLUSION	80

REFERENCES.....	82
APPENDICES	
A MAMMALIAN CELL CULTURE PROPERTIES	98
B BACTERIAL CULTURE MEDIUM.....	99
C PRIMERS AND DUPLEX PCR OPTIMIZATION CONDITIONS.....	100
D MAPS OF VECTORS.....	101

LIST OF TABLES

TABLES

Table 1.1: Different types of seed sequences (miRNA binding sites) in humans.....	7
Table 1.2: Various miRNAs up- or down-regulated in tumors relative to normal tissues.....	10
Table 1.3: Representative oncogenic or tumor suppressive miRNAs and their direct target genes	14
Table 1.4: Recent confirmed targets of oncogenic or tumor suppressive miRNAs in breast cancer.....	17
Table 2.1: DNase I reaction mixture	29
Table 2.2: cDNA synthesis (RT) protocol and reaction mixture by RevertAid First strand cDNA synthesis kit (Fermentas).....	31
Table 2.3: List of primers used in semi-quantitative duplex RT-PCR.....	32
Table 2.4: Duplex RT-PCR mixture to amplify pre- miRNA and <i>GAPDH</i>	33
Table 2.5: Duplex PCR cycling conditions for pre-miRNA	34
Table 2.6: List of primer set used in confirmation of ectopic expression.....	39
Table 2.7: Cloning primers for <i>ARID3B</i> 3'UTR.....	46
Table 2.8: Site-directed Mutagenesis PCR Program.....	51
Table 3.1: miR-125b target prediction scores for <i>ARID3B</i> 3'UTR.	69
Table A.1: Mammalian cell lines' properties.....	98
Table C.1: List of primers used in PCR.....	100
Table C.2: Duplex PCR Optimization Conditions.....	100

LIST OF FIGURES

FIGURES

Figure 1.1: Possible mechanisms of Drosha and Dicer actions.	2
Figure 1.2: Biogenesis of miRNAs.	4
Figure 1.3: mRNA cleavage by miRNAs.	6
Figure 1.4: Translational repression by miRNAs	6
Figure 1.5: miRNAs can function as tumor suppressors and oncogenes.....	12
Figure 1.6: Precursor structures of miR-125 family members.....	18
Figure 1.7: Mature miR-125a and miR-125b sequences.	19
Figure 2.1: cDNA primer design for hsa-mir-125b-1 pre-miRNA.....	32
Figure 2.2: Example oligonucleotide design for pSUPER system	35
Figure 2.3: Differences in sequence between native pre-miR-125b-1 and cloned construct.	36
Figure 2.4: Reduction of MTT to formazan.	40
Figure 2.5: A. Side view of a Transwell, lower and upper chambers B. Top view of upper chamber.....	42
Figure 2.6: TargetScan web interface	43
Figure 2.7: microRNA.org web interface	44
Figure 2.8: PicTar web interface.....	44
Figure 2.9: PITA downloadable target search interface.....	45
Figure 2.10: TOPO Reaction	46
Figure 2.11: Bioluminescent reactions catalyzed by Firefly and <i>Renilla</i> luciferases.	48
Figure 2.12: Mutagenesis specific primers' design by <i>Stratagene's</i> web-based QuikChange Primer Design Program.....	50
Figure 3.1 pre-miR-125a expression analysis by semi-quantitative duplex RT-PCR.	53
Figure 3.2: pre-miR-125b-2 expression analysis by semi-quantitative duplex RT- PCR.	54
Figure 3.3: pre-miR-125b-2 expression analysis by semi-quantitative duplex RT- PCR.....	55

Figure 3.4: pSUPER-125b-1 BLAST analysis.....	57
Figure 3.5: Genome integration confirmation of pSUPER-125b-1 and pSUPER constructs.	58
Figure 3.6: Ectopic expression confirmation of miR-125b-1 transfections.....	59
Figure 3.7: MTT assay of miR-125b-1 transfected and empty vector transfected MCF7 cells.....	60
Figure 3.8: Wound healing images of MCF7-125b-1 and MCF7-EV.....	62
Figure 3.9: Distance travelled by MCF-125b-1 and MCF7-EV cells.....	63
Figure 3.10: Transwell migration assay of MCF7-125b-1 and MCF7-EV cells.	64
Figure 3.11: Representative figures of MCF7-EV and MCF7-125b-1 cells migrated through membrane.	65
Figure 3.12: TargetScan predictions for miR-125b- <i>ARID3B</i> interaction.	67
Figure 3.13: microRNA.org prediction for miR-125b- <i>ARID3B</i> interaction.	67
Figure 3.14: PicTar prediction for miR-125b- <i>ARID3B</i> interaction.	68
Figure 3.15: PITA prediction for miR-125b- <i>ARID3B</i> interaction.....	69
Figure 3.16: Alignment of <i>ARID3B</i> 3'UTR and the predicted miR-125b binding sites.....	70
Figure 3.17: BLAST analysis of sequencing results for three different constructs. A) 472 bp C1 region B) 422 bp C2 region C) 300 bp C3 region..	72
Figure 3.18: Double digestion and colony PCR results. A) 472 bp C1 insert confirmation: B) 422 bp C2 insert and 300 bp C3 insert confirmations:.....	73
Figure 3.19: Interaction of miR-125b with <i>ARID3B</i> 3' UTR constructs.	75
Figure 3.20: Mutagenesis specific PCR results.....	76
Figure 3.21: BLAST analysis of sequencing result for C1-MUT construct..	77
Figure 3.22: Interaction of miR-125b with <i>ARID3B</i> 3' UTR C1 and C1-MUT constructs.	78

LIST OF ABBREVIATIONS

BLAST	Basic Local Alignment Search Tool
bp	Base Pairs
cDNA	Complementary Deoxyribonucleic Acid
DEPC	Diethyl Pyrocarbonate
DMSO	Dimethyl Sulfoxide
DNA	Deoxyribonucleic Acid
DNase I	Deoxyribonuclease I
dNTP	Deoxyribonucleotide Triphosphate
DTT	Dithiothreitol
EDTA	Ethylenediaminetetraacetic Acid
g	Centrifuge gravity force
<i>GAPDH</i>	Glyceraldehyde 3-Phosphate Dehydrogenase
NCBI	National Center for Biotechnology Information
LOH	Loss of Heterozygosity
miRNA	microRNA
mRNA	Messenger RNA
PCR	Polymerase Chain Reaction
PBS	Phosphate Buffered Saline
Pri-miRNA	Primary microRNA
Pre-miRNA	Precursor microRNA
RISC	RNA-induced Silencing Complex
RNA	Ribonucleic Acid
RNase	Ribonuclease
rpm	Revolution Per Minute
RT-PCR	Reverse Transcription Polymerase Chain Reaction
TBE	Tris-Boric acid-EDTA
UTR	Untranslated Region

CHAPTER 1

INTRODUCTION

1.1 microRNAs

microRNAs, also designated as miRNAs, were first discovered in 1993 by Victor Ambros and his colleagues while studying developmental timing in *Caenorhabditis elegans* [1]. Since then, miRNAs were discovered in various organisms; mammals [2], plants [3], *Drosophila* [4] and viruses [5]. According to miRBase release15.0, April 2010, over 14,000 miRNAs have been identified in 63 different species (<http://www.mirbase.org/>). To date, 940 human miRNA sequences have been registered to miRBase. It is predicted that genes encoding miRNAs contribute more than 1% to the total gene content of the so far investigated organisms [6]. Number of human miRNA genes has far exceeded this prediction.

miRNAs are thought to be at least 400 million years old [7], [8]. Many miRNAs and their targets are conserved across unrelated species. This conservation among different species with their targets may indicate an evolutionary conserved mechanism of gene regulation.

1.1.1 miRNA Biogenesis

Transcription of miRNAs is generally done by RNA polymerase II and miRNAs have a 3' poly (A) tail and a 5' cap [9]. However, for some miRNAs that are located downstream of a RNA Pol-III promoter, RNA polymerase III is thought to be responsible for transcription of the primary miRNA transcript [10]. The length of primary miRNA (pri-miRNA) transcripts varies from several hundred (unclustered monocistronic) to several thousand nucleotides (clustered polycistronic).

The pri-miRNA molecule forms a stem and loop structure. This structure is processed in the nucleus into a shorter, approximately 60-70 nucleotides long, hairpin precursor miRNA (pre-miRNA) by the ribonuclease (RNase III), Drosha, [11], and double strand RNA-binding protein, DGCR8 (DiGeorge syndrome critical region gene 8), [12], in a protein complex named “Microprocessor”. After Drosha processing, pre-miRNA has a 2 nucleotide overhang at the 3’end which defines one end of the mature miRNA strand [13]. Following overhang recognition, pre-miRNAs are exported from the nucleus by Exportin-5 together with Ran-GTP [14]. Further processing of pre-miRNA is done in the cytoplasm by a cytoplasmic ribonuclease Dicer [15], [16]. Dicer enzyme has several functional domains: the Piwi-Argonaute-Zwille (PAZ) domain which binds to the 3’overhang in pre-miRNA structure, the helicase domain, the double-strand RNA binding domain and two ribonuclease III catalytic domains that form an intramolecular dimer during pre-miRNA cleavage [17].

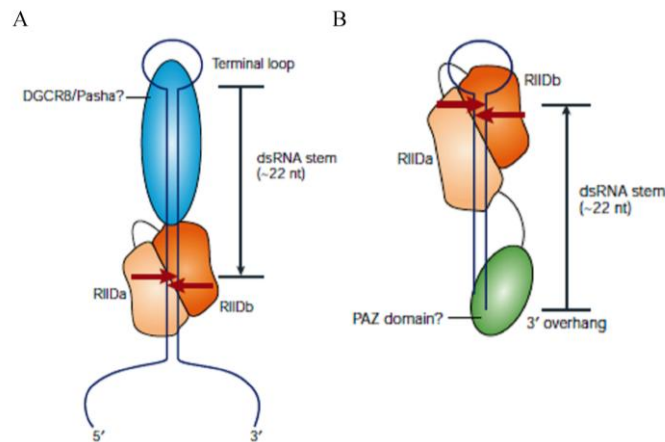


Figure 1.1: Possible mechanisms of Drosha and Dicer actions. A) Drosha recognizes double strand-single strand RNA boundaries and cleaves primary miRNA and produce precursor miRNA with 2 nucleotide long overhangs at the 3’end. B) Dicer recognizes loop structure and 3’ overhangs and cleaves precursor miRNA, finally forming mature miRNA duplex intermediate. (Figure taken from Kim *et al* 2005) [13].

Following Dicer processing, 20–25 nucleotide long mature miRNA duplex intermediate is formed. By the help of Dicer protein, mature miRNA duplex is incorporated into a multi-protein complex termed RNA-induced silencing complex (RISC). RISC contains Dicer, TRBP (human immunodeficiency virus (HIV)-1 trans-activating responsive element (TAR) RNA-binding protein), and Argonaute2 (Ago2) proteins [13], [12], [18], [19]. Only the mature miRNA strand (also termed as guide strand) of the excised duplex intermediate successfully enters RISC and is stabilized. RISC is also required for bringing mature miRNA and target mRNA together. The antisense miRNA* strand (also termed as the passenger strand) and the remainder of precursor structure is degraded [20]. Thermodynamic characteristics of the parent and passenger strands determine which strand of the duplex mature intermediate enters the RISC. Generally less stable strand remains in the RISC [21]. Figure 1.2 summarizes the biogenesis of miRNAs. However, in some cases, both strands of the miRNA duplex may be functional and may target different mRNAs in a tissue specific manner [22].

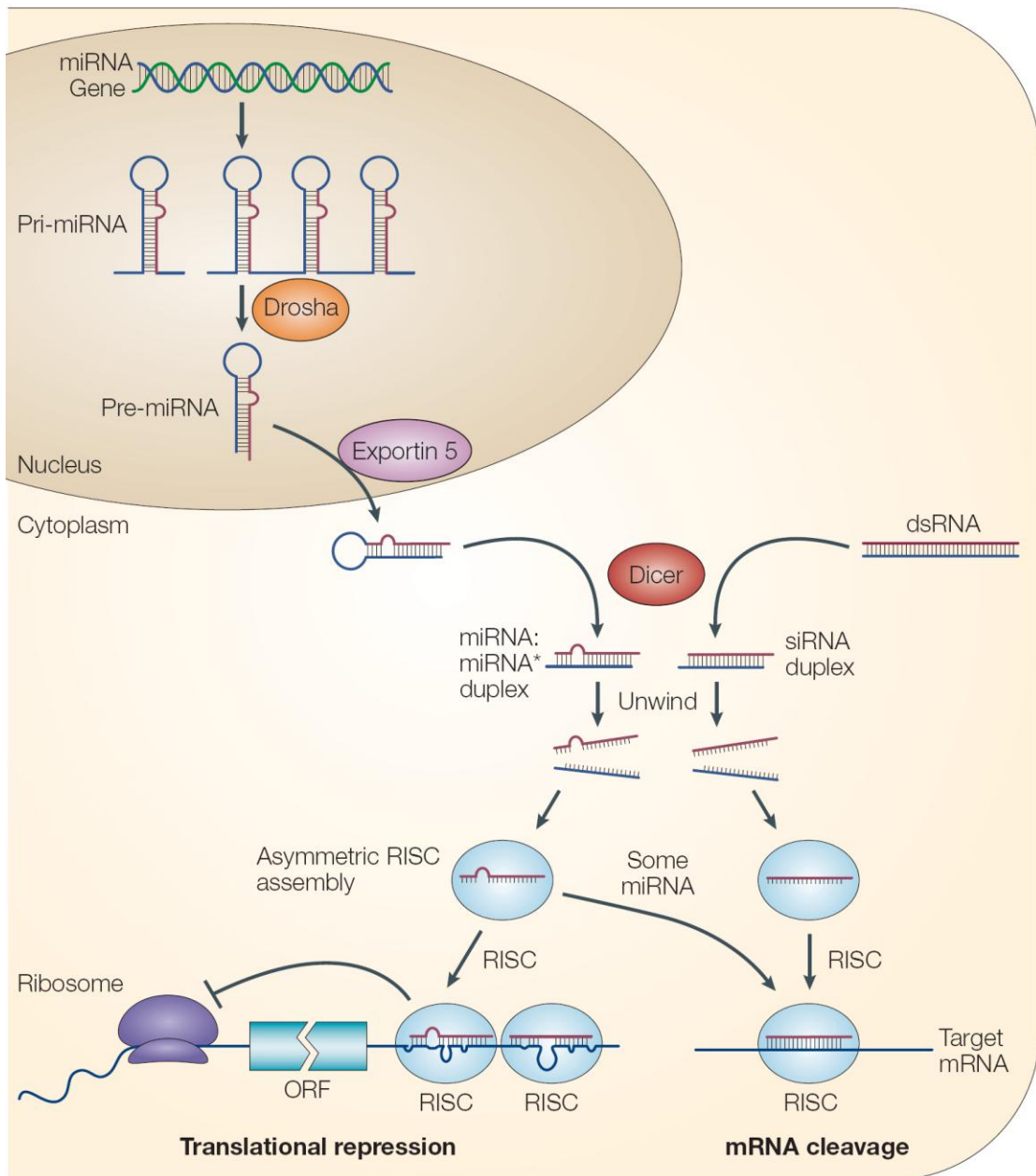


Figure 1.2: Biogenesis of miRNAs. miRNAs are first transcribed as primary transcript. Drosha cleaves primary miRNA and forms precursor miRNA. Through Exportin 5 mediated export, precursor miRNA is transported into cytoplasm. In the cytoplasm, Dicer further process precursor miRNA into mature miRNA. (Figure taken from He and Hannon, 2004) [23].

30% of mammalian miRNA genes are located in intergenic regions, whereas remaining 70% of miRNA genes are located within introns and/or exons of protein coding genes [24]. Intergenic miRNAs usually have their independent transcription units [25]. Intronic miRNAs are generally transcribed by the Pol-II promoters of their encoded genes. After RNA splicing and further processing, the spliced intron may function as primary miRNA [26]. In some cases, through splicing these introns form debranched structures. These debranched introns mimic the structural feature of precursor miRNA. By that way, intronic miRNAs, also known as mirtrons, enter the miRNA processing pathway without being processed by Drosha [27].

1.1.2 Gene Regulation by miRNAs

Human miRNAs are predicted to control the expression of a large number of genes (about 30% of all human genes) [28]. Post-transcriptional regulation of gene expression by miRNAs occurs by two different mechanisms: mRNA cleavage (Figure 1.3) or translational repression (Figure 1.4) [1], [28], [29], [23]. Translational repression occurs via miRNA-RISC binding to target mRNA 3'UTR (untranslated region). It has also been reported that, although rarely, translational repression of target mRNA occurs by binding of miRNA-RISC to 5'UTR of target mRNA and inhibiting translation initiation [30]. Translational repression of target mRNA occurs via imperfect binding of miRNA to its target. This event is commonly observed in animals whereas perfect binding of miRNAs to targets is observed in plants causing target mRNA cleavage [31], [28]. Although it is rare, perfect binding of miRNA to its target has been reported in animals [32].

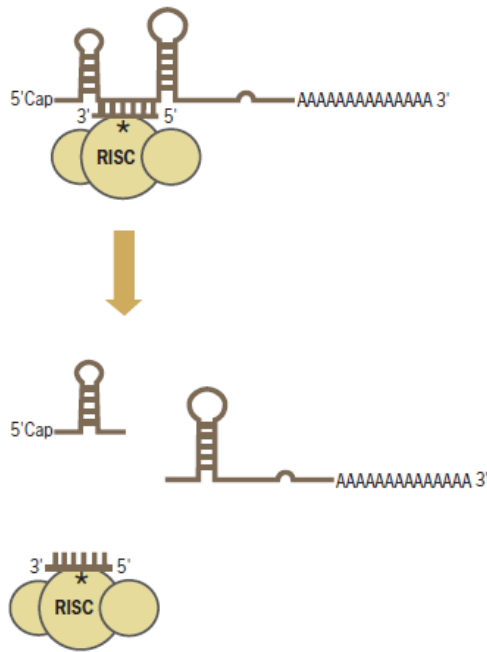


Figure 1.3: mRNA cleavage by miRNAs (Figure taken http://www.ambion.com/techlib/resources/miRNA/mirna_fun.html).

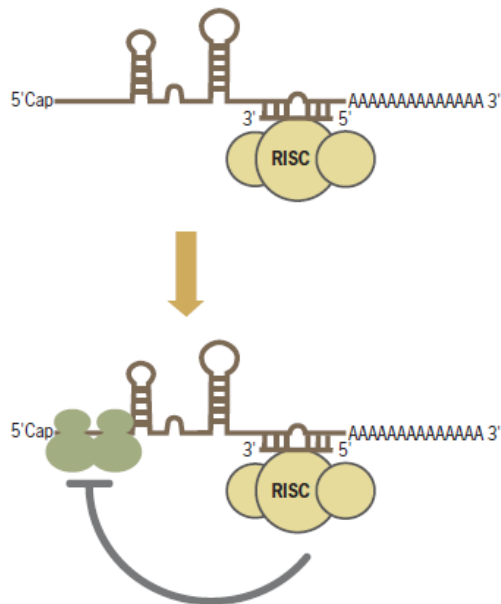


Figure 1.4: Translational repression by miRNAs (Figure taken http://www.ambion.com/techlib/resources/miRNA/mirna_fun.html).

According to previous studies mRNA down-regulation by miRNAs is usually due to translational repression [1], [33]. However, it has also been reported that, miRNAs can induce deadenylation of target mRNAs, causing both translational repression and a reduction in mRNA levels [34]. This mechanism depends on destabilizing target mRNA through imperfect binding with miRNA-RISC and removal of the poly-A tails of mRNAs and finally degradation of target mRNAs [35].

Plant miRNAs bind to their targets with perfect complementarity whereas mammalian miRNAs bind to their targets with imperfect complementarity as previously mentioned. Although this is the case, there is a highly conserved region of perfect match between miRNA and mRNA termed as the ‘seed region’ in this imperfect complementarity. This seed region starts from the second nucleotide of the mature miRNA. The size of seed sequence varies: 7mer-m8, 7mer-1A and 8mer [36]. Table 1.1 lists the different types of seed sequences.

Table 1.1: Different types of seed sequences (miRNA binding sites) in humans.

Seed Type	Definition	Example
7mer-m8	miRNA-mRNA matching to positions 2-8 of the mature miRNA (the seed + position 8)	<pre> 5' ...GGCCAGUAUGUCUUUCAGGGG... 3' AGUGUCAAUCCAGAGUCCCU </pre>
7mer-1A	miRNA-mRNA matching to positions 2-7 of the mature miRNA (the seed) followed by an 'A'	<pre> 5' ...GACAGCGUUGUCCAUCAGGGAU... 3' AGUGUCAAUCCAGAGUCCCU </pre>
8mer	miRNA-mRNA matching to positions 2-8 of the mature miRNA (the seed + position 8) followed by an 'A'	<pre> 5' ...AUGCAGGGGAGACGUCAGGGA... 3' AGUGUCAAUCCAGAGUCCCU </pre>

The hierarchy of site efficacy is as follows: 8mer >> 7mer-m8 > 7mer-A1 > >6mer > no site, with the 6mer differing only slightly from no site at all [37], [38]. Due to small length of seed sequences, as 7 nucleotide long seed region may be present in several targets, a single miRNA can potentially target several mRNAs [36]. Due to this reasons, computational methods are used to predict potential miRNA targets (binding sites in 3' UTR) by using degrees of complementarity, conserved regions among related species and thermodynamics of binding. Some most commonly used prediction tools are: TargetScan, version 5.1 [39], [37], [40], miRNA.org [41], PicTar [42], and PITA [43].

1.1.3 miRNAs and Cancer

The first link between miRNAs and cancer has been proposed by Calin *et al* in 2002 [44]. 13q14 chromosomal region contains miR-15a and miR-16-1. This is a region that is deleted in more than half of B cell chronic lymphocytic leukemias (B-CLL). In that study, deletion and downregulated expression of these miRNA genes in 68% of analyzed CLL patients were shown. Further studies also indicated that, these miRNAs target anti-apoptotic BCL2 protein in CLL patient samples [45].

In a genome-wide analysis, genomic instability and miRNA relationship was further investigated by the same group 98 out of 186 miRNA genes (52.5%) were found to be located on cancer related genomic instability regions [46]. In a recent study, 242 of 715 miRNA genes were reported to be located on cancer related genomic instability regions [47]. Moreover, in addition to these 242 miRNA genes, 317 miRNA genes (44.3%) were also reported to be located within genes which reside in translocation regions in cancer. From these 317 miRNA genes, 87 of them (27.4%) were also reported to be mapping to fragile sites.

miRNAs are differentially expressed across different organisms, developmental stages, tissues or cell types [2], [48], [49]. Through Northern blot analyses and miRNA microarrays, differential expression of miRNAs in different organisms and tissues has been reported [50], [51], [52], [53].

As miRNA expression differs in a time dependent and tissue specific manner, miRNAs show different expression patterns in different tissues and cancer types [54]. When expression profiles of mRNA and miRNAs were compared by microarray, 12 of 17 tumor samples were classified by miRNA expression profiles whereas mRNA expression profiles could discriminate only 1 of 17 samples [55]. This showed the power of using miRNAs as a diagnostic tool given that in that study the mRNA array contained 15,000 genes whereas the miRNA array harbored only 200 miRNA genes. More miRNA-expression profile studies also showed that miRNAs are powerful discriminators of human cancers [56], [57], [58]. For that reason, miRNAs can be used as diagnostic and prognostic markers for cancer.

To date, deregulated expression of miRNAs in cancers has been reported. In one study 540 tumor samples including lung, breast, stomach, prostate, colon and pancreatic tumors were analyzed for their miRNA expression levels and detected consistently downregulated or upregulated miRNAs in these tumor samples [56]. Similar studies were conducted for breast cancer, ovary cancer and chronic lymphocytic leukemia samples [57], [59], [60]. In all studies, deregulation of miRNA expression in different cancers was reported. Table 1.2 shows deregulated expression of selected miRNAs in several different cancers [61].

Table 1.2: Various miRNAs up- or down-regulated in tumors relative to normal tissues. (Table adapted from Lee and Dutta, 2009) [61].

miRNA	up/down	Cancer
let-7	down	breast cancer
	down	prostate cancer
	down	hepatocellular cancer
	down	gastric tumor
	down	lung cancer
	up	colon cancer
	up	uterine leiomyoma
	up	pancreatic cancer
	up	hepatocellular carcinoma
miR-10b	up	breast cancer
	up	glioblastoma
miR-21	down	pituitary adenomas
	up	breast cancer
	up	colorectal cancer
	up	ovarian cancer
	up	hepatocellular cancer
	up	cervical cancer
	up	pancreatic cancer
	up	chronic lymphocytic leukemia
	up	uterine leiomyoma
	up	pancreatic cancer
	up	breast tumor
	up	pancreatic tumor
	up	hepatocellular carcinoma
	up	cholangiocarcinoma
	up	lung cancer
	up	breast cancer
	up	glioblastoma

miRNA	up/down	Cancer
miR-125a	down	neuroblastoma
miR-125b	down	breast cancer
	down	prostate cancer
	down	ovarian cancer
	down	thyroid cancer
	down	neuroblastoma
	up	pancreatic cancer
miR-145	down	B-cell malignancies
	down	prostate cancer
	down	ovarian cancer
	down	colorectal cancer
	down	breast cancer
	down	colorectal neoplasia
miR-155	down	pancreatic tumor
	up	breast cancer
	up	pancreatic cancer
	up	chronic lymphocytic leukemia
	up	pancreatic cancer
	up	Hodgkin's lymphomas
	up	Burkitt lymphoma
	up	hepatocellular cancer
	up	chronic lymphocytic leukemia
miR-221	down	chronic lymphocytic leukemia
	up	pancreatic cancer
	up	papillary thyroid carcinoma
	up	glioblastoma
miR-222	up	glioblastoma
	up	pancreatic cancer
	up	papillary thyroid carcinoma

Deregulated miRNA expression may be caused by several reasons. Genomic abnormalities (amplification, deletion, translocation, etc) may cause changes in miRNA expression. In support of this, a significant fraction of miRNA genes are known to be located at genomic instability and fragile sites in human genome [46], [47].

Epigenetic factors may also change the expression pattern of miRNAs. An *in silico* analysis revealed that several miRNAs are located near CpG islands [62]. In addition, some miRNAs were up-regulated upon exposure of cells to the demethylating agent 5-aza-2'-deoxycytidine [63], upon mutation of DNMTs (DNA methyltransferases) [64], or upon HDAC (histone deacetylase) inhibitor treatment [65].

Another factor affecting miRNA expression is transcriptional regulation of miRNA transcripts. Transcription factors such as *TP53* and *MYC*, may change transcript levels of miRNAs. Tumor suppressor *TP53* induces the expression of tumor suppressor miR-34 cluster [66], whereas *MYC* transcription factor, an oncogene, induces the expression of oncogenic miR-17-92 cluster [67].

Due to such alterations of miRNA expression, levels of potentially many target mRNAs do change, as well. Target mRNA of a miRNA may be either an oncogene or a tumor suppressor gene. If miRNA's target is an oncogene, and this miRNA's expression is downregulated, then increase in proliferation, invasion and angiogenesis capacities and decrease in apoptosis in cancer cells may be observed. These changes can also be observed if miRNA's target is a tumor suppressor gene and the miRNA's expression is upregulated. According to the target mRNAs' role in cancer, miRNAs can be classified as oncogenes (also termed as oncomiR) or tumor suppressors. It is also possible that some miRNAs may target both oncogenes and tumor suppressor genes in different tissues and in different cancer types. Thus, for the classification of miRNAs, their targets should be taken into consideration. Figure 1.5 summarizes the miRNA and cancer relationship.

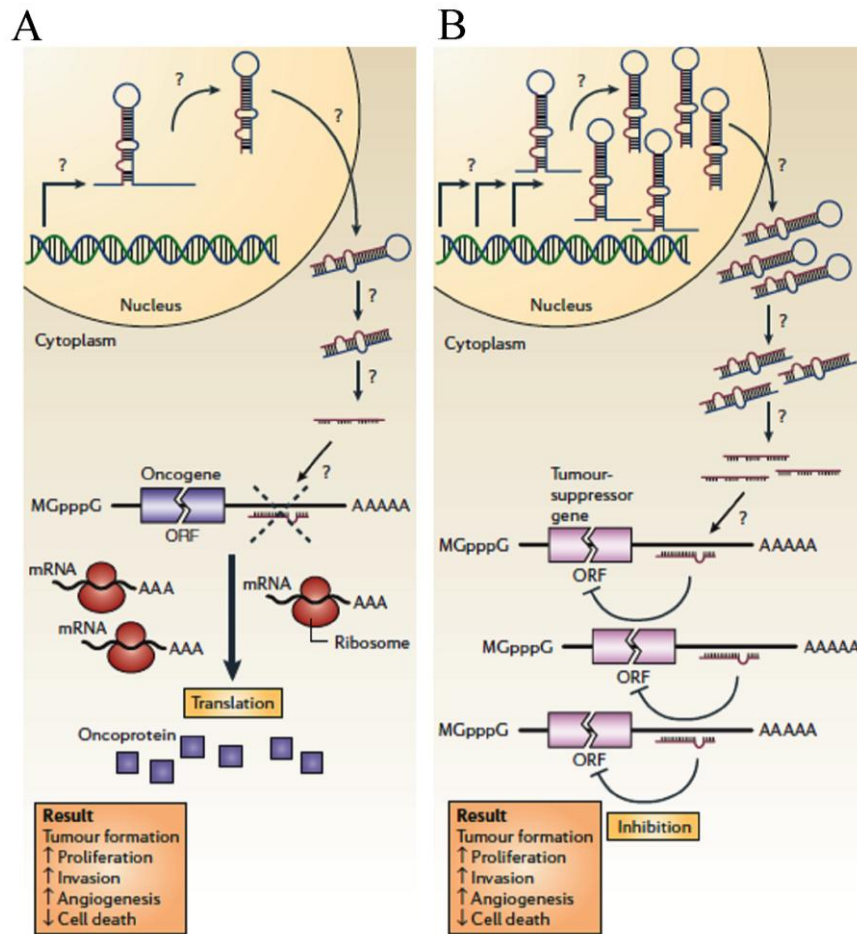


Figure 1.5: miRNAs can function as tumor suppressors and oncogenes (Figure taken from Aurora Esquela-Kerscher and Frank J. Slack, 2006) [68]. A) Downregulation of a miRNA that functions as a tumor suppressor leads to tumor formation. Downregulation may be caused by any stage of miRNA biogenesis and ultimately leads to the inappropriate expression of the miRNA-target oncoprotein. B) Upregulation of a miRNA that has an oncogenic role would result in tumor formation. Increased amounts of a miRNA would eliminate the expression of a miRNA-target tumor-suppressor gene. Increased levels of mature miRNA might occur due to several reasons. Amplification of the miRNA gene, translocation of miRNA gene under a constitutively active promoter, changes causing increase in efficiency of miRNA processing or increased stability of the miRNA. For both cases, the overall outcome might involve increased proliferation, invasiveness or angiogenesis, decreased levels of apoptosis, or undifferentiated or de-differentiated tissue, ultimately leading to tumor formation.

Human miRNAs bind to their target with imperfect complementarity. Seven nucleotides long seed sequence in the target 3'UTR determines the binding of miRNA to its target. miRNAs can potentially target several mRNAs [36]. Several tools are available for miRNA target predictions. Among thousands of predicted targets of miRNAs, several miRNA targets have been experimentally verified in several cancers. For instance several targets of hsa-let-7 were experimentally confirmed in different cancers. For let-7 miRNA, *RAS* in lung cancer [69], *CCND2*, *CDK6* and *CDC25A* in several cancer cell lines such as A549, HepG2, HeLa [70], *HMGA2* in ovarian cancer and in lung cancer cell lines [71], [72], *C-MYC* in liver tumors [73], were confirmed. Table 1.3 summarizes some of the confirmed targets of some miRNAs in different cancer types [61].

It is also possible that single target may be regulated by several miRNAs [36]. *TP53* (also designated as *p53*) is a well known tumor suppressor. Several miRNAs have been shown to target *TP53* in different cancer types. One of the miRNAs targeting *TP53* is miR-1285 [74]. Ectopic expression of miR-1285 inhibits expression of *TP53* mRNA and protein. Furthermore, decreased level of p21 transcript was observed upon miR-1285 expression. Another miRNA targeting *p53* is miR-504 [75]. miR-504 binds to two sites in *TP53* 3' UTR. Overexpression of miR-504 decreases *TP53* protein levels and activity in cells, including *TP53* transcriptional activity, *TP53*-mediated apoptosis, and cell-cycle arrest in response to stress. miR-125 family also targets p53 [76], [77]. On the other hand, as *TP53* is a transcription factor, it induces expression of many miRNAs which have tumor suppressor function. miR-34 family is one of the miRNAs that are induced by p53 [78], [79], [80].

Table 1.3: Representative oncogenic or tumor suppressive miRNAs and their direct target genes (Table adapted from Lee and Dutta, 2009) [61].

miRNA	Target gene	Note (cancer type, etc)
let-7	RAS	lung cancer
	CCND2, CDK6, CDC25A	cancer cell lines (A549,HepG2, HeLa)
	HMGA2	ovarian cancer
	c-Myc	liver tumors
	HMGA2	lung cancer cell lines
	NF2	cholangiocarcinoma cell lines
miR-10b	HOXD10	breast cancer
miR-16-1,-15a	Bcl2	chronic lymphocytic leukemia
miR-17-5p	AIB1	breast cancer
miR-18	CTGF (connective tissue growth factor)	colon cancer model of angiogenesis
miR-19	Thrombospondin-1	colon cancer model of angiogenesis
miR-20a	E2F1, 2, 3	
miR-21	PDCD4	colorectal cancer
	PTEN	hepatocellular cancer
	Tropomyosin 1 (TPM1)	
miR-27b	CYP1B1	breast cancer
miR-29a, b, c	DNMT3A, DNMT3B	non small cell lung cancer
	TCL1	chronic lymphocytic leukemia
	E2F3	neuroblastoma
	cyclin E2 (CCNE2),	
	hepatocyte growth factor receptor (MET)	
miR-34a, -34b,-34c	Bcl2	non small cell lung cancer
miR-106a cluster	MyIip (myosin regulatory light chaininteracting protein)	T-cell leukemia
	Hipk3 (homeodomain-interacting protein kinase3)	T-cell leukemia
	Rbp1-like (retinoblastoma-binding protein 1-like)	T-cell leukemia
miR-122a	Cyclin G1	hepatocellular cancer
miR-125a, -125b	ERBB2 and ERBB3	breast cancer
miR-125b	Bak-1	prostate cancer
miR-127	Bcl6	bladder and prostate cancer
miR-206	ER alpha	breast cancer
miR-221, -222	p27 (Kip)	glioblastoma
	p27 (Kip)	prostate cancer

1.1.4 miRNAs and Breast Cancer

As other cancer types, breast cancer also has a unique miRNA expression profile. Microarray analysis of 10 normal and 76 primary breast tumors showed that, hsa-miR-125b, hsa-miR-145, hsa-miR-21, and hsa-miR-155 were significantly deregulated in breast cancer [57]. Among those miRNAs, miR-155 and miR-21 were found to be upregulated whereas other indicated miRNAs were found to be downregulated in breast cancer samples.

In another study, miRNA expression profile in breast cancer cell lines and tumors were compared [81]. Ten *ERBB2* positive breast tumors and SKBR3 cell line were used in the study. According to results a unique set of miRNAs were associated with phenotypic status (*ERBB2* status) of breast cancer samples. miRNA expression profile similarities between *ERBB2* positive cell line and *ERBB2* positive tumor samples were identified.

Estrogen regulates genes directly through binding to estrogen receptors alpha and beta (*ER α* and *ER β*) that are ligand-activated transcription factors. Through binding to receptor, intracellular signaling cascades are activated, ultimately leading to altered gene expression. As estrogen has ability to change gene expression, miRNA expression in breast cancer samples was analyzed upon estrogen treatment in MCF7 cells [82]. According to this study, 38 miRNA genes were regulated by estrogen: 9 miRNAs were found to be downregulated and 29 miRNAs were found to be upregulated. However it is not clear whether this change was directly caused by *ER α* and *ER β* or their indirect effects

As miRNAs are powerful discriminators for identifying different cancer types, they are also capable of discriminating cancer subtypes. Breast cancer subtypes according to estrogen receptor, progesterone receptor and HER2/*neu* receptor status were categorized by miRNA expression profile [83]. In this study, expression of miR-342, miR-299, miR-217, miR-190, miR-135b and miR-218 were correlated with estrogen receptor expression, expression of miR-520g, miR-377, miR-527-518a and miR-520f-520c were correlated with progesterone receptor

expression and finally expression of miR-520d, miR-181c, miR-302c, miR-376b and miR-30e were correlated with HER2/*neu* receptor expression.

One of the most studied miRNAs is miR-21. It is found to be a well defined oncogene especially in breast cancer [84]. In several breast cancer cell lines oncogenic properties of miR-21 have been shown. Knockdown of miR-21 in MCF7 significantly reduced cell growth and reduced tumor growth in mouse xenograft [85]. In MDA-MB-231 cells, knockdown of miR-21 reduced invasive potential of MDA-MB-231 cells [86]. Moreover, in 344 fresh tumor samples, miR-21 overexpression was correlated with aggressiveness of the disease and high tumor grade [87]. In other cancers, tumor suppressor targets of miR-21 were identified; *PTEN* (phosphatase and tensin homologue deleted on chromosome 10) in hepatocellular carcinoma [88], *PDCD4* (programmed cell death 4) in colorectal cancer [89] and *IL-6* (interleukin-6) in myeloma cells [90]. Furthermore, in several studies anti-apoptotic effects of miR-21 in HeLa cells [91], neuroepithelial cells [92] and glioblastoma cells [93] were shown. Together with these findings, miR-21 is now accepted as an important oncogene not only in breast cancer but others as well.

Several oncogene and tumor suppressor targets of miRNAs have been identified in breast cancer samples. Table 1.4 summarizes the recent confirmed targets of several miRNAs in breast cancer.

Table 1.4: Recent confirmed targets of oncogenic or tumor suppressive miRNAs in breast cancer

miRNA	Target	Cell type	Reference
let-7 family	ER-alpha	MCF7	[94]
miR-10b	HOXD10	tumor-bearing mice	[95]
	TIAM1	breast cancer cell lines	[96]
miR-16	WIP1	MCF7 and mouse mammary tumor stem cells	[97]
miR-17-5p	HBP1	MCF7 and MDA-MB-231	[98]
miRNA 17/20	IL-8	MCF7 and MDA-MB-231	[99]
miR-20b	VEGF	MCF7	[100]
miR-92	ER-beta1	MCF7	[101]
miR-155	FOXO3A	breast cancer cell lines	[102]
	SOCS1	breast cancer cell lines	[103]
miR-185	SIX1	breast cancer cell lines	[104]
miR-200bc/429	PLCG1	breast cancer cell lines	[105]
miR-221,-222	ER-alpha	MCF-7 and T47D	[106]
miR-328	BCRP/ABCG2	MCF7	[107]
miR-520b, -520e	CD46	HBL-100 ,MCF-7 and MDA-MB-231	[108]
miR-661	Nectin-1 and StarD10	MCF7	[109]

1.2 miR-125 Family

miRNAs are grouped into families according to their mature sequence similarities. For instance according to miRBase, human miRNA let7, as largest miRNA family in human, has 8 isoforms encoded by 11 distinct genes. miR-125 family is another well known family in humans. This family has 2 isoforms encoded by 3 distinct genes: hsa-miR-125a, hsa-miR-125b-1 and hsa-miR-125b-2. miR-125a maps to 19q13.33 and codes for the mature form of miR-125a. miR-125b-1 and miR-125b-2 map to 11q24.1 and 21q21.1, respectively. miR-125b-1 locus (11q24.1) and miR-125b-2 (21q21.1) locus are known as loss of heterozygosity (LOH) regions [110], [111].

Precursor structures of these miRNAs are completely different from each other whereas there are only minor differences near the 3' end of their mature sequence. Figure 1.6 shows the precursor structures of these miRNAs.

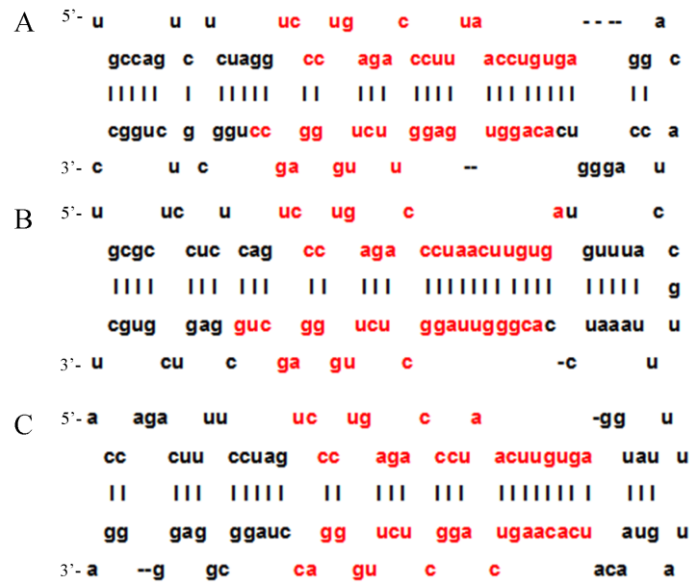


Figure 1.6: Precursor structures of miR-125 family members. Nucleotides in red indicates mature miRNA (near to 5' end) and miRNA*(near to 3' end) sequences A) pre-miR-125a hairpin structure B) pre-miR-125b-1 hairpin structure C) pre-miR-125b-2 hairpin structure

miR-125b-1 and miR-125b-2 produce the same mature miR-125b whereas there is only one source (hsa-miR-125a gene at chromosome 19q13.33) for mature miR-125a. There are only minor differences between mature sequences of miR-125a and miR-125b in 3' region. There are two extra U residues in 14th and 15th positions of mature miR-125a and there is C instead of U in the 19th nucleotide with respect to mature miR-125a. Figure 1.7 shows the differences between mature miR-125a and miR-125b. Seed regions for these two mature miRNAs are exactly the same. For that reason, target predictions for these miRNAs yield same results for the programs that only predict targets for seed sequence matching.

hsa-mir-125a: 5'- ucccugagacccuuuaaccuguga - 3'
hsa-mir-125b: 5'- ucccugagacccu__aacuguga - 3'

Figure 1.7: Mature miR-125a and miR-125b sequences. Figure shows the differences between mature sequences.

Deregulated expression of miR-125 family members in various cancers has been reported. One of the most studied cancer type for miR-125 family is breast cancer. 76 primary breast tumors, 11 breast cancer cell lines and 5 normal breast tissues were compared for their miRNA expression levels by both microarray and Northern blot analyses [57]. Downregulation of miR-125b was confirmed by both techniques in tumor and cell line samples compared to normal tissues whereas no significant change was observed for miR-125a expression. In another study, decreased expression of miR-125b was detected in 13 ERBB2 positive compared to 7 ERBB2 negative breast cancer biopsy samples [81]. miRNA expression levels in MCF7 breast cancer adenocarcinoma cell line were compared to HBL-100 cell line (derived from an early lactation sample of human milk) by miRNA microarray [112]. Similarly, downregulation of miR-125b was confirmed whereas no significant changes could be observed for miR-125a expression.

miR-125b expression has been studied in other cancers. In two independent studies carried out in ovarian cancer, downregulation of miR-125b was shown [59], [113]. Both groups confirmed the downregulation of miR-125b in primary ovarian tumors by miRNA array and Northern blot analyses. In non-small cell lung cancer, downregulation of miR-125a was confirmed by qPCR [114]. In this study, inhibitory effect of miR-125a on invasion and migration was confirmed in non-small cell lung cancer. In another study conducted in A549, H1299 and PC-9 lung cancer cell lines, inhibitory effects of miR-125a on metastasis was confirmed. Downregulation of miR-125b in squamous cell carcinoma of tongue [115], in oral cancer [116] and in prostate cancer [117] were detected.

miR-125b is also reported to have functions in proliferation and differentiation switch. Incompatibility between proliferation and differentiation and the switch between proliferation and differentiation have been demonstrated for many different cell types [118], [119]. By analyzing mouse mesenchymal stem cells, ST2, downregulation of cell proliferation rate by miR-125 was reported [120]. This inhibition of proliferation ultimately inhibited osteoblastic differentiation. In another study conducted with mouse embryonic stem cell line, D3, it has been reported that the depletion of miR-125b-2, but not miR-125b-1, caused a decrease in cell proliferation [121]. These results suggested that, for the proliferation of differentiated mouse embryonic stem cells, miR-125b-2 is required. Controversially, upregulation of miR-125b caused growth inhibition of U251 glioma stem cells *in vitro* [122]. miR-125b has also functions in neuronal differentiation in the human neuroblastoma cell line SH-SY5Y [123]. Ectopic expression of miR-125b increased the percentage of differentiated SH-SY5Y cells. In a different study, miR-125b overexpression inhibited the differentiation of primary B cells by targeting B lymphocyte-induced maturation protein-1 (*BLIMP-1*) and IFN regulatory protein-4 (*IRF-4*) transcription factor [124]. By this way, miR-125b inhibited premature utilization of these two transcription factors for plasma cell differentiation.

As mentioned previously, it is possible that miRNAs may target both oncogenes and tumor suppressor genes in different tissues and in different cancer types. Thus, for the classification of miRNAs, their targets should be taken into consideration. miR-125 family members were shown to target many oncogenes and tumor suppressor genes in several types of cancers.

1.2.1 Targets of miR-125 Family Members

First confirmed targets of miR-125a and miR-125b were *ERBB2* and *ERBB3* (epidermal growth factor, EGF, receptor family of receptor tyrosine kinases) oncogenes [125]. By ectopic expression miR-125a and miR-125b in *ERBB2* and *ERBB3* dependent breast cancer cell line, SKBR3, oncogenic properties such as proliferation, motility and invasiveness were decreased. Together with previous data

on downregulated levels of miR-125b, these initial results suggested that, miR-125b is a potential tumor suppressor.

Pro-apoptotic Bcl-2 antagonist killer 1 (*BAK1*) is a positive regulator of apoptosis. *BAK1* was confirmed as a target of miR-125b by two different groups. First, in prostate cancer cell lines, miR-125b was found to be targeting *BAK1* and stimulating prostate cancer cell line growth [126]. The other study was done in Taxol (mitotic inhibitor) resistant and sensitive breast cancer cell lines. Taxol sensitivity causing apoptosis was recovered by restoring *BAK1* expression either by inhibition of miR-125b or by re-expression of *BAK1* in miR-125b overexpressing cells [127]. These results suggested that, considering the target, miR-125b may also act as a potential oncogene.

Other targets of miR-125b were Vitamin D Receptor (*VDR*) and Human vitamin D₃ hydroxylase (*CYP24*) that have roles in calcitriol metabolism. Hormonally active form of vitamin D, 1 α ,25-dihydroxyvitamin D₃ (calcitriol) exerts antiproliferative effects. There are two important proteins for calcitriol metabolism: Vitamin D Receptor (*VDR*) and Human vitamin D₃ hydroxylase (*CYP24*). While *VDR* internalize the calcitriol into cells, *CYP24* catalyze the inactivation of calcitriol. Although, these two proteins have opposing functions in calcitriol metabolism, they are both regulated by miR-125b. In MCF7 cells, antiproliferative effect of calcitriol was abolished upon miR-125b overexpression [128], whereas endogenous expression levels of miR-125b and *CYP24* expression had a negative correlation 2009 [129]. Dual luciferase assays for both mRNAs indicated that these two proteins with opposite functions were both regulated by miR-125b. Moreover, *CYP24* is regulated by transcription factor vitamin D receptor (*VDR*) [130]. All these findings indicate an autoregulatory loop that miR-125b participate.

BCL3 protein has functional domains that are similar to I kappa B proteins (*IKB*). This protein activates NF-kappa B homodimers through interacting with this protein and acts as a transcriptional co-activator For that reason, *BCL3* may function as an oncogene. In ovarian cancer samples, interaction between *BCL3* and miR-125b was reported [131]. Through this interaction, cell cycle arrest and cell proliferation

reduction was observed. These results suggest that, lack of miR-125b contributes to ovarian cancer progression.

First study in bladder cancer about miR-125 family indicated that miR-125b was downregulated in bladder cancer tissues and four bladder cancer cell lines [132]. Furthermore, it was also shown that miR-125b downregulates protein levels of *E2F3* in bladder cancer. The E2F family proteins play crucial roles in the control of cell cycle. *E2F3* specifically binds to retinoblastoma protein pRB in a cell-cycle dependent manner and inhibits it. This downregulation of *E2F3* resulted in decreased expression levels of Cyclin A2 suggesting that miR-125b may regulate G1/S transition through the E2F3-Cyclin A2 signaling pathway.

In a different study carried in breast cancer cell lines, a negative correlation between miR-125a and HuR (*ELAVL1*) protein was found [133]. HuR is an RNA binding protein that stabilizes mRNAs of genes that regulate cell proliferation, angiogenesis, apoptosis, rapid inflammatory response and the stress response. Upon ectopic expression of miR-125a in breast cancer cell lines, cell proliferation rate was decreased and apoptosis was induced. These results indicate the tumor suppressor properties of miR-125a in breast cancer.

Another confirmed target of miR-125 family is *MUC I* protein [134]. Mucin I functions in cell signaling. Deregulated intracellular localization and overexpression of *MUC I* have been reported in carcinomas. Silencing of miR-125b in BT-549 breast cancer cell line both increased *MUC I* protein level and growth rate of the cells. *MUC I* interacts with I kappa B protein and has function in activation of NF-kappa B pathway. By having functions in activation of NF-kappa B pathway and being regulated by miR-125b, *MUC I* and *BCL3* have similarities.

As well as Pro-apoptotic Bcl-2 antagonist killer 11 (*BAK1*), miR-125b has another pro-apoptotic target; *BMF* (Bcl2 modifying factor). Study conducted in U343 and U251 human glioma cell lines proved the downregulation of *BMF* protein levels upon miR-125b-1 and miR-125b-2 transfections and an increase in *BMF* protein levels upon miR-125b inhibition [135]. Moreover, silencing of *BMF* by miR-125b inhibits apoptosis in U343 cells. These results suggest that miR-125b is an oncogene

for glioma cells and it may have function in abnormal development of nervous system.

C-RAF is an important MAP kinase kinase kinase (MAP3K), which functions in activating *ERK1* and *ERK2*, which have regulatory role in gene expression involved in cell cycle, apoptosis, cell differentiation and cell migration. *C-RAF* expression levels were downregulated by a short DNA hairpin analogous of miR-125b in breast cancer cell lines MDA-MB-453 and MDA-MB-231 [136]. Not only *C-RAF* and downstream targets' expression levels decreased but also decreased proliferation and induced apoptosis were reported.

One of the major tumor suppressor genes is p53 protein (*TP53*). As a transcription factor, it has functions for regulating target genes that induce cell cycle arrest, apoptosis, senescence, DNA repair, or changes in metabolism. Two different groups independently reported that miR-125 family members target p53 protein. In one study, miR-125b was shown to be a regulator of p53 in HEK-293T (human embryonic kidney) cells, SH-SY5Y neuroblastoma cells, p53-null human lung carcinoma H1299 cells and mouse Swiss-3T3 cells [137]. In other study, miR-125a was shown to regulate p53 tumor suppressor gene in HEK293T, HepG2 and MCF7 cell lines [77].

AT-rich interactive domain 3B (*ARID3B*) protein has roles in embryonic modelling, cell lineage gene regulation, cell cycle control, transcriptional regulation of several genes and possibly in chromatin structure modification. *ARID3B* was reported as an oncogene in neuroblastoma samples [138]. In a different study, *ARID3B* was shown to be essential for development of embryonic mesenchymal cells [139]. The epithelial-to-mesenchymal transition (EMT) is an important process during morphogenesis of multi-cellular organisms. EMT is required for a normal developmental process. However EMT was shown to have roles in tumor invasion and metastasis [140]. Role of *ARID3B* in EMT is yet to be understood. *ARID3B* was found to be regulated by miR-125a in ovarian cancer. Interaction between *ARID3B* and miR-125a was confirmed in ovarian cancer cell lines, OVCA433 and DOV13

[141]. Overexpression of miR-125a caused both a decrease in *ARID3B* protein level and induces a mesenchymal-to-epithelial transition.

1.3 Aim of the Study

miRNAs are known to have functions in cancer related pathways either as oncogenes or tumor suppressors. Identifying targets of miRNAs will elucidate their functions better in different cancer types. In this study, our aim was to investigate functions of miR-125b in breast cancer cells.

As a potential tumor suppressor in breast cancers, we aimed to investigate the role of miR-125b expression in breast cancer cells. This thesis consists of expression analysis of miR-125b in a panel of 11 breast cancer cells. Based on these results, low miR-125b expressing cells were further investigated in terms of miR-125b expression restoration and several functional studies were performed to understand the effect of this restoration.

CHAPTER 2

MATERIALS AND METHODS

2.1 Cancer Cell Lines

Eleven breast cancer cell lines (BT474, CAL51, CAL85-1 EFM-19, JIMT-1, HCC1937, HCC1143, HDQ-P1, MDA-MB-231, MCF7 and T47D) and one non-tumorigenic immortalized mammary cell line (MCF10A) were used in semi-quantitative duplex RT-PCR experiments. MCF10A, BT474 and CAL51 cell lines were obtained from ATCC (LGC Standards GmbH, Germany). MDA-MB-231 and MCF7 cell lines were a kind gift from Dr. Uygur Tazebay (Bilkent University, Ankara). EFM-19, JIMT-1, HCC1937, HCC1143, HDQ-P1, CAL85-1 and T47D cell lines were obtained from DSMZ (Braunschweig, Germany).

2.2 Mammalian Cell Culture Conditions

MCF7 cell line was grown in Minimum Essential Medium (MEM) with Earle's salts of Biochrom AG (Cat# FG0325) supplied with 10% Fetal Bovine Serum, PAA (Cat# A11-649) and 1% Penicillin / Streptomycin (10,000 IU / 10,000 µg/ml), (Biowhittaker, DE17-602E). FBS and Penicillin / Streptomycin were added into MEM by filtrating through Millipore 0.45µm HV Durapore membrane (Cat# SCHVU065RE). EFM-19 and HCC-1937 cells were grown in RPMI 1640 medium supplied with 10% FBS and 1% penicillin/streptomycin. HCC-1143 cells were grown in RPMI 1640 medium supplied with 20% FBS and 1% penicillin/streptomycin. BT474 cells were grown in RPMI 1640 medium supplied with 20% FBS, 1% penicillin/streptomycin, 10µg/mL human insulin and 2mM L-Glutamine. HDQ-P1, JIMT1 and MDA-MB-231 cells were grown in Dulbecco's

MEM medium supplied with 10% FBS and 1% penicillin/streptomycin. Cal-85-1 cells were grown in Dulbecco's MEM medium supplied with 10% FBS, 1% penicillin/streptomycin, 2mM L-Glutamine and 1mM NAPYR. Cal-51 cells were grown in Dulbecco's MEM medium supplied with 20% FBS, 1% penicillin/streptomycin and 4,5g/L Glucose. T47D cells were grown in Dulbecco's MEM, medium supplied with 10% FBS, 1% penicillin/streptomycin and 0.1% Non Essential Amino Acids. Finally, MCF10A cells were grown in DMEM/F12 medium supplied with 5% Horse Serum, 100 mg/mL EGF, 1 mg/mL Hydrocortizone, 1mg/mL Cholera Toxin, 10mg/mL insulin and 1% penicillin/streptomycin. Basic properties of cell lines such as *ER* (estrogen receptor) and *PR* (progesterone receptor) status, *ERBB2* protein status, source that cell line was formed, tumor type and subtype are given in Appendix A.

All cell lines were grown as monolayer and were incubated at 37°C with 95% air and 5% CO₂ in a hepa filtered Heraeus Hera Cell 150 incubator. All cell lines were handled in a Bilsler Class II laminar flow cabinet by using appropriate cell culture techniques.

According to doubling times of cell lines, media were changed 2-4 times a week and subculturing was done with 1X Trypsin-EDTA (PAA, Cat# L11-022) when the cells reached ~80% confluency. Total RNA isolation was done at ~70% confluency. Hank's Balanced Salt Solution of Biochrome AG (Cat# L2055) was used in cell culture washings before subculturing and RNA isolation.

Cells were frozen in liquid nitrogen when they reached 90% confluency. Ten percent DMSO (dimethyl sulfoxide) (Sigma, Cat# 154938) was used in the corresponding media for each cell line for long term storage of frozen cells. Cells were frozen and kept at -80°C for 24 hours and transferred to liquid nitrogen. Cells were thawed in a 37°C water bath. Centrifugation to pellet the cells during RNA isolation and freezing was done at 1400 rpm for 5 minutes.

All the reagents and chemicals used in cell culture studies were cell culture grade.

2.3 Bacterial Culture Media and Culture Conditions

DH5 α strain of *E.coli* was grown in LB (Luria Broth) media. For selection purposes, either 100 μ g/mL ampicillin or 100 μ g/mL spectinomycin was included in the media. In Appendix B, ingredients of bacterial media are listed. Sterilization of the medium was done by autoclaving at 121°C for 15 minutes. When solid media were used, 1.5% agar was added to solidify the media. All bacterial cultures were grown at 37°C with a 200 rpm (revolution per minute) shaking speed. Bacterial cultures were frozen in liquid nitrogen with 20% glycerol and kept at -80°C for long term storage.

2.4 Expression Analysis of miRNAs in Breast Cancer Cell Lines

Expression analysis of 3 candidate precursor miRNA, from now on designated as pre-miRNAs, (hsa-miR-125a, hsa-miR-125b-1 and hsa-miR-125b-2) was done by semi-quantitative duplex RT-PCR with precursor structure specific miRNA primers. In semi-quantitative duplex RT-PCR, miRNA primers were co-amplified with *GAPDH* primers, a housekeeping control gene, in the same reaction tube, as described previously [142], in eleven breast cancer cell lines (BT474, CAL51, CAL85-1, EFM-19, JIMT-1, HCC1937, HCC1143, HDQ-P1, MDA-MB231, MCF7 and T47D) and one non-tumorigenic immortalized mammary cell line (MCF10A).

2.4.1 RNA Isolation by Trizol Reagent

All the solutions used in RNA isolation were prepared with DEPC-treated water. Working area was cleaned by RNase AWAY from Molecular BioProducts (Cat# 7000) and DNA AWAY from Molecular BioProducts (Cat# 7010).

Cells were grown in T75 cell culture flasks to 70% confluency. Growing medium was sucked off from the flask and 8mL of Trizol reagent (Guanidium thiocyanate) from Invitrogen (Cat# 15596-018) was used to lyse the cells. After waiting for 5 minutes at room temperature (RT) for complete dissociation of nucleoprotein complexes, lysates were transferred into 15mL sterile tubes and 1.6

mL chloroform was added. Tubes were shaken vigorously for 15 seconds by hand. After 3 minutes incubation at RT, samples were centrifuged at 4700g for 20 minutes at 8°C. At the end of this stage, phases were separated and RNA remained in the aqueous phase with an approximate volume of 5mL. For RNA precipitation, 4 mL of isopropanol was added to each 5mL aqueous phase containing RNA. The samples were again incubated at RT for 15 minutes and centrifuged at 4700g at 4°C for 20 minutes. At the end of this stage, RNA formed a gel-like pellet at the bottom of tube. After removing supernatant, RNA pellet was washed by 75% ethanol with gentle vortexing. To remove ethanol, samples were centrifuged again at 4700g for 7 minutes at 4°C. Without disturbing the RNA pellet, ethanol was removed from the tube and samples were allowed to dry at RT for 10 minutes. RNA pellet was suspended in 20-50µL RNase-free water. RNA was stored at -80°C.

2.4.2 RNA Isolation by High Pure RNA Isolation Kit

Seventy percent confluent cells in T75 flasks were washed twice with 5mL Hank's Balanced Salt Solution. 3mL of 1X Trypsin-EDTA was added to detach the cells and cells were incubated at 37°C, 5% CO₂ incubator for 10-15 minutes. Double volume of growth medium was added to samples to stop the action of trypsin. Supernatant was removed by centrifuging the cells at 1400 rpm for 5 minutes in 5-6mL culture medium. The media were removed, cells were washed once with 1x PBS, cell pellet was dissolved in PBS and kept on ice. 400µL Lysis-Binding Buffer was added to cell suspension. All contents were applied into filter tube after addition of Lysis-Binding Buffer and collection tube assembly and cells were centrifuged for 30 seconds at 8000g. 10µL DNase I and 90µL DNase I incubation buffer was mixed and applied to filter tube. Samples were incubated for 15 minutes at RT. After this step, two consecutive washing steps (500µL Wash Buffer) were performed with 30 seconds 8000g centrifugations followed by 13000g centrifugation for 2 minutes for complete removal of ethanol of wash buffers. RNA was eluted from filter tube by applying 25-50µL RNase free water. RNA was stored at -80°C.

2.4.3 Determination of RNA Quantity and Quality

The RNA concentration was determined by measuring absorbance at 260 nm on a spectrophotometer in distilled water. One absorbance unit equals to 40 μ g/mL RNA. According to this, RNA concentration was determined as follows:

$$\text{RNA } (\mu\text{g/mL}) = 40 \times \text{Dilution Factor} \times \text{OD}_{260}$$

Moreover, A260/A280 and A260/A230 ratios were checked. Nucleic acids are detected at 260nm, proteins are detected at 230nm and 280nm, salt and solvents are detected at 230nm. For that reason A260/A280 ratio must be between 1.8 and 2 and A260/A230 ratio must be higher than 1.8 [143].

2.4.4 DNase I Treatment

All the solutions used in DNase treatment were prepared with DEPC-treated water. Working area was cleaned by RNase AWAY from Molecular BioProducts (Cat# 7000) and DNA AWAY from Molecular BioProducts (Cat# 7010). All isolated RNAs were treated with Deoxyribonuclease I (DNase I) from Fermentas (Cat # EN0521) in order to obtain DNA-free RNA. Reaction mix is listed in Table 2.1.

Table 2.1: DNase I reaction mixture

RNA (1 μ g/ μ L)	10 μ L
10x Reaction Buffer	10 μ L
DNase I (1u/ μ L)	10 μ L
Ribonuclease Inhibitor (40u/ μ L)	5 μ L
DEPC-dH ₂ O	65 μ L
Total Volume	100 μ L

Reaction mixture was prepared on ice and reaction was carried out at 37°C for 60 minutes in a water bath. Equal amount of Phenol: Chloroform: Isoamyl Alcohol (25: 24: 1) was added to stop the reaction (100µL). Tube was vortexed for 30 seconds and incubated on ice for 10 minutes. Samples were centrifuged at 14000g for 20 minutes at 4°C. Then, upper phase containing RNA was taken into a fresh tube. According to volume of upper phase, 3X volume 100% ice cold ethanol and 1/10X volume 3M NaAc was added to samples and samples were incubated at -20°C overnight to precipitate RNA. After overnight incubation, samples were centrifuged for 30 minutes at 14000g at 4°C. After discarding the supernatant, samples were washed with 70% cold ethanol and again centrifuged for 10 minutes at 14000g at 4°C. Finally, pellet was dissolved in 20-50µL RNase-free dH₂O. RNA was quantified as previously described. Lack of DNA in RNA samples were further confirmed by PCR.

2.4.5 cDNA Synthesis

RevertAid First Strand cDNA Synthesis Kit from Fermentas (Cat# K1632) was used for first strand cDNA synthesis. Random hexamer primers were used in the reaction. Table 2.2 shows master mix preparation and protocol for the kit used.

Table 2.2: cDNA synthesis (RT) protocol and reaction mixture by RevertAid First strand cDNA synthesis kit (Fermentas).

RNA	1µg (1-2µL)
Primer (oligodT or random hexamer)	1µL
dNTP mix	2µL
DEPC- treated water	variable
TOTAL	12µL
Briefly centrifuged, incubated at 70°C for 5 minutes, chilled on ice and briefly centrifuged.	
5X reaction buffer	4µL
Ribolock RNase inhibitor	1µL
Briefly centrifuged and incubated at 37°C for 5 minutes (25°C for random hexamer primers)	
RevertAid RT enzyme	1µL
TOTAL	20µL
Tubes were mixed and incubated at 25°C for 10 minutes, 42°C for 60 minutes for random hexamer primers; reaction was stopped by heating at 70°C for 10 minutes and chilling on ice.	

2.4.6 Primer Design for Precursor miRNA (pre-miRNA)

For expression analysis of pre-miRNA, sequences were obtained from miRBase database (<http://www.mirbase.org>) and cDNA primers were designed manually. hsa-mir-125b-1 pre-miRNA primers are shown in Figure 2.1.

5'- UGCGCUCCUCUCAGUCCUGAGACCCUAACUUGUGAUGUUUACCGUU
 UAAAUCCACGGGUUAGGCUCUUGGGAGCUGCGAGUCGUGCU - 3'

chr11: 121475675-121475762 88bp

Forward: 5'- tgcgetcctcctcagtcctgag -3'

Reverse: 5'- agcacgactcgcagctccaag -3'

Figure 2.1: cDNA primer design for hsa-mir-125b-1 pre-miRNA. Red; mature miRNA sequence, underlined sequences; forward (22 nucleotides) and reverse (22 nucleotides) primers, green; stem-loop region. UCSC In-Silico PCR primer specificity program (<http://genome.ucsc.edu/cgi-bin/hgPcr>) confirmed the 88 bp product size for hsa-mir-125b-1.

PCR product sizes for precursor miRNAs were 75bp for hsa-miR-125a, 88bp for hsa-miR-125b-1, and 70bp for hsa-miR-125b-2. *GAPDH* primers were designed to yield a PCR product of 115bp. Table 2.3 shows the primer list used in expression analysis of precursor miRNAs. Specificity of designed primers was checked by using UCSC *in-silico* PCR program (<http://genome.brc.mcw.edu/cgi-bin/hgPcr>). All primers were resuspended in RNase-free water to a final concentration of 100µM.

Table 2.3: List of primers used in semi-quantitative duplex RT-PCR. miRNA primers are precursor structure specific.

Primers		Expected Size
<i>GAPDH</i>	Forward: 5'-TATGACAACGAATTTGGCTAC-3'	115bp
	Reverse: 5'-TCTCTCTTCTCTTGTGCTCT-3'	
hsa-miR-125a	Forward: 5'-TGCCAGTCTCTAGGTCCCTG-3'	75bp
	Reverse: 5'-AGGCTCCCAAGAACCTCACC-3'	
hsa-miR-125b-1	Forward: 5'-TGCGCTCCTCTCAGTCCCTGAG-3'	88bp
	Reverse: 5'-AGCACGACTCGCAGCTCCCAAG-3'	
hsa-miR-125b-2	Forward: 5'-ACCAGACTTTTCCTAGTCCC-3'	70bp
	Reverse: 5'-AAGAGCCTGACTTGTGATGT-3'	

2.4.7 Semi-quantitative Duplex RT-PCR

Precursor specific miRNA primers (hsa-miR-125a, hsa-miR-125b-1 and hsa-miR-125b-2) and *GAPDH* were co-amplified in the same duplex RT-PCR tubes in eleven breast cancer cell lines and one non-tumorigenic immortalized mammary cell line cDNAs. Reaction setup and PCR program details are given in Table 2.4 and Table 2.5. 15 μ L of the final PCR products of all reactions were electrophoresed on a 2% agarose gel at 100V and photographed under UV light. All PCR optimization conditions are given in Appendix C.

Table 2.4: Duplex RT-PCR reaction mixture to amplify pre- miRNA and *GAPDH*.

1X master mix	
Molecular grade dH ₂ O	7.35 μ L
10 X buffer	3 μ L
dNTP mix (2mM each)	3 μ L
miRNA forward primer (5 μ m)	3 μ L
miRNA reverse primer (5 μ m)	3 μ L
<i>GAPDH</i> forward primer (5 μ m)	1.5 μ L
<i>GAPDH</i> reverse primer (5 μ m)	1.5 μ L
MgCl ₂ (25mM)	2.4 μ L
DMSO	3 μ L
Taq Polymerase	0.25 μ L
cDNA	2 μ L
TOTAL	30 μ L

Table 2.5: Duplex PCR cycling conditions for pre-miRNA (Annealing temperature differed for all miRNAs).

94°C	3:00 min	} 35 cycles
94°C	0:30 min	
56°C	0:30 min	
72°C	0:30 min	
72°C	10:00 min	

2.4.8 Densitometry Analysis of Semi-quantitative Duplex RT-PCR

Semi-quantitative duplex RT-PCR gel images were analyzed using Scion Image program (National Institute of Health). Fold changes calculated for MCF10A cDNA for *GAPDH* and miRNA band intensities were used to normalize the cancer cell line cDNA fold changes. The formula used in calculation of fold change of miRNAs in cancer cell lines normalized to normal DNAs is shown below.

$$\text{Fold Change} = \frac{\text{C (microRNA/GAPDH)}}{\text{MCF10A (microRNA/GAPDH)}}$$

C stands for cancer cell line samples. Band intensities of miRNA PCR products were divided to band intensities of *GAPDH* PCR products. Results were further normalized by the value determined for MCF10A.

2.5 Ectopic Expression of pre-miR-125b

In order to ectopically express miR-125b in MCF7 cells, pSUPER RNAi System (Cat# VEC-PRT-0005/0006) was used.

2.5.1 Oligonucleotide Design

Oligonucleotides to be cloned into pSUPER RNAi system were designed according to pSUPER manual. Figure 2.2 shows the properties that the oligonucleotides had; 5' *Bgl*III and 3' *Hind*III sticky ends, sense and antisense sequences and a hairpin sequence in the middle of oligos.

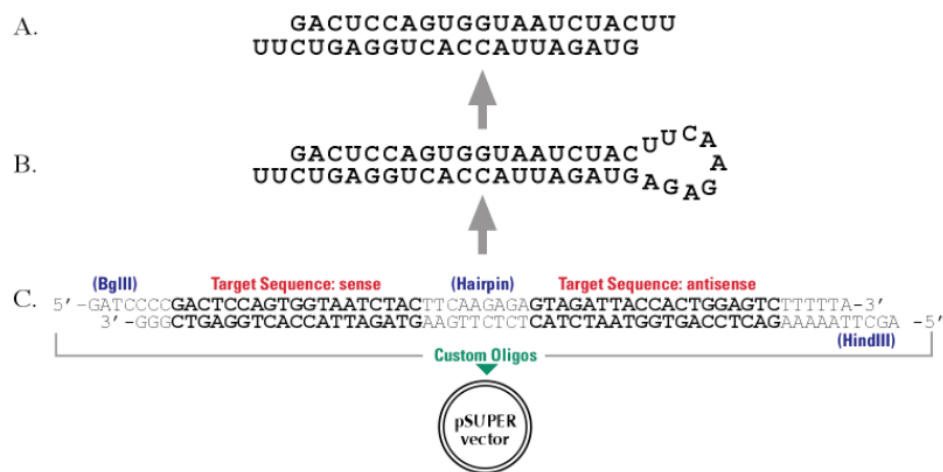


Figure 2.2: Example oligonucleotide design for pSUPER system (pSUPER RNAi System).

Oligonucleotides contained sticky ends for *Bgl*III restriction enzyme (target sequence: 5'-A/GATCT-3') at the 5' end and *Hind*III (target sequence: 5'-A/AGCTT-3') restriction enzyme at the 3' end, so that after linearization of vector, through these sites, oligos were ligated into pSUPER. Although *Bgl*III produces 5'-GATCT-3' sticky end, in oligo design it was 5'-GATCC-3'. This was done to demolish *Bgl*III recognition site and eliminate negative clones. Sense oligonucleotides have modified sticky end for *Bgl*III restriction enzyme at the 5' end (5'-GATCC-3') and antisense oligonucleotides have sticky end for *Hind*III (5'-AGCTT-3') at the 3' end. There are also additional sequences which enhances hairpin structure formation with 2 nucleotides overhangs at the 3' ends after transcription, which is required for further processing of transcript. For that reason two extra cytosine (C) nucleotides at the 5' end just after *Bgl*III sticky end and five extra thymidine (T) nucleotides at the 5' end just after *Hind*III sticky end were introduced. These extra nucleotides were suggested

by manufacturers for efficient processing by Dicer enzyme after transcription from the vector. miRNA precursor structure was used instead of sense target, hairpin and anti-sense target sequences as shown in Figure 2.2. However, as pre-miR-125b is 88bp long, 11 nucleotides from both 5'end and 3'end were omitted for size limitations of vector, forming a final 66bp precursor structure. Figure 2.3 shows the differences in sequence between native pre-miR-125b-1 and cloned construct. Oligonucleotides sequences were also given Figure 2.3.

A
 TGCGCTCCTCTCAGTCCCTGAGACCCTAACTTGTGATGTTTACCGTTTAAATCCACGGGTTAGGCTCTTGGGAGCTGCGAGTCGTGCT

B
GATCCCCCAGTCCCTGAGACCCTAACTTGTGATGTTTACCGTTTAAATCCACGGGTTAGGCTCTTGGGAGCTGTTTTTA

C
 Sense: 5'/Phos/- *GATCCCCCAGTCCCTGAGACCCTAACTTGTGATGTTTACCGTTTAAATCCACGGGTTAGGCTCTTGGGAGCTGTTTTTA*-3'
 Anti-sense: 5'/Phos/ - *AGCTTAAAAACAGCTCCCAAGAGCCTAACCCGTGGATTTAAACGGTAAACATCACAAAGTTAGGGTCTCAGGGACTGGGG*-3'

Figure 2.3: Differences in sequence between native pre-miR-125b-1 and cloned construct. Underlined sequences are same in both native and cloned pre-miR-125b-1 A. Native pre-miR-125b-1 B. Cloned pre-miR-125b-1. Italics sequences are added according to pSUPER system. C. Sense and antisense oligonucleotides used for cloning into pSUPER vector.

2.5.2 Oligonucleotide Cloning into pSUPER Vector

2.5.2.1 Preparation of Competent *E.coli* Cells

Competent *E.coli* preparation protocol was adapted from the book; Molecular Cloning: A Laboratory Manual [143]. Several *E.coli* colonies were grown in 50mL of LB medium as described previously in bacterial culture conditions, at 37°C with a 200 rpm (revolution per minute) shaking speed. 300µL grown cell suspension was further grown in LB medium until OD₆₀₀ reaches to 0.6, indicating the log phase of bacterial growth. Cell suspension was then divided into 2 sterile prechilled centrifuge tubes and was incubated on ice for 10 minutes. Cells were centrifuged at 4000 rpm

for 10 minutes. Pellet was resuspended in 5 mL ice cold 10mM CaCl₂ and was recentrifuged at 3000 rpm for 10 minutes at 4°C. Finally, pellet was dissolved in 1mL of 75mM CaCl₂ and 200µL ice cold glycerol was added. After making aliquots, cells were frozen in liquid nitrogen and stored at -80°C.

2.5.2.2 Oligo Annealing

The annealing procedure was performed as described in the pSUPER manual. Designed oligos were first dissolved in sterile nuclease-free H₂O to have a final concentration of 3mg/ml. Annealing buffer was prepared according to pSUPER manual, (100mM NaCl and 50mM HEPES at pH 7.4). Reaction setup was prepared by using 1µL of each oligo (sense + antisense) with 48µL annealing buffer. Reaction mixture was incubated at 90°C for 4 minutes and then at 70°C for 10 minutes. Then stepwise cooling was performed; 60°C for 10 minutes, 50°C for 10 minutes, 37°C for 30 minutes and finally reaction was cooled to 10°C.

2.5.2.3 Linearization of pSUPER Vector and Ligation Reaction

pSUPER vector was linearized by *Bgl*III and *Hind*III restriction enzymes. The map of pSUPER vector is given in Appendix D. 10 units of each enzyme were incubated with 10µg pSUPER vector with 2X Tango buffer (Fermentas) at 37°C for overnight. Reaction was stopped by incubating the mixture at 65°C for 10 minutes. Digested vector was run on 1% agarose gel containing 0.5µg/mL EtBr. DNA was extracted from the gel by using agarose gel extraction kit, Roche (Cat# 11696505001), and quantified on a Hoefer fluorometer.

Annealed oligos and linearized vector were ligated by T4 DNA ligase enzyme. By adding 2µL of the annealed oligos to 1µL of T4 DNA ligase buffer with 0.5µg of pSUPER vector and 1 unit of T4 DNA ligase, ligation reaction was performed for overnight at 16°C with a total volume of 10µL.

2.5.2.4 Transformation of Competent *E.coli* Cells

Competent *E.coli* cells were transformed according to Molecular Cloning: A Laboratory Manual [143]. For each transformation reaction, 50 μ L chemically competent *E.coli* cells were thawed on ice. 2 μ L of ligation reaction product was added into tubes containing competent cells and incubated for 30 minutes on ice. Cells were exposed to heat shock for 45 seconds at 42°C and were incubated on ice for 5 minutes. 500 μ L LB medium was added to each reaction mix. Cells were grown at 37°C for 1 hour with 200 rpm shaking. LB-Agar plates containing 100 μ g/mL ampicillin were prepared and 250 μ L cell suspension was spread over these plates. Plates were incubated overnight at 37°C.

Plasmids isolated from colonies were screened for positivity by isolating double digestion with *Eco*RI (target sequence: 5'-G/AATTC-3') and *Hind*III as suggested by pSUPER manual. *Bgl*II site had already been lost during cloning as mentioned previously. Plasmid isolations were done by Roche High Pure Plasmid Isolation kit (Cat# 11754777001). Correct clones with inserts (pSUPER-125b) were expanded and insert was further confirmed by sequencing.

2.5.3 Stable Transfection of MCF7 Cells with pSUPER-125b

MCF7 cells were seeded in 6-well plates the day before transfection at confluency of 80% ($\sim 2 \times 10^6$ cells). Before the transfections, MEM-Earle's complete culture medium was changed to an antibiotic free medium, containing 10% FBS. FuGENE HD was used as a transfection reagent in 3:2 (FuGENE:plasmid) ratio. For 3 μ g plasmid, 4.5 μ L FuGENE HD was included in the mixture and the mixture volume was completed to 100 μ L with Optimem medium. The ingredients were added into a sterile eppendorf tube in the order of Optimem, DNA and FuGENE HD. Mixtures were left at RT for 15 minutes before adding into 6-well plate.

500µg/mL of G418 antibiotic, Gentamycin, from Roche (Cat# 4727878001) was first added after 24 hours of transfection for stable selection of cells. After elimination of non-transfected cells, concentration of antibiotic was reduced to 250µg/mL for long term maintenance of transfected cells.

2.5.4 Confirmation of pSUPER Genomic Integration and Ectopic Expression

For DNA isolation, GeneJET Genomic DNA Purification Kit from Fermentas (Cat# K0721) was used. PCR was performed with pSUPER plasmid specific primers according to pSUPER manual. Sequences of primer and PCR optimization conditions are given in Appendix C.

For confirmation of ectopic expression, RNA was isolated and cDNA synthesis was done as previously described. For confirmation of miR-125b expression, a different set of primers were designed, as cloned precursor miR-125b lacked a total number of 22 nucleotides due to pSUPER size limitations. *GAPDH* PCR was also used to test the quality of cDNA samples for normalization of samples. Primer set used for confirmation of ectopic expression is given in Table 2.6.

Table 2.6: List of primer set used in confirmation of ectopic expression.

Primers		Expected Size
hsa-miR-125b-1	Forward: 5'-CAGTCCCTAGACCCTAA -3'	66bp
	Reverse: 5'-CAGCTCCCAAGAGCCTAA -3'	

Cloned pre-miR-125b-1 PCR thermal cycling conditions used consisted of an initial denaturation at 94°C for 2 minutes followed by 35 cycles of 94°C for 30 seconds, 56°C for 30 seconds, 72°C for 30 seconds and final extension at 72°C for 10 minutes by using 3µL primers from 5µM stock. *GAPDH* PCR thermal cycling conditions used consisted of an initial denaturation at 94°C for 2 minutes followed

by 35 cycles of 94°C for 30 seconds, 56°C for 30 seconds, 72°C for 30 seconds and final extension at 72°C for 10 minutes by using 3µL primers from 5µM stock. PCR products were run on ethidium bromide stained 3% agarose gels, visualized and documented under UV.

2.6 Functional Assays

2.6.1 Cellular Proliferation Assay

The effects of hsa-miR-125b-1 expression on cell proliferation was measured by Cell Proliferation Kit I (MTT), Roche (Cat# 11 465 007 001). The water soluble MTT (3-(4,5-dimethylthiazol-2-yl)-2,5-diphenyltetrazoliumbromide) is converted to an insoluble formazan by mitochondrial reductase in the mitochondria of viable cell as shown in Figure 2.4. Formazan is then solubilized by solubilization buffer and by this way; spectrophotometrically, the solubilized formazan product is quantified by using an ELISA plate reader. An increase in number of living cells indicated in an increase in the total metabolic activity of the sample. This increase directly indicates the total amount of purple formazan crystals formed.

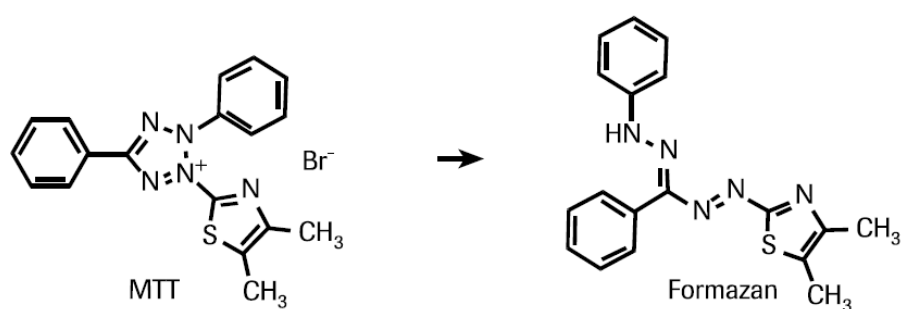


Figure 2.4: Reduction of MTT to formazan, (Cell Proliferation Kit I (MTT), Roche.)

One thousand pSUPER-125b-1 transfected MCF7 cells, from now on designated as MCF7-125b-1, and one thousand empty pSUPER transfected MCF7 cells, from now on designated as MCF7-EV, were plated in 96-well plates in MEM-Earle's medium to be assayed at 1, 3, 5, 7 and 9 days for the MTT assay. Cells were incubated with 10 μ L of MTT solution for four hours. After incubation with MTT solution, formazan crystals were formed. These crystals become solubilized by incubating with solubilization solution overnight. The medium with the MTT reagent was used as a blank for the microplate reading. The absorbance was measured with Bio-Rad microplate reader at 570nm. MTT assay was repeated twice at different times. Each sample had 10 replicates. Data were statistically evaluated by Mann Whitney test using GraphPad Prism Software and significance was set to $P < 0.0001$

2.6.2 *In vitro* Wound Closure Assay

To investigate the proliferation and directional migration behavior of cells, an *in vitro* wound closure assay was performed [144]. MCF7-125b-1 and MCF7-EV cells were seeded in 6-well plates and were grown until they were 90% confluent. A wound was introduced by a sterile pipette tip in monolayer cells. Cell debris was removed by washing twice with Hank's Salt solution. Cells were then grown in MEM-Earle's complete medium. Wound areas were marked with a permanent marker to determine the size of the initial wound area. 0, 24, 48 and 72 hours after wounding, images were captured using an inverted Olympus phase contrast microscope with 4X objective (total magnification 40X) and Moticam 2300 camera system. Distances traveled by the cells were measured by Motic ImagePlus 2.0 software. Experiment was repeated twice with 4 replicates for each sample.

Data were statistically evaluated by one way ANOVA test using GraphPad Prism Software. In order to find groups whose mean differences were significant, Tukey's multiple comparison tests was carried out. Significance was tested by Mann Whitney test.

2.6.3 Transwell Migration Assay

Transwell migration assay was done in 24-well plates using migration chambers from Corning (Cat# 3422). Figure 2.5 shows the structure of migration chamber.

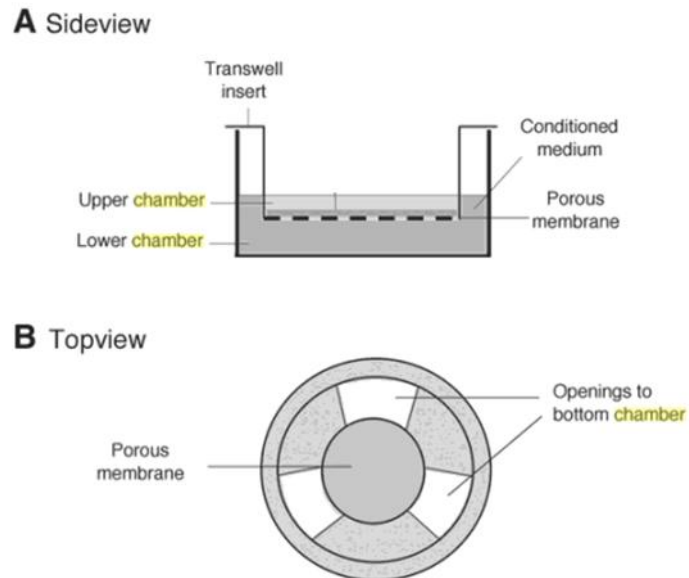


Figure 2.5: A. Side view of a Transwell, lower and upper chambers B. Top view of upper chamber, Figure taken from the book, Cell Migration: Developmental Methods and Protocols [145].

Basically, 30,000 cells in 0.1mL MEM-Earle's medium with 1% FBS were plated on the upper wells of transwell migration chambers. MEM-Earle's medium with 10% FBS (0.6mL) was added to lower wells. Cells were allowed to migrate through an 8 μ m pore membrane for 72 hours. Cells on the upper surface of the membrane were removed by scrubbing with sterile cotton swabs. 100% methanol was used to fix cells on the lower surface of the membrane for 10 minutes. Fixed cells were stained with Giemsa for 2 minutes and membranes were washed twice with distilled water and membranes were left to air dry. After the membrane filters were dry, they were cut out and mounted onto a glass slide upside down with a drop

of oil. Cells on the upper side of the membrane were counted under a Leica light microscope with 4X objective (total magnification 40X).

4 membranes were used for each sample and 3 random fields were counted per membrane. Data were evaluated by Mann-Whitney test, using GraphPad Prism Software. Significance level was set to $P < 0.0001$.

2.7 Target Search for hsa-miR-125b

Four miRNA target prediction programs available online, TargetScan, version 5.1 (<http://www.targetscan.org/>) (For web interface, see Figure 2.6), [39], [37], [40]; microRNA.org (<http://www.microRNA.org>) (For web interface, see Figure 2.7) [41]; PicTar (<http://pictar.bio.nyu.edu/>) (For web interface, see Figure 2.8) [42] and PITA (http://genie.weizmann.ac.il/pubs/mir07/mir07_data.html) (For web interface, see Figure 2.9) [43], were used to find predicted target genes of hsa-miR-125b-1. All programs were screened and listed for high scored predictions.

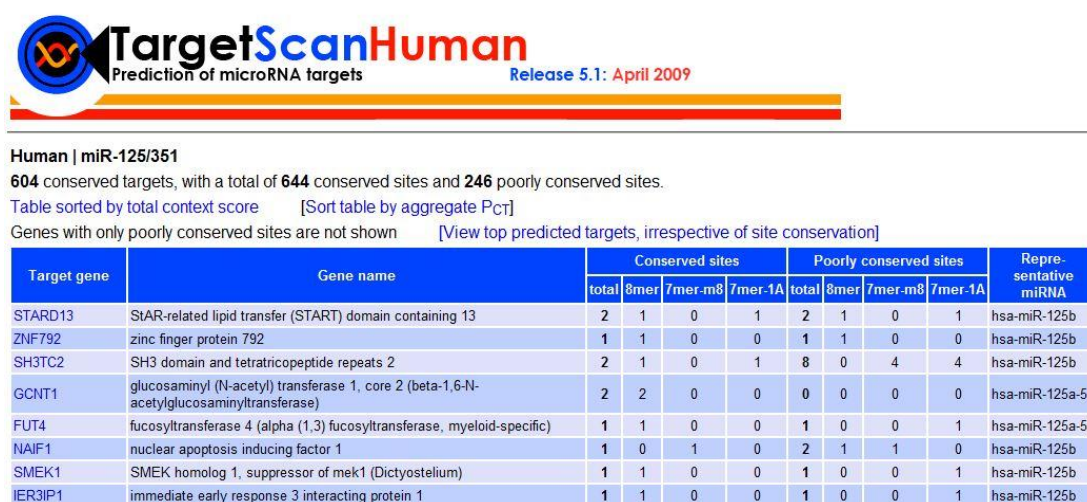


Figure 2.6: TargetScan web interface, miRNA targets search page (<http://www.targetscan.org/>)

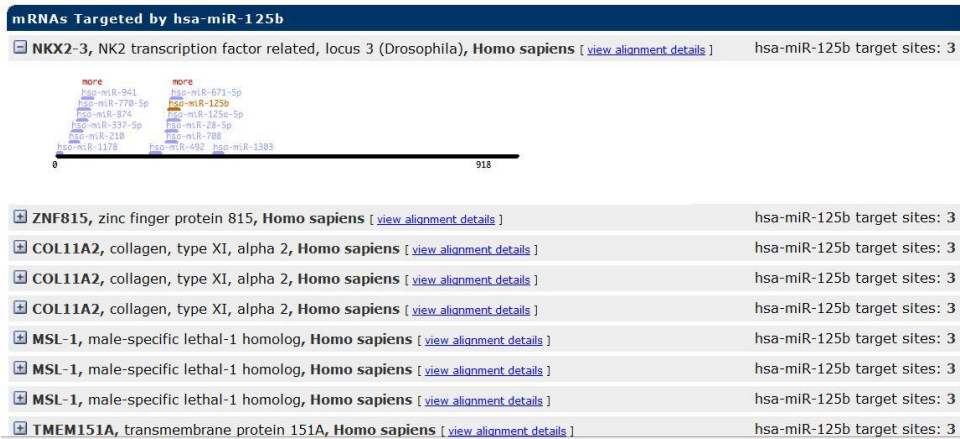


Figure 2.7: microRNA.org web interface, miRNA targets search page (<http://www.microRNA.org/miRNA/home.do>)

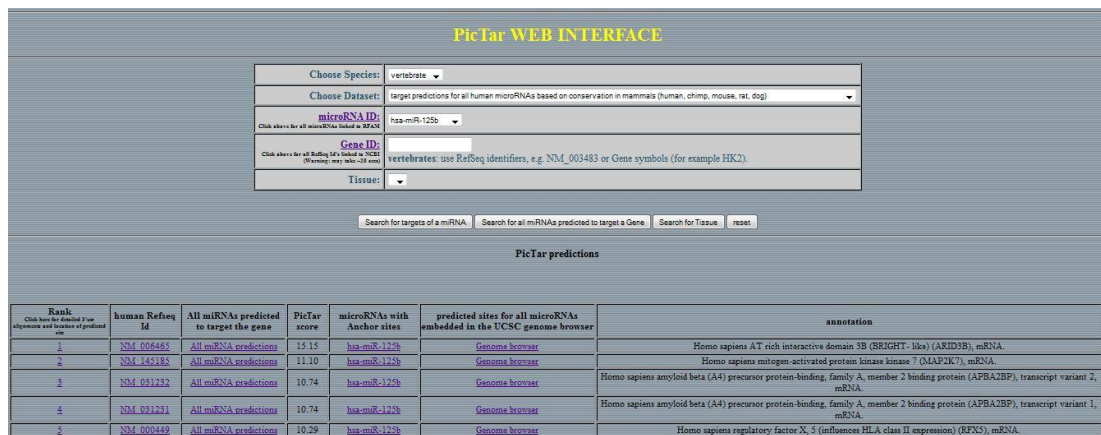


Figure 2. 8: PicTar web interface, miRNA targets search page (<http://pictar.mdc-berlin.de/>)

Organism	RefSeq	Gene Name	microRNA	Sites	Score
Human	NM_012296;NM_080491	GAB2	hsa-miR-125b	4	-21.56
Human	NM_016293	BIN2	hsa-miR-125b	1	-19.34
Human	NM_152460	C17orf77	hsa-miR-125b	1	-19.26
Human	NM_022749	RAI16	hsa-miR-125b	2	-18.78
Human	NM_133334	WHSC1	hsa-miR-125b	3	-18.35
Human	NM_001100598;NM_001100599	CZNF707	hsa-miR-125b	3	-18.25
Human	NM_001042550;NM_001042551	SMC2	hsa-miR-125b	2	-17.70
Human	NM_001013690	LOC401720	hsa-miR-125b	2	-17.51
Human	NM_152383	DIS3L2	hsa-miR-125b	1	-17.26
Human	NM_153442	GPR26	hsa-miR-125b	4	-17.04
Human	NM_020398;NM_181502	SPINLW1	hsa-miR-125b	1	-16.98
Human	NM_207517	ADAMTSL3	hsa-miR-125b	2	-16.89
Human	NM_021961	TEAD1	hsa-miR-125b	2	-16.79
Human	NM_002711	PPP1R3A	hsa-miR-125b	3	-16.69
Human	NM_003807;NM_172014	TNFSF14	hsa-miR-125b	1	-16.5
Human	NM_144679	C17orf56	hsa-miR-125b	2	-16.40
Human	NM_018947	CYCS	hsa-miR-125b	2	-16.34
Human	NM_032376	TMEM101	hsa-miR-125b	1	-16.32
Human	NM_024562	TMCO7	hsa-miR-125b	2	-16.14
Human	NM_002206	ITGA7	hsa-miR-125b	2	-16.12
Human	NM_032351	MRPL45	hsa-miR-125b	1	-16.08
Human	NM_014913	KIAA0863	hsa-miR-125b	1	-15.95
Human	NM_001010845	ACSM2A	hsa-miR-125b	2	-15.94

Figure 2. 9: PITA downloadable target search interface, miRNA targets search page (http://genie.weizmann.ac.il/pubs/mir07/mir07_data.html)

2.8 Analysis of Target 3'UTR and miRNA Interaction

For analysis of 3'UTR and miRNA interaction, dual-luciferase assay was performed. Sequence of interest was cloned downstream of the Firefly luciferase gene in pMIR vector. Renilla luciferase was used for normalizing the ratios. For Firefly luciferase construct pMIR-REPORT Luciferase vector (Ambion) and for Renilla luciferase construct phRL-TK vector (Promega) were used.

2.8.1 ARID3B 3'UTR Cloning

ARID3B (NM_006465.2) 3'UTR is 2369 nucleotides long. Due to vector's size limitations whole UTR region was divided into 3 regions named as C1, C2 and C3. Primers with restriction enzyme recognition sites were designed. Table 2.7 list the primers used in cloning. By PCR, these regions initially were cloned into pCR8/GW/TOPO subcloning vector then were cloned into pMIR vector. *SacI* sites into the 5' end and *HindIII* sites into the 3' end were integrated into PCR products through primers. Details of PCR optimization conditions are given in Appendix C.

Table 2.7: Cloning primers for *ARID3B* 3'UTR. Underlined sequences indicate restriction enzyme recognition sites; *Sac*I sites in forward primers and *Hind* III sites in reverse primers.

Primers		Expected Size
C1	Forward: 5'-ATTTGGCCAGACATTGAGAGCTCGGA-3'	472bp
	Reverse: 5'-CCCAAGCTTCACAGCCTCTTCCTTCAGACTA-3'	
C2	Forward: 5'-TATGTGTTGAGCTCACTTTTGTTTTTTTTT-3'	422bp
	Reverse: 5'-CCCAAGCTTGGAGCTGTGGAGTTATT-3'	
C3	Forward: 5'-ACACATACCCGAGCTCCCGAGGGCTG-3'	309bp
	Reverse: 5'-CCCAAGCTTAGGGCAGTGAGGGTTCACTCCA-3'	

After PCR was performed; samples were incubated at 72°C for 10 minutes for “A” tailing of PCR product. PCR products were then subcloned into pCR8/GW/TOPO vector (detailed map was given in Appendix D). TOPO reaction was prepared by adding 4 µL PCR product, 1 µL salt solution 1.2M NaCl 0.06M MgCl₂ and finally adding 1µL TOPO vector and incubating the tubes at 23°C for 20 minutes. After this reaction PCR product was ligated to pCR8/GW/TOPO subcloning vector by T-A annealing and Topoisomerase function as shown in Figure 2.10.

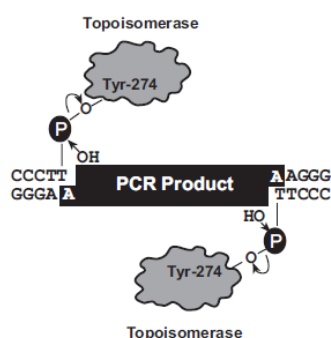


Figure 2.10: TOPO Reaction (pCR8/GW/TOPO TA Cloning Kit manual)

As previously described, ligation product was transformed into *E.coli* DH5 α cells. Positive clones were selected by spectinomycin. First screening was done by colony PCR. Further confirmation was done by double digestion of isolated plasmids with *SacI* (target sequence: 5'-GAGCT/C-3') and *HindIII* (target sequence: 5'-A/AGCTT-3'). Finally by DNA sequencing, constructs were confirmed. After this step, both TOPO vector bearing the insert and empty pMIR vector were double digested with same enzymes at 37°C for overnight as previously described. All digested samples were run on agarose gel. Insert and double digested pMIR vector were extracted from agarose. By adding 3 fold molar excess of insert according to vector were to 1 μ L of T4 DNA ligase buffer, 100ng pMIR vector and 1 unit of T4 DNA ligase, ligation reaction was performed overnight at 16°C with a total volume of 10 μ L. Positive clones were selected by ampicillin. Final confirmation was done by again double digesting pMIR vector with *SacI* and *HindIII* enzymes. Digestion products were run on agarose gel. After this final confirmation, pMIR constructs were ready for transfection into MCF7-125b and MCF7-EV cells.

2.8.2 Transient Transfections of Luciferase Constructs into MCF7 Cells

Transient transfections were done by Lipofectamine 2000 from Invitrogen according to manufacturers' instructions. $\sim 5 \times 10^5$ cells were seeded into 24-well plate. Cells were grown overnight in medium containing serum but no antibiotics. At the time of transfection, cells were 90% confluent. For each well, a total amount of 800ng DNA was used. 3:1 Firefly Luciferase (pMIR) to Renilla Luciferase (phRL-TK) ratio was used. 600ng pMIR vector and 200ng phRL-TK vector was used. Total amount of DNA, 800ng, was diluted with Optimem to have a final volume of 50 μ L. For each well 2 μ L Lipofectamine 2000 was used and it was also diluted with Optimem to have a final volume of 50 μ L. Lipofectamine 2000 and Optimem mix was incubated at RT for 5 minutes. Then, two mixes were combined together. Final mixture was incubated at RT for 20 minutes for DNA-Lipofectamine 2000 complex formation. After 20 minutes, DNA-Lipofectamine 2000 complex was added to each well containing the cells and was mixed gently by rocking the plate back and forth. Then cells were incubated for 48 hours at 37°C, in a 5% CO₂ incubator as suggested by Dual-luciferase Reporter Assay System's (Promega) manual.

2.8.3 Dual Luciferase Assay

In dual-luciferase assay, two vectors bearing two different types of luciferase genes were used; Firefly and Renilla. The differences between these two luciferase enzymes depend on the substrate. Figure 2.11 shows the different enzymatic reaction performed by these two different luciferases.

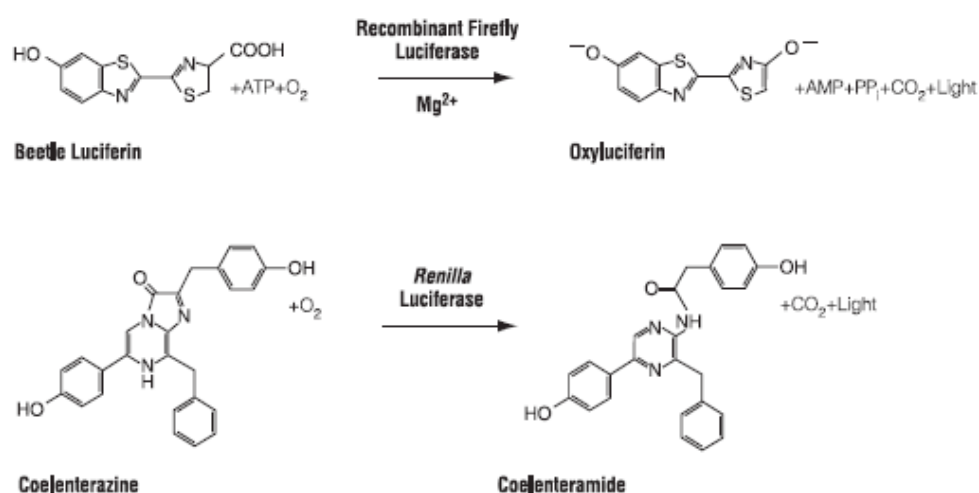


Figure 2.11: Bioluminescent reactions catalyzed by Firefly and *Renilla* luciferases (Dual-Luciferase Reporter Assay System, Promega).

Dual-luciferase assay was performed by Dual-luciferase Reporter Assay System from Promega according to manufacturers' guidelines. Dual-luciferase activities were measured using Modulus Microplate Multimode Reader (Turner Biosystems, USA). Injectors of the microplate reader were primed with LAR II and Stop & Glo Reagents. LAR II is Firefly luciferase substrate and Stop & Glo Reagent stops Firefly luciferase reaction and provides substrate for Renilla luciferase. Injectors 1 and 2 were set to dispense 100 μ L of LAR II and Stop & Glo Reagent, respectively. For measurements, 2 seconds delay and 10 seconds read time was adjusted.

Growth medium was removed and cells were washed with PBS. Cells were lysed by 100µL passive lysis buffer by incubating 15 minutes at RT and by rocking the plate back and forth. After lysis, 20µL from each lysate was transferred to 96-well plates. 100 µL of LAR II was dispensed and Firefly luciferase activity was measured. Then 100 µL of Stop & Glo Reagent was dispensed and Renilla luciferase activity was measured. This cycle was repeated for all samples to get a ratio of Firefly/Renilla.

Four replicates were used for each sample and experiment was performed twice. Data were statistically evaluated by one way ANOVA test using GraphPad Prism Software. In order to find groups whose mean differences were significant, Tukey's multiple comparison tests was carried out and significance level was set to $P < 0.0001$.

2.8.4 Site Directed Mutagenesis

Site directed mutagenesis was performed as previously described [146]. First PCR was performed with mutagenesis primers and a high fidelity polymerase and then digest parental (non-mutated) strands with a restriction enzyme. As *PfuTurbo* DNA polymerase has 6-fold higher fidelity in DNA synthesis than *Taq* DNA polymerase, *PfuTurbo* was used in PCR reaction [147]. Next step is to digest parental, non-mutated, strand with *DpnI*. The *DpnI* endonuclease (Fermentas Cat# ER1702) (target sequence: 5'-Gm6ATC-3') is specific for methylated and hemimethylated DNA and is used to digest the parental, unmethylated DNA template and to select for mutation-containing newly synthesized DNA. Finally, mutated construct was transformed into *E.coli* DH5α cells. After confirmation of mutation was done by sequencing, constructs was used in dual-luciferase assay.

Mutagenesis specific primers were designed by using *Stratagene's* web-based QuikChange Primer Design Program (<http://www.stratagene.com/qcprimerdesign>). Figure 2.12 shows mutagenesis primers. By using these primers, highly conserved binding regions, corresponding to 2102nd - 2108th nucleotides of *ARID3B* mRNA,

218th-224th of *ARID3B* 3'UTR and 74th -80th nucleotides of pMIR-C1 construct, were deleted.

Primer Name	Primer-Template Duplex
del174-80	<pre> 5'-cagacagcgttggtccaa-----ttgtcctggagaactg-3' cctgtctgtcgcaacaggttagtcacctaacaggacctcttgaccca </pre>
del174-80- antisense	<pre> ggacagacagcgttggtccaatcagggattgtcctggagaactgggt 3'-qtctqtcqcaacaqqt-----aacaqqacctcttqac-5' </pre>

Figure 2.12: Mutagenesis specific primers' design by *Stratagene's* web-based QuikChange Primer Design Program. Mutagenesis primers were shown in blue. Nucleotides corresponding to 74th-80th of pMIR-C1 constructs were deleted (sequence corresponding to 218th-224th of *ARID3B* 3'UTR and 2102nd - 2108th nucleotides of *ARID3B* mRNA).

PCR conditions were used as suggested [146]. 5µL of 10x reaction buffer of *PfuTurbo* DNA polymerase supplied with enzyme, 125ng of each deletion specific sense and anti-sense primers, 1µL of dNTP mix (from 2 mM stock dNTP solution), 50ng of dsDNA (pMIR-C1 construct) and 1µL of *PfuTurbo* DNA polymerase (2.5U/µL) was added and the volume was completed to 50µL with sterile dH₂O. Reaction was incubated in the following program given in Table 2.8.

Table 2.8: Site-Directed Mutagenesis PCR Program

Segment	Cycles	Temperature	Time
1	1	95°C	30 seconds
2	18	95°C	30 seconds
		55°C	1 minute
		68°C	10 minutes

Following the completion of the reaction and cooling to 4°C, 10µL of sample was run in agarose gel electrophoresis for confirmation. Remaining PCR product was digested by *DpnI* enzyme. 1µL of the *DpnI* restriction enzyme (10U/µL) was directly added to each amplification reaction. Each reaction mixture was mixed by pipetting the solution up and down several times. Reaction mixtures were spun down in a microcentrifuge for 1 minute and each reaction was immediately incubated at 37°C for 1 hour to digest the parental (the nonmutated) supercoiled dsDNA.

After 1 hour of digestion, samples were transformed into *E.coli* DH5α cells. Positive clones were selected by ampicillin as the vector pMIR contains ampicillin resistance gene. Positive clones were screened by colony PCR. Deletion was confirmed by sequencing the pMIR-C1-MUT construct. Mutated construct was used in dual-luciferase assay.

CHAPTER 3

RESULTS AND DISCUSSION

3.1 Expression Analysis of pre-miR-125a, pre-miR-125b-1 and pre-miR-125b-2 in Breast Cancer Cell Lines

miR-125a, miR-125b-1 and miR-125b-2 are members of the same miRNA family. miR-125b-1 and miR-125b-2 produce the same mature miRNA whereas there is only 3 nucleotides difference between mature miR-125a and mature miR-125b. miR-125a and miR-125b expression were shown to be downregulated in primary breast tumors and breast cancer cell lines [57], [81],[148]. To determine the expression status of miRNA-125 family members in breast cancer cell lines, semi-quantitative duplex RT-PCR, as described previously [142], was performed for pre-miR-125a, pre-miR-125b-1 and pre-miR-125b-2 in 11 breast cancer cell lines and an immortalized non- tumorigenic mammary cell line, MCF10A. *GAPDH* PCR product (115bp) was used as an internal control in each PCR. Densitometry analysis was done after agarose gel electrophoresis of PCR products using Scion Image program (National Institute of Health). Band intensities of miRNA/*GAPDH* were calculated for each cell line and these values were normalized to the values of MCF10A.

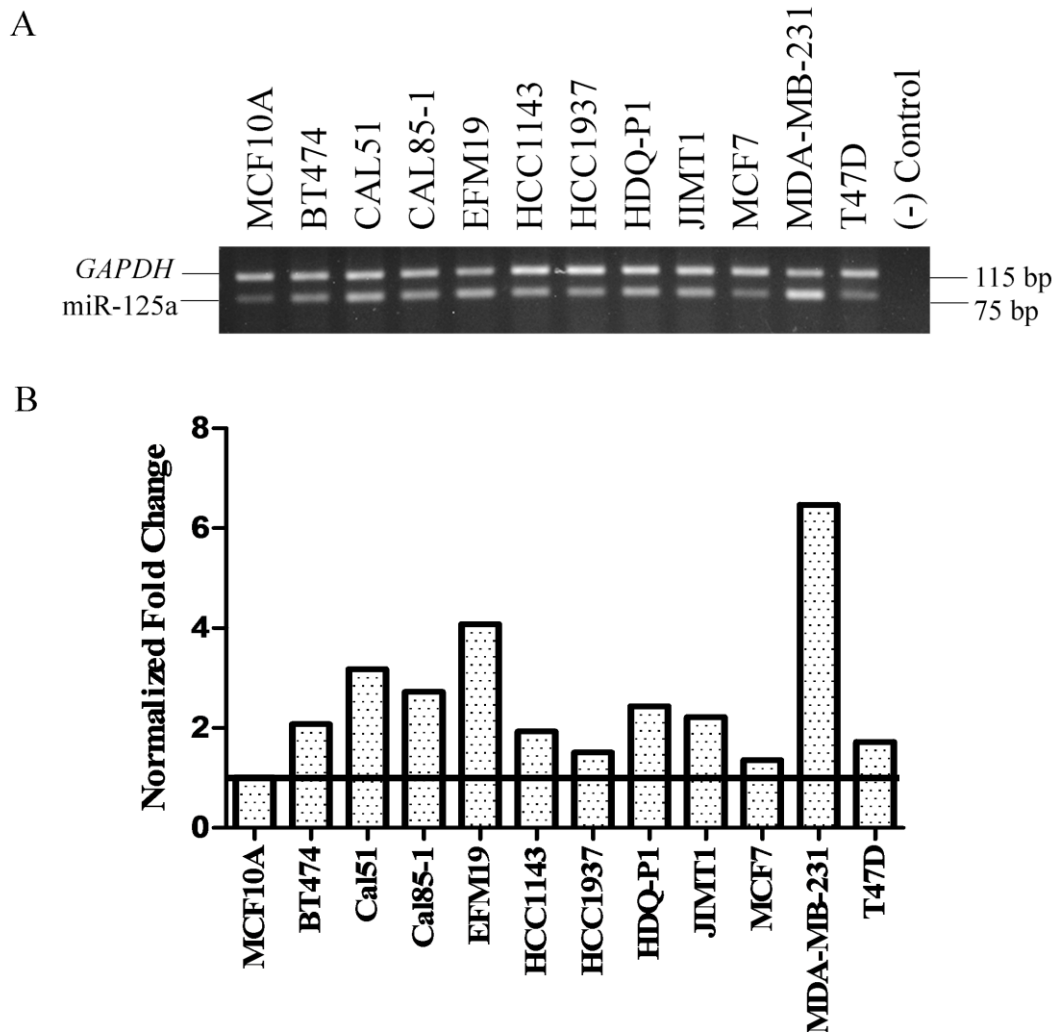


Figure 3.1: pre-miR-125a expression analysis by semi-quantitative duplex RT-PCR. A) 75bp pre-miR-125a and 115bp *GAPDH* PCR products were separated on 2% agarose gel. B) Densitometry results were normalized according to miRNA/*GAPDH* band intensity values of MCF10A. miRNA/*GAPDH* ratio of MCF10A cells was set to 1.

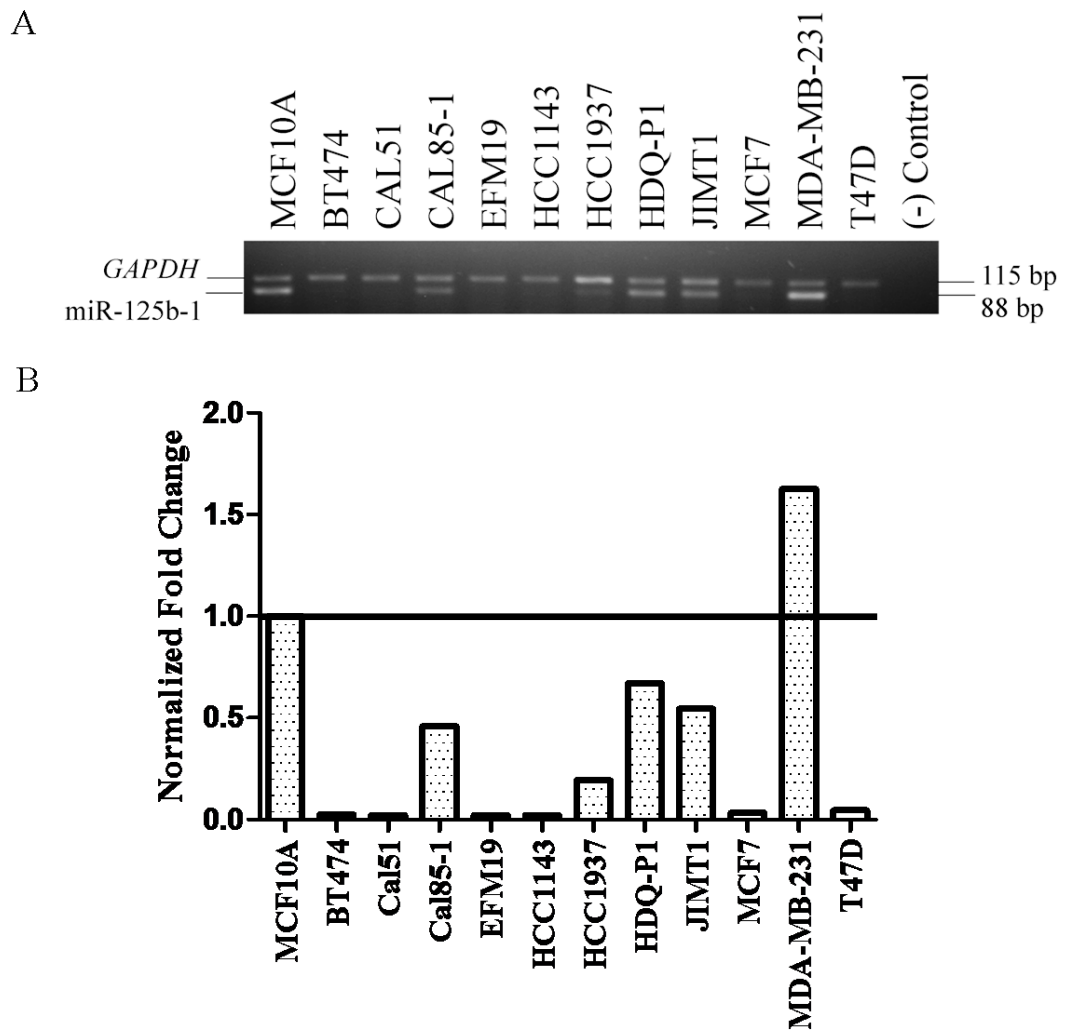


Figure 3.2: pre-miR-125b-2 expression analysis by semi-quantitative duplex RT-PCR. A) 88bp pre-miR-125b-1 and 115bp *GAPDH* PCR products were separated on 2% agarose gel. B) Densitometry results were normalized according to miRNA/*GAPDH* band intensity values of MCF10A. miRNA/*GAPDH* ratio of MCF10A cells was set to 1.

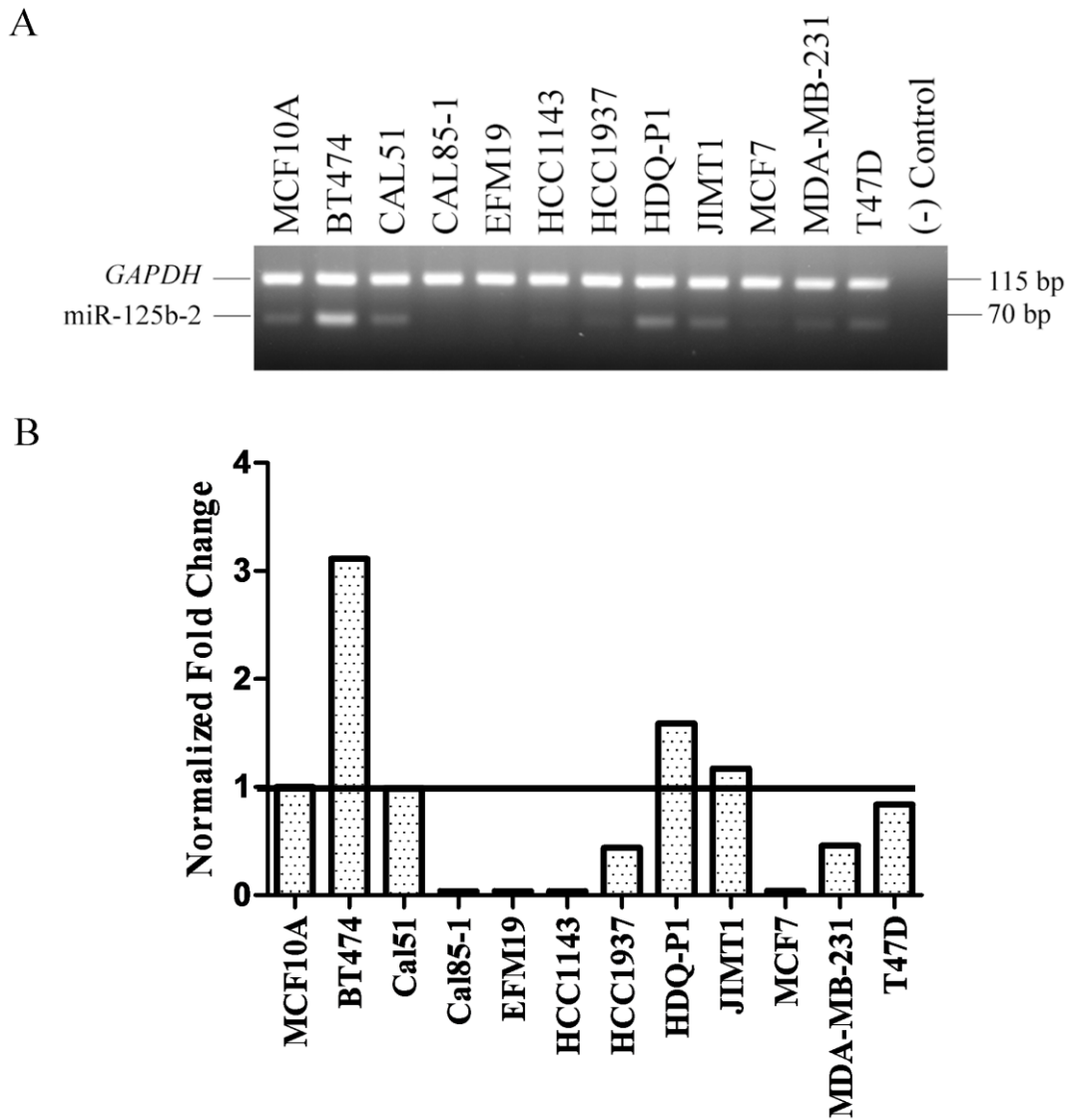


Figure 3.3: pre-miR-125b-2 expression analysis by semi-quantitative duplex RT-PCR. A) 70bp pre-miR-125b-2 and 115bp *GAPDH* PCR products were separated on 2% agarose gel. B) Densitometry results were normalized according to miRNA/*GAPDH* band intensity values of MCF10A. miRNA/*GAPDH* ratio of MCF10A cells was set to 1.

Results in Figure 3.1, 3.2 and 3.3 showed different expression patterns for all three precursor miRNAs. The most significant changes were seen for pre-miR-125b-1 and pre-miR-125b-2. Only for MDA-MB-231 sample, increase in pre-miR-125a transcript level was observed; whereas pre-miR-125b-1 levels were found to be low or absent in 7 of 11 breast cancer cell lines. pre-miR-125b-2 levels were found to be low or absent in almost all cell lines including MCF10A. Although pre-miR-125b-1 and pre-miR-125b-2 produce same mature miRNA, as these two different precursor miRNAs have different genomic locations (miR-125b-1 and miR-125b-2 map to 11q24.1 and 21q21.1, respectively), expression pattern of these miRNAs in breast cancer cell lines might be different.

Decreased expression of miR-125b in breast cancer was also reported in several studies. Microarray analysis of 10 normal and 76 primary breast tumors and Northern blot analysis of 1 normal, 11 human breast carcinomas and 7 breast cancer cell lines indicated decreased miR-125b expression [57]. In another study, miRNA microarray analysis of 79 breast cancer tumors and 6 normal tissues showed decreased miR-125b and miR-125a expression [56].

pre-miR-125b-1 and pre-miR-125b-2 produce the same mature miRNA, miR-125b. We did not detect pre-miR-125b-1 and pre-miR-125b-2 expression in MCF7 cell line (Figure 3.2 and Figure 3.3). Moreover according to Cancer Genome Project (<http://www.sanger.ac.uk/genetics/CGP>), which is an SNP array based LOH and copy number analysis database, pre-miR-125b-1 locus was found in an LOH region in 18 of 45 breast tumors, whereas pre-miR-125b-2 locus was found to be in an LOH region in 12 of 45 breast tumors. Therefore according to above results, to better understand the roles of miR-125b in breast cancer, as one of the frequently downregulated miRNAs in breast cancer, we decided to transfect miR-125b precursor into MCF7 cell line.

3.2 Ectopic Expression of pre-miR-125b-1 in MCF7 Breast Cancer Cell Line

In order to ectopically express miR-125b in MCF7 cells, pSUPER RNAi System was used. pSUPER RNAi system is designed for shRNA (short hairpin RNA) transfections. pSUPER vector produces a transcript that produces substrates for the Dicer enzyme. Both precursor miRNA and shRNA are substrates for Dicer enzyme [149]. For that reason precursor structure of miR-125b-1 was cloned into pSUPER vector.

Sense and antisense oligonucleotides for pre-miR-125b-1 to be cloned into pSUPER.retro.neo +GFP vector were designed according to pSUPER manual. Sense and antisense oligonucleotides were annealed and were cloned into vector. Positive clones were confirmed by restriction digestion and sequencing. Confirmed pSUPER constructs were transfected into MCF7 cells. Integration of construct into MCF7 genome was confirmed by PCR with DNA and ectopic expression of miR-125b was confirmed by RT-PCR with cDNA.

Figure 3.4 shows the result of sequencing and NCBI BLAST (Basic Local Alignment Search Tool) (<http://www.ncbi.nlm.nih.gov/blast/Blast.cgi>) confirmation of cloned pre-miR-125b-1 compared to the pre-miR-125b-1 sequence in miRBase database.

```
>lcl|1179
Length=855

Score = 122 bits (66), Expect = 6e-33
Identities = 66/66 (100%), Gaps = 0/66 (0%)
Strand=Plus/Minus

Query 12  CAGTCCCTGAGACCCCTAACTTGIGATGTTTACCGTTTAAATCCACGGGTAGGCTCTTGG 71
          |||
Sbjct 245  CAGTCCCTGAGACCCCTAACTTGIGATGTTTACCGTTTAAATCCACGGGTAGGCTCTTGG 186

Query 72  GAGCTG 77
          |||
Sbjct 185  GAGCTG 180
```

Figure 3.4: pSUPER-125b-1 BLAST analysis. Highlighted region indicates mature sequence. The remaining region is the cloned pre-miR-125b-1.

After confirmation of constructs by DNA sequencing, pSUPER-125b-1 construct was transfected into MCF7 cell line. In order to establish stably miR-125b expressing cells, cells were selected by 500 μ g/mL G418 antibiotic and were maintained with 250 μ g/mL G418. Integration of vector into MCF7 genome was confirmed by PCR with pSUPER specific sequencing primers. Figure 3.5 shows the confirmation of stable transfection results for pSUPER-125b-1.



Figure 3.5: Genome integration confirmation of pSUPER-125b-1 and pSUPER constructs. M: DNA Ladder; Lane 1, 2 and 3: Polyclones for pSUPER-125b-1 transfection (MCF7-125b-1); Lane 4: polyclonal selection for empty pSUPER(MCF7-EV); Lane 5: Negative control; Lane 6: pSUPER-125b-1 construct as a positive control; Lane 7: empty pSUPER vector, positive control for empty vector transfection.

Empty pSUPER sample gave a longer PCR product due to stuffer region which was excluded from the vector after cloning. Empty pSUPER and pSUPER-125b-1 vector itself were used as positive control. According to Figure 3.5, plasmids were integrated into MCF7 cell line genome in the polyclonal transfectants.

Analysis of ectopic expression of pre-miR-125b-1 from stably transfected cells were done by RT-PCR. Stable polyclone confirmed in the lane 3 of Figure 3.5 was used for expression analysis. Results are shown in Figure 3.6. As 66 bp of pre-miR-125b-1 was cloned into pSUPER vector, a new set of primers (66 bp) were used to confirm the expression.

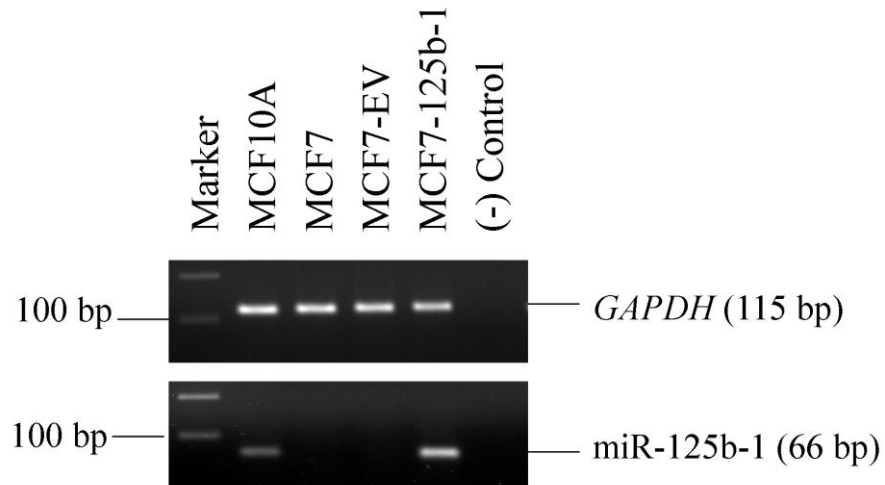


Figure 3.6: Ectopic expression confirmation of miR-125b-1 transfections. 66 bp pre-miR-125b-1 transcript and 115 bp *GAPDH* transcript were run on 2% agarose gel. M: DNA Ladder; Lane 1: MCF10A; Lane 2: Untransfected MCF7; Lane 3: empty pSUPER transfected MCF7 (MCF7-EV); Lane 4: pSUPER-125b-1 transfected MCF7 cells (MCF7-125b-1); Lane 5: Negative control.

MCF10A sample was used as a positive control for miR-125b expression. MCF7-EV cells were empty pSUPER vector transfected cells. Parental MCF7 cells (untransfected) were also included in the RT-PCR. *GAPDH* transcript (115 bp) was also amplified to confirm the quality of cDNA samples. MCF7-125b-1 cells (pre-miR-125b-1 transfected MCF7 cells) were used for functional assays.

3.3 Functional Assays

To better understand the effects of miR-125b-1 expression in MCF7 cells and potential inhibitory roles in breast tumorigenesis, assays related with proliferation and migration was performed with MCF7-125b-1 cells.

3.3.1 Cellular Proliferation Assay

To investigate whether miR-125b-1 expression had an effect on cell proliferation, an MTT assay for MCF7-125b-1 and MCF7-EV cells was performed according to manufacturer's instructions (Roche). MTT test is used for determination of cellular proliferation and viability of cells. In fact, MTT test determines the metabolically active cells. By comparing the metabolic activity, difference in proliferation rate was deduced. The results of MTT assay are shown in Figure 3.7.

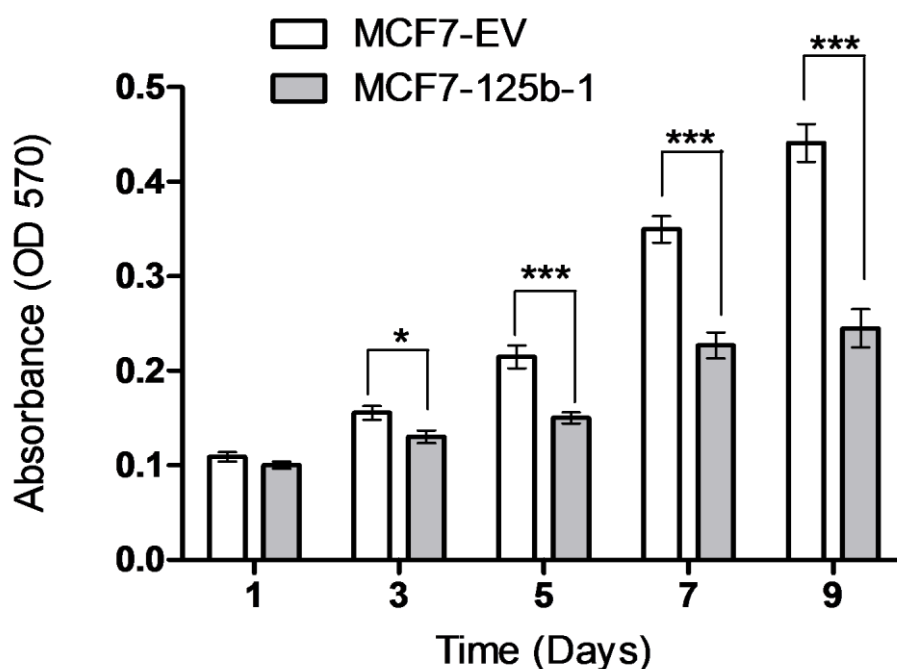


Figure 3.7: MTT assay of miR-125b-1 transfected and empty vector transfected MCF7 cells. Error bars represent the SD of two independent experiments with 10 replicates. One thousand MCF7-125b-1 cells and one thousand MCF7-EV cells were plated in 96-well plates in MEM-Earle's medium to be assayed at 1, 3, 5, 7 and 9 days. At the 9th day, difference in proliferation between MCF7-125b-1 and MCF7-EV was significant (***) $P < 0.0001$.

From the 3rd day, difference in proliferation rate was observed between MCF7-125b-1 and MCF7-EV. MCF7-125b-1 cells had a 45% decrease in the proliferation rate compared to MCF7-EV cells at the end of the 9th day (***P*<0.0001). Similar reduction in proliferation rates after miR-125b transfection has been reported in several studies. In breast cancer cell lines SKBR3 [125], BT-549 [134], and MDA-MB-453 [136], transfection of miR-125b decreased proliferation. Moreover, human glioma cell line (U251) and osteoblastic differentiated cells (ST2) showed similar reduction in proliferation upon miR-125b transfection [122], [120]. We used MCF7-125b and MCF7-EV cells as a model system to further understand the roles of miR-125b expression.

3.3.2 *In vitro* Wound Closure Assay

In vitro wound closure assay is used to investigate directional cell migration *in vitro* [144]. The assay mimics cell migration during wound healing *in vivo* [150]. After cells reached confluency, a wound was introduced by a sterile plastic pipette tip and during wound closure; distances travelled by the cells were tracked until MCF7-EV cells almost closed the wound. 72 hours after wound was introduced, MCF7-EV cells almost closed the gap whereas MCF7-125b-1 cells had a slower rate for wound closure and a decreased travelled distance compared to MCF7-EV cells, as can be seen from Figure 3.8 and Figure 3.9.

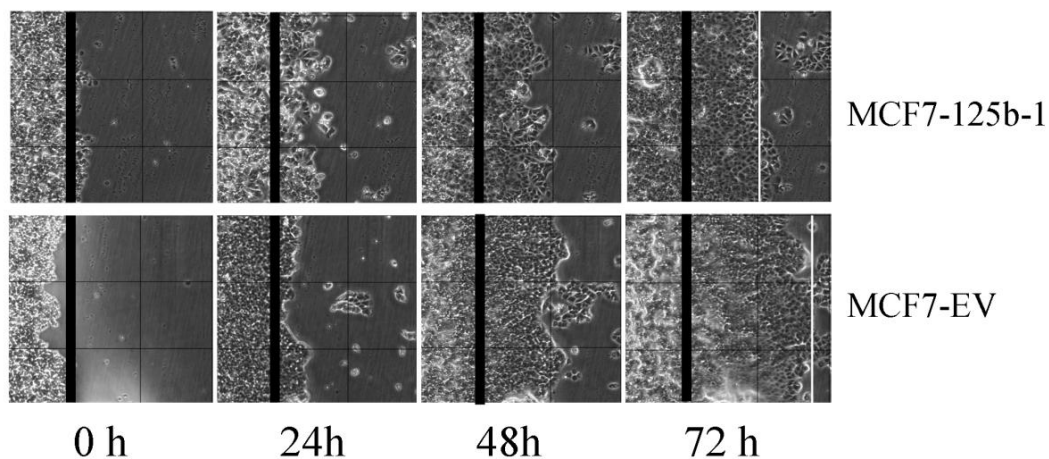


Figure 3.8: Wound healing images of MCF7-125b-1 and MCF7-EV (overall magnification: 40 X). A wound by a sterile pipette tip was introduced to confluent cells on 6-well plate. Distances travelled by the cells were tracked until the gap was closed. Black bars indicate initial wound location. White bars indicate the final location that the cells travelled.

The images were taken every 24 hours using a phase contrast microscope with a 4 X objective (overall magnification: 40 X) until all the gaps were closed by cells. Image analyses were carried out and distances travelled by the cells were calculated by Motic ImagePlus 2.0 software, as a bar graph. Experiment was performed twice with 4 replicates for each sample. Data were statistically evaluated by one way ANOVA test following Mann Whitney test by using GraphPad Prism Software and the mean difference was significant at the 0.0001 level ($P < 0.0001$) as shown in Figure 3.9.

Compared to MCF7-EV cells, miR-125b-1 caused a delayed motility in MCF7-125b-1 cells at 72 hours. By this assay, decrease in migration capacity upon miR-125b-1 transfection was confirmed.

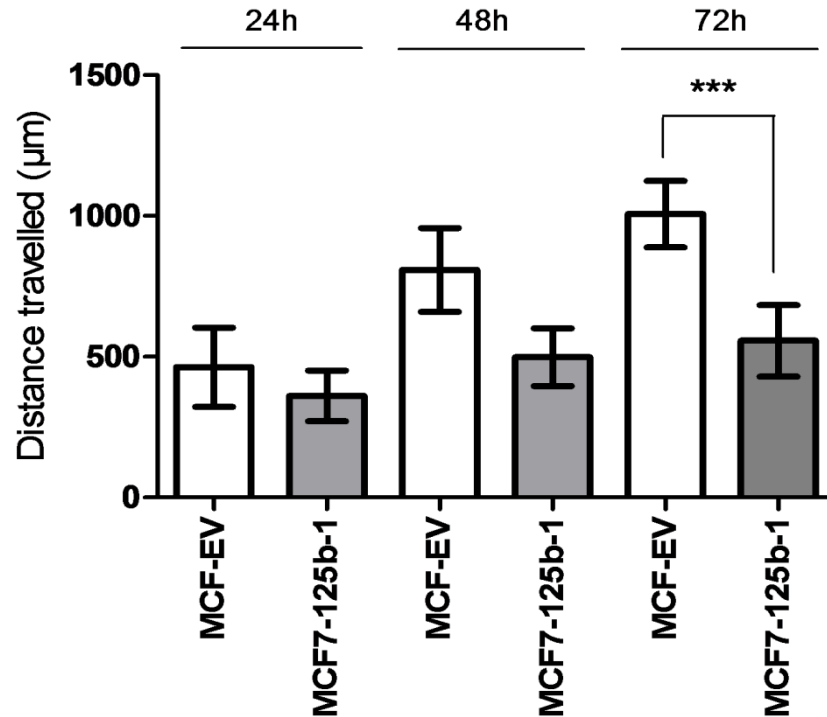


Figure 3.9: Distance travelled by MCF7-125b-1 and MCF7-EV cells. Error bars represent the SD of two independent experiments with 4 replicates. At the 72nd hour, difference in distance travelled by the cells between MCF7-125b-1 and MCF7-EV was significant (***) $P < 0.0001$).

3.3.3 Transwell Migration Assay

Tissue invasion and metastasis are among the hallmarks of cancer according to Hanahan and Weinberg [151]. For tumor metastasis, migration is one of the first steps. Migration capacities of the cells can be compared by a transwell migration assay. MCF7-EV cells were compared with MCF7-125b-1 cells for their difference in migration capacity

Thirty thousand cells were added to transwell inserts containing membranes with 8µm pores. This upper chamber contained medium with 1% FBS whereas 10% FBS in growth medium was present in the bottom chamber, creating a serum concentration gradient. After 72 hours, time which the highest difference was observed in *in vitro* wound closure assay, the membranes were fixed and stained and

the number of cells which moved through the pores in membrane was counted under a Leica light microscope (10 X objective). MCF7-125b-1 cells showed a significant decrease in the number of migrated cells compared to MCF7-EV cells. Figure 3.10 shows the differences in the number of migrated cells.

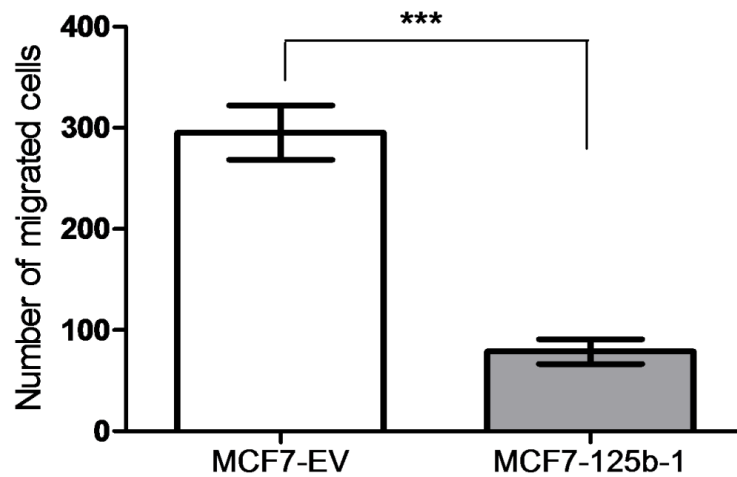


Figure 3.10: Transwell migration assay of MCF7-125b-1 and MCF7-EV cells. The bar diagram represents the number of cells that migrated through the Transwell in MCF7-EV and MCF7-125b-1 cells at 72 hours. (***) $P < 0.0001$). The experiment was carried out with 4 replicates for each sample.

Representative membrane images for MCF7-EV and MCF7-125b-1 are given in Figure 3.11.

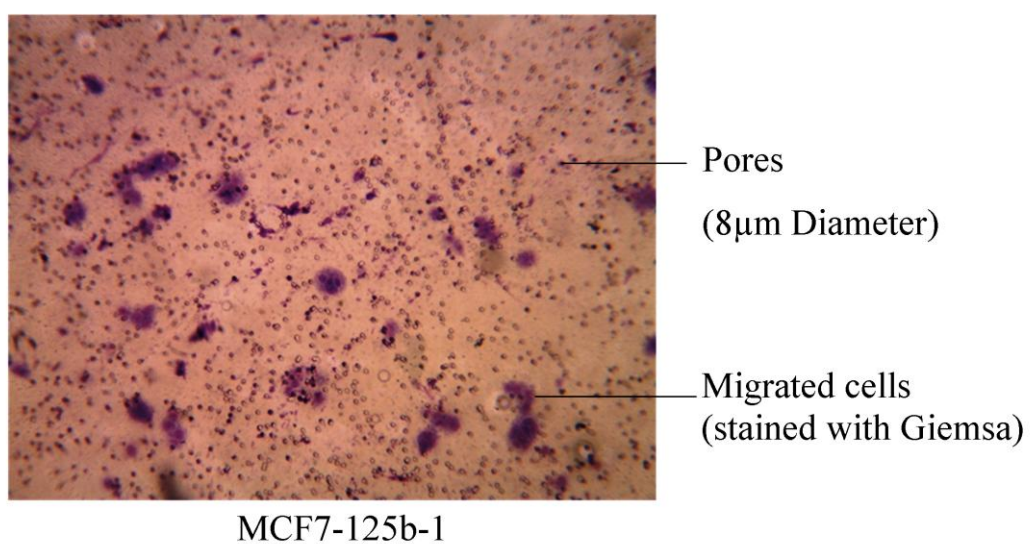
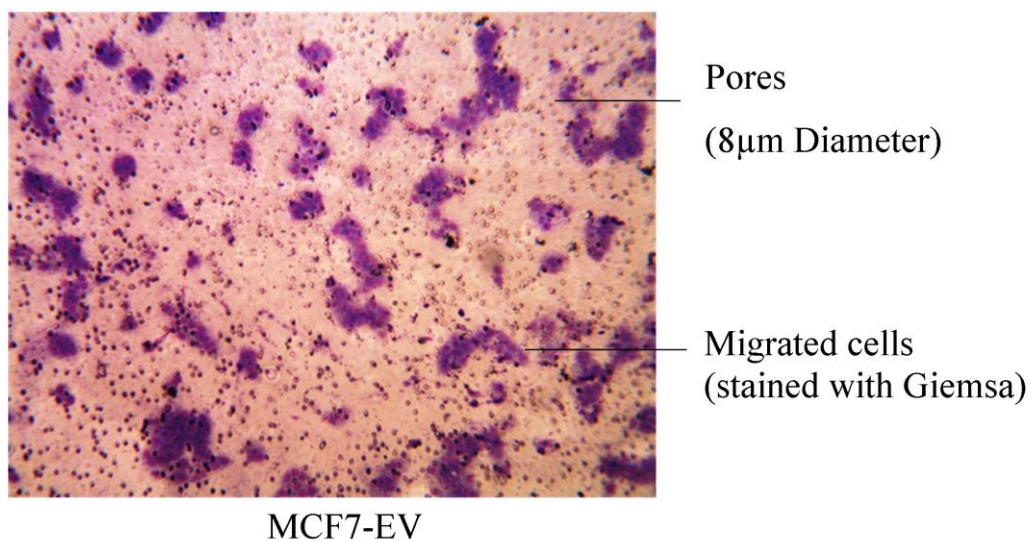


Figure 3.11: Representative figures of MCF7-EV and MCF7-125b-1 cells migrated through membrane.

Through three different functional assays, inhibitory effects of miR-125b-1 expression in MCF7 breast cancer cells were determined. Upon stable transfection of pre-miR-125b-1, MCF7 cells reduced proliferation rate. These cells also had reduced migration and motility capacities, identified by *in vitro* wound closure assay and transwell migration assays.

3.4 Target Search for hsa-miR-125b

A single miRNA can potentially target several mRNAs [40]. To identify miRNA targets, bioinformatic tools are used for target predictions. There are several target prediction programs available online. Each prediction tool uses a different algorithm based on sequence conservation, site accessibility or combination of both. Our main criterion for choosing a target gene was that target was predicted by all four programs. *ARID3B* was found to be predicted by TargetScan, microRNA.org, PicTar and PITA with high scores.

3.4.1 TargetScan

TargetScan, version 5.1 (<http://www.targetscan.org/>) [39], [37], [40], predicts miRNA targets by searching conserved seed sequences. Seed sequences are classified according to the seed length; 8mer or 7mer. All predictions are given a score according to the site numbers in the target mRNA, site types and site contexts which also affect target UTR-miRNA binding. The site-type contribution reflects the average contribution of each site type. The 3' pairing contribution reflects target UTR-miRNA binding outside the seed region. The local AU content reflects the transcript's AU content in a region of 30 nucleotides upstream and downstream of predicted site. The position contribution reflects the distance of binding sequence to the nearest end of the annotated UTR of the target gene. The context score is the sum of the contribution of these four features. In short, a more negative score is associated with a more favorable site. Figure 3.12 shows TargetScan prediction for a miR-125b target: *ARID3B*. TargetScan program predicts 3 conserved and 3 poorly conserved miR-125b binding sites in the *ARID3B* 3'UTR.

3.4.3 PicTar

PicTar (<http://pictar.bio.nyu.edu/>) [42], prediction program uses statistical tests using genome-wide alignments of eight vertebrate genomes. By this way program predicts targets according to conservation among vertebrates as well as free energies of miR binding to target UTR. Figure 3.14 shows PicTar prediction for miR-125b target: *ARID3B*. PicTar program predicts totally 6 binding sites for miR-125b in *ARID3B* 3'UTR.

Rank <small>Click here for detailed 3'utr alignments and location of predicted site.</small>	human Refseq Id	All miRNAs predicted to target the gene	PicTar score	microRNAs with Anchor sites	annotation		
1	NM_006465	All miRNA predictions	15.15	hsa-miR-125b	Homo sapiens AT rich interactive domain 3B (BRIGHT-like) (<i>ARID3B</i>), mRNA.		

Org	PicTar score	PicTar score per species	microRNA	Probabilities	Nuclei mapped to alignments	Nuclei mapped to sequence	Free Energies kcal/mol
hs	15.15	20.42	hsa-miR-125b	0.97 0.96 0.96 0.97 0.96 0.96	312 389 712 1371 1559 2202	218 295 575 1173 1333 1907	-21.8 -18.6 -24.8 -27.2 -20.3 -21.3

Figure 3.14: PicTar prediction for miR-125b-*ARID3B* interaction.

3.4.4 PITA

PITA prediction program combines several properties of other programs (http://genie.weizmann.ac.il/pubs/mir07/mir07_data.html [43]). It predicts miRNA targets according to sequence complementarity of target mRNA and miRNA. Furthermore, it also gives score for conservation among species. Finally, the most important feature of the program is that program computes miRNA-target interaction thermodynamically according to the difference between the free energy gained from the formation of the miRNA-target duplex and the energetic cost of unpairing the target to make it accessible to the miRNA. Figure 3.15 shows PITA prediction for miR-125b target: *ARID3B*. PITA program predicts totally 8 binding sites for miR-125b in *ARID3B* 3'UTR.

Gene Name	microRNA	Position	Seed	dGduplex	dGopen	ddG	Conservation	Name	Chromosome	Start	End	Strand
ARID3B	hsa-miR-125b	302	7:0:0	-17.06	-7.85	-9.2	0.12	ARID3B hsa-miR-125b 5	15	72675463	72675469	+
ARID3B	hsa-miR-125b	1179	7:0:0	-20.4	-11.77	-8.62	0.99	ARID3B hsa-miR-125b 1	15	72676340	72676346	+
ARID3B	hsa-miR-125b	582	7:0:0	-19.72	-13.13	-6.58	0.003	ARID3B hsa-miR-125b 6	15	72675743	72675749	+
ARID3B	hsa-miR-125b	224	6:0:0	-17.81	-11.54	-6.26	1	ARID3B hsa-miR-125b 4	15	72675386	72675391	+
ARID3B	hsa-miR-125b	1340	7:0:0	-15.25	-10.96	-4.28	0	ARID3B hsa-miR-125b 2	15	72676501	72676507	+
ARID3B	hsa-miR-125b	1914	8:0:0	-16.2	-12.59	-3.6	0.97	ARID3B hsa-miR-125b 3	15	72677074	72677081	+
ARID3B	hsa-miR-125b	683	7:0:1	-18.36	-15.6	-2.75	0	ARID3B hsa-miR-125b 8	15	72675844	72675850	+
ARID3B	hsa-miR-125b	637	6:0:0	-19	-20.94	1.94	0.00016	ARID3B hsa-miR-125b 7	15	72675799	72675804	+

Figure 3.15: PITA prediction for miR-125b-*ARID3B* interaction

Table 3.1 summarizes predictions by four programs for miR-125b - *ARID3B* 3'UTR. For TargetScan and PITA predictions, more negative scores suggest stronger targets. A positive score predicted by PicTar indicates more likely to be a target. No comparison among predicted targets can be made for microRNA.org predictions. It just gives alignment scores for individual bindings.

In short, *ARID3B* gene was predicted as a target of miR-125b by all four programs with high scores even with different algorithms.

Table 3.1: miR-125b target prediction scores for *ARID3B* 3'UTR.

	Score	Binding Sites	Prediction based on
TargetScan	-0.51	3 conserved	Conservation among species
		3 poorly conserved	Seed binding
microRNA.org	-	2	Sequence similarity
PicTar	15.15	6	Genome-wide conservation
			Sequence similarity
PITA	-9.72	8	Conservation among species
			Seed binding
			Site Accessibility

3.5 Analysis of *ARID3B* 3'UTR and miR-125b Interaction

According to 4 prediction programs, *ARID3B* (AT rich interactive domain 3B (BRIGHT-like)) was selected as a putative target for miR-125b. In a recent study, miR-125a was shown to target *ARID3B* and cause a decrease in protein level shown by Western blotting in ovarian cancer cells [141]. As miR-125a and miR-125b have the same seed sequence, *ARID3B* 3'UTR was investigated as a potential miR-125b target in breast cancer cell line. Two widely used programs, TargetScan and PITA, usually have consistent predictions. Due to this reason, regions to be analyzed were determined according to these programs. TargetScan predicts a total number of 6 binding sites on the *ARID3B* 3'UTR for miR-125b and PITA predicted a total number of 8 binding sites. Last 2 binding sites listed in Figure 3.15 (Position 683 and 637) were omitted as the $\Delta \Delta G$ values for these sites were too low and as these sites were not predicted by TargetScan. Figure 3.16 shows the borders of regions to be analyzed and the binding sites predicted by two programs.

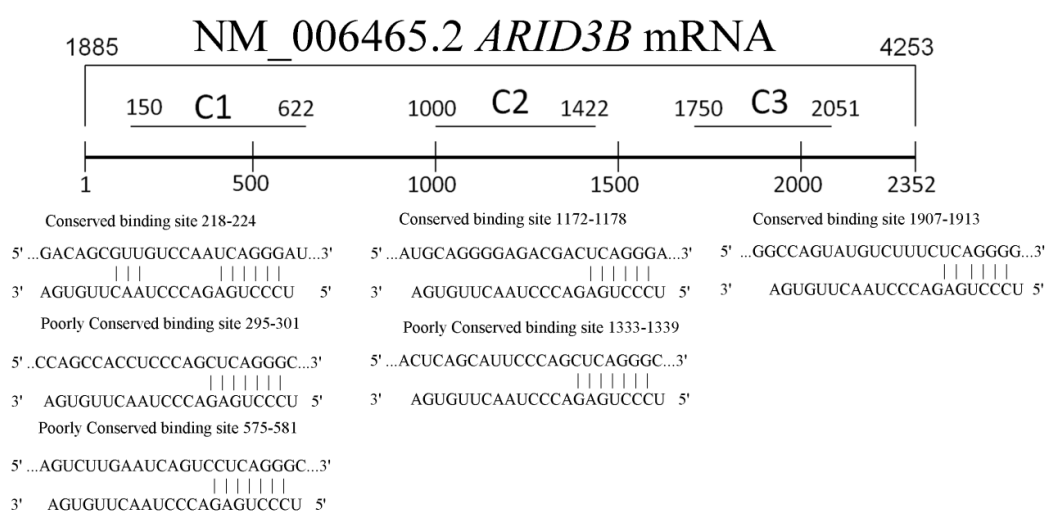


Figure 3.16: Alignment of *ARID3B* 3'UTR and the predicted miR-125b binding sites. 3 conserved and 3 poorly conserved miR-125b binding sites were predicted (by TargetScan and PITA) between the 1885th and 4237th bases of the *ARID3B* mRNA.

Three different regions were selected for analysis as shown in Figure 3.16. C1 region contains 1 conserved (218th-224th) and 2 poorly conserved binding sites (295th-301st and 575th-581st). C2 region contains 1 conserved (1172nd-1178th) and 1 poorly conserved binding site (1333th-1339th). C3 region contains 1 conserved (1907th-1913th) binding sites. All these regions were amplified by PCR, and cloned into pMIR Luciferase Reporter Vector for further analysis by dual-luciferase.

As described in Materials and Methods, primers with *HindIII* and *SacI* restriction enzymes recognition sites were used for PCR amplification of *ARID3B* 3'UTR using genomic DNA as a template. Regions were first cloned into TOPO subcloning vector. After confirmation of regions by sequencing (Figure 3.17 shows BLAST analysis of sequenced region), inserts were then cloned into pMIR vector. Further confirmations of regions were done by double digesting with *SacI* and *HindIII* and colony PCR.

```

A. >lcl|51501
Length=485

Score = 893 bits (483), Expect = 0.0
Identities = 483/483 (100%), Gaps = 0/483 (0%)
Strand=Plus/Minus

Query 51  AAGCTTCACAGCCTCTTCCTTCAGACTGTTAGAAGGGGGATCTGGGGCCCTGAGGACTGA 110
Sbjct 485  AAGCTTCACAGCCTCTTCCTTCAGACTGTTAGAAGGGGGATCTGGGGCCCTGAGGACTGA 426

Query 111  TTCAGACTTGTGTTTGGGGACCCGTACCCAGGAACCTAACAGTAGGCAAGTGGGCT 170
Sbjct 425  TTCAGACTTGTGTTTGGGGACCCGTACCCAGGAACCTAACAGTAGGCAAGTGGGCT 366

Query 171  GGAAGGGCCCCATCCCATGCTCTGCAGAGAAGGGCATGAAGGCATGCTCTTGGCTCCTGG 230
Sbjct 365  GGAAGGGCCCCATCCCATGCTCTGCAGAGAAGGGCATGAAGGCATGCTCTTGGCTCCTGG 306

Query 231  CAGCCCCACATGGGACTTAAAAACAGGGGAGAGACTAGTGGCCCTGGGGTCATGGCAGA 290
Sbjct 305  CAGCCCCACATGGGACTTAAAAACAGGGGAGAGACTAGTGGCCCTGGGGTCATGGCAGA 246

Query 291  AGGCAGGGTCAGGGAATAAATAAAGGGGAGGGAATGGAGGGCCTCCAGCCCTGGGT 350
Sbjct 245  AGGCAGGGTCAGGGAATAAATAAAGGGGAGGGAATGGAGGGCCTCCAGCCCTGGGT 186

Query 351  CGCTGACAGATTGTCGATACACTGTGCCCTGAGCTGGAGTGGCTGGGGAACCTGGA 410
Sbjct 185  CGCTGACAGATTGTCGATACACTGTGCCCTGAGCTGGAGTGGCTGGGGAACCTGGA 126

Query 411  GGAAGCTGGACACCCACAGACCCCAACCCAGTCTCCAGGACAATCCCTGATTGGACAC 470
Sbjct 125  GGAAGCTGGACACCCACAGACCCCAACCCAGTCTCCAGGACAATCCCTGATTGGACAC 66

Query 471  GCTGCTGTCTCTGCCCTCTAGCCTCTCCCTGCCCCAGAGTACAGCAGGACCTGAATGG 530
Sbjct 65  GCTGCTGTCTCTGCCCTCTAGCCTCTCCCTGCCCCAGAGTACAGCAGGACCTGAATGG 6

Query 531  AGC 533
Sbjct 5  AGC 3

B. >lcl|10265
Length=433

Score = 771 bits (417), Expect = 0.0
Identities = 417/417 (100%), Gaps = 0/417 (0%)
Strand=Plus/Minus

Query 107  AAGCTTGGAGCTGTGGAGTATTTCATCTCCTCATACCTGGGGCGGCTCAACCTCTGGCA 166
Sbjct 433  AAGCTTGGAGCTGTGGAGTATTTCATCTCCTCATACCTGGGGCGGCTCAACCTCTGGCA 374

Query 167  AGGCCAGCGAGGACCCAGCCTGCCTGTGCCCTGAGCTGGGAATGCTGAGTGGGGAG 226
Sbjct 373  AGGCCAGCGAGGACCCAGCCTGCCTGTGCCCTGAGCTGGGAATGCTGAGTGGGGAG 314

Query 227  GTGTCTCTGCCCTCCCTGGTCAGCTGGGGGTGGGGGTGGGCAAAAACGGTCTCTCAGAA 286
Sbjct 313  GTGTCTCTGCCCTCCCTGGTCAGCTGGGGGTGGGGGTGGGCAAAAACGGTCTCTCAGAA 254

Query 287  CTGGTACAGTTTCAGGGCCGACCCGGTGTGAGAGCGGGCCTCTCCACTCCACCTCCCGG 346
Sbjct 253  CTGGTACAGTTTCAGGGCCGACCCGGTGTGAGAGCGGGCCTCTCCACTCCACCTCCCGG 194

Query 347  CCCCOCGATCCCTGAGTCTCTCCCTGCAATGCCTCCACCCACTCTCTCACTGGGCTTG 406
Sbjct 193  CCCCOCGATCCCTGAGTCTCTCCCTGCAATGCCTCCACCCACTCTCTCACTGGGCTTG 134

Query 407  AGGGAAGGGCCAGAGGGCCGGGTACCCAATCACTTGGCTTGGGCTTGGGGTGTATCTGT 466
Sbjct 133  AGGGAAGGGCCAGAGGGCCGGGTACCCAATCACTTGGCTTGGGCTTGGGGTGTATCTGT 74

Query 467  TTTCATTTCTTTGGTGTACGATaaaaattttaaaatgaaaaaaaaaaaaaGTGAGC 523
Sbjct 73  TTTCATTTCTTTGGTGTACGATAAAAATTTTAAATGAAAAAARCAAAAGTGTGAGC 17

C. >lcl|61395
Length=313

Score = 568 bits (307), Expect = 2e-166
Identities = 307/307 (100%), Gaps = 0/307 (0%)
Strand=Plus/Minus

Query 53  AAGCTTAGGGCAGTGGGGTTCACCTCCTTACGGTGTGGCCAGGGAGCTGCCTGGGAAA 112
Sbjct 313  AAGCTTAGGGCAGTGGGGTTCACCTCCTTACGGTGTGGCCAGGGAGCTGCCTGGGAAA 254

Query 113  GGGAGAGGATCCAATGACCGGAAAGACACAGTGTGCTTTCCTGCACTCCTCTGGGTGGGA 172
Sbjct 253  GGGAGAGGATCCAATGACCGGAAAGACACAGTGTGCTTTCCTGCACTCCTCTGGGTGGGA 194

Query 173  AGAGTCCATCCTTTGTGACCAAAACCCCTGAGAAAGACATACTGGCCAAATGCTGAGACA 232
Sbjct 193  AGAGTCCATCCTTTGTGACCAAAACCCCTGAGAAAGACATACTGGCCAAATGCTGAGACA 134

Query 233  CCTTCAAATGGGCCAGTGCACCCCACTGGGCTCCTCACTGGCACCAGTCCCAATGTC 292
Sbjct 133  CCTTCAAATGGGCCAGTGCACCCCACTGGGCTCCTCACTGGCACCAGTCCCAATGTC 74

Query 293  CCTTCTCTGCCACACCCCTGACGGCTGAGGCCAGGAGGTCAGCCCTCCGGAGCTCGGG 352
Sbjct 73  CCTTCTCTGCCACACCCCTGACGGCTGAGGCCAGGAGGTCAGCCCTCCGGAGCTCGGG 14

Query 353  TAATGT 359
Sbjct 13  TAATGT 7

```

Figure 3.17: BLAST analysis of sequencing results for three different constructs. A) 472 bp C1 region B) 422 bp C2 region C) 300 bp C3 region. All sequences were blasted with *ARID3B* mRNA sequence (Accession number: NM_006465_2).

All constructs were confirmed by both colony PCR and double digestion with *SacI* and *HindIII*. Correct colonies were picked for further experiments. Screened colonies gave positive results for both colony PCR and double digestion. After confirmation of correct sequences of selected regions in pMIR vector by sequencing, constructs were used in dual-luciferase assay. Figure 3.18 shows results for double digestion and colony PCR.

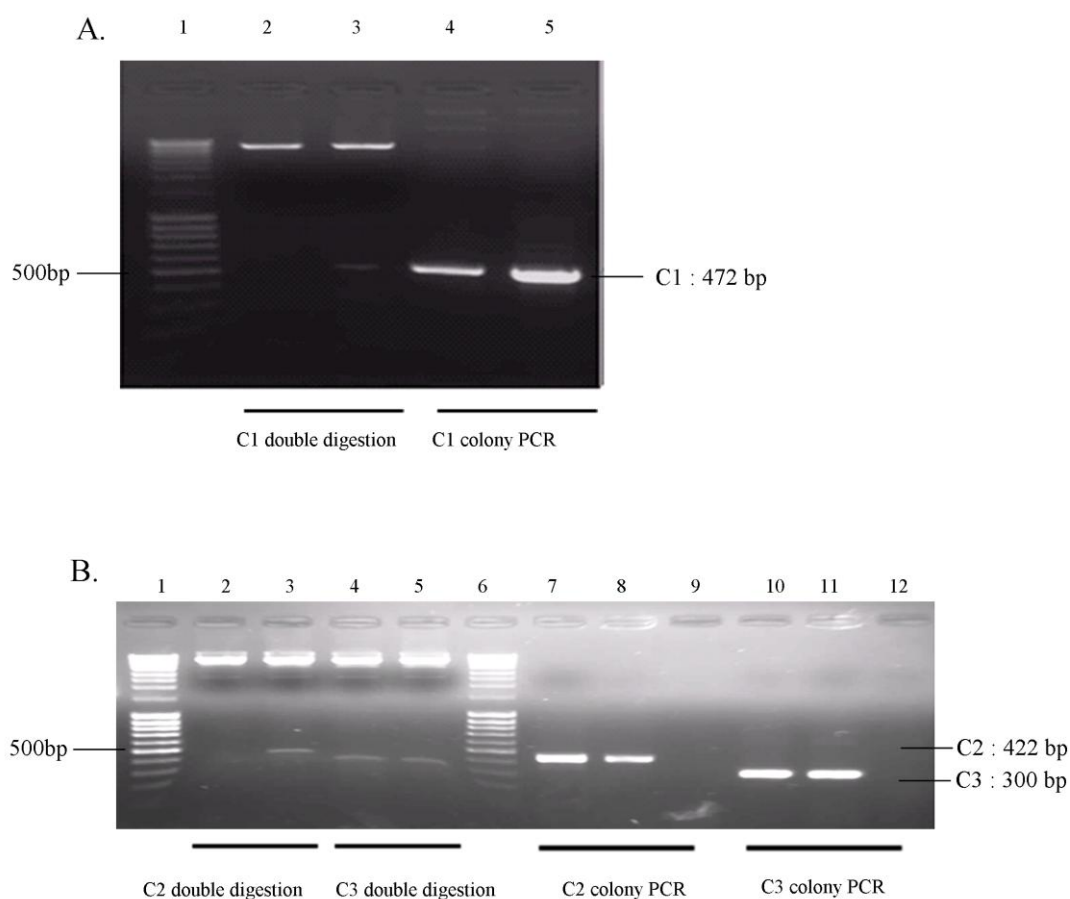


Figure 3.18: Double digestion and colony PCR results. A) 472 bp C1 insert confirmation: Lane 1: DNA ladder; Lane 2 and 3: double digestion of 2 different colonies of C1; Lane 4: colony PCR of 2 different colonies of C1. B) 422 bp C2 insert and 300 bp C3 insert confirmations: Lane 1: DNA ladder; Lane 2 and 3: double digestion of 2 different colonies of C2; Lane 4 and 5: double digestion of 2 different colonies of C3; Lane 6: DNA ladder; Lane 7 and 8: colony PCR of 2 different colonies of C2; Lane 9: Negative control; Lane 10 and 11: colony PCR of 2 different colonies of C3; Lane 12: Negative control.

Luciferase assay had been widely used for determination of miRNA-mRNA interaction [152]. Interest of UTR is cloned downstream of luciferase gene. If miRNA interacts with this cloned UTR then, decrease in luciferase activity is observed. This is the main idea how luciferase assay is used for detection of miRNA-mRNA interaction.

Firefly Luciferase vector pMIR and Renilla Luciferase vector phRL-TK were used during transfection. Renilla Luciferase vector phRL-TK was used as a transfection normalizer. For dual-luciferase experiments, both MCF7-EV and MCF7-125b-1 cells were transfected with empty pMIR, C1, C2 and C3 constructs.

Dual-luciferase assay was done by co-transfecting pMIR and phRL-TK vectors in 3:1 ratio (800ng vector in total). 600 ng for all pMIR constructs and 200 ng phRL-TK vectors were used. 2 μ L Lipofectamine 2000 and plasmids were diluted in Optimem to have a final volume of 100 μ L. 48 hours after transfections, cells were lysed and luciferase assays were performed. Figure 3.19 shows the results of dual-luciferase assay with all three constructs; C1, C2 and C3 with empty pMIR vector in MCF7-EV and MCF7-125b-1 cells. Normalization of the samples was done by co-transfecting all the constructs with pMIR and phRL-TK Renilla Luciferase vectors.

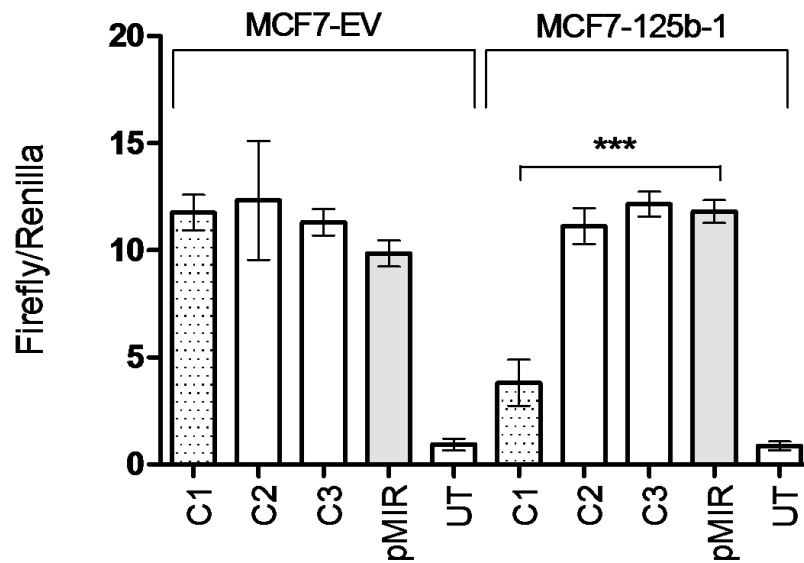


Figure 3.19: Interaction of miR-125b with *ARID3B* 3' UTR constructs. MCF7-EV and MCF7-125b-1 cells were co-transfected with pMIR (C1,C2,C3 constructs and empty pMIR) and phRL-TK vectors. 48 hours after transfection, luciferase activities were measured. UT stands for untransfected cells. Transfection efficiencies were normalized by Renilla luciferase. Data shown is a result of two independent experiments with a total of 8 replicates. Data were analysed by one way ANOVA followed by Tukey's multiple Comparison test. *** indicates statistical significance ($P < 0.0001$).

According to these results, for MCF7-EV samples, there were no significant changes in Luciferase activity among all constructs, including empty pMIR vector. When MCF7-125b-1 samples were considered, only C1 construct showed a significant reduction in luciferase activity due to miR-125b-1 expression. C1 construct showed ~60% decrease in luciferase activity compared to empty pMIR transfected samples. There were no significant differences between C2, C3 and empty pMIR transfected cells. Since there was only a reduction in luciferase activity in C1 construct transfected MCF7-125b-1 cells, it was suggestive that expression of miR-125b in MCF7-125b-1 cells was causing a decrease in the C1-mRNA translation.

In order to confirm the direct binding of miR-125b to *ARID3B* 3'UTR in C1, one conserved seed binding site was selected to be deleted by site-directed mutagenesis. C1 region contained 1 conserved (218th-224th) and 2 poorly conserved binding sites (295th-301st and 575th-581st). Among these sites, conserved binding site had more score points according to TargetScan prediction program. For that reason, in order to confirm that the decrease in luciferase activity was directly caused by miR-125b-1 transfection, 218th-224th sites were deleted by site directed mutagenesis as previously described [146].

For site directed mutagenesis, with mutagenesis primers and *PfuTurbo* DNA polymerase, PCR was performed. Details of mutagenesis primers and PCR for site directed mutagenesis are given in Figure 2.12 and Table. 2.7. Figure 3.20 shows the results for site-directed mutagenesis PCR.

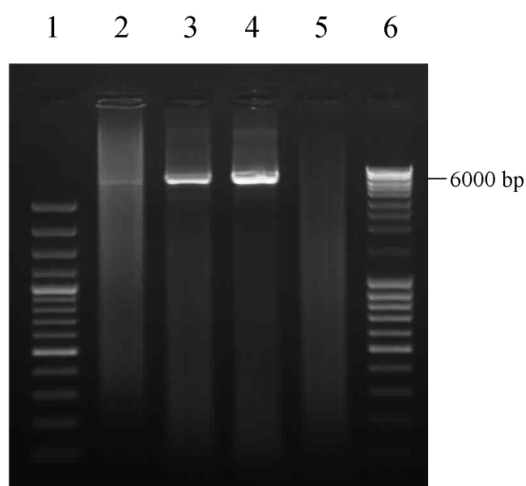


Figure 3.20: Mutagenesis specific PCR results. Lane 1: 100 bp DNA ladder; Lane 2: 10 ng template DNA; Lane 3: 25 ng template DNA; Lane 4: 50 ng template DNA; Lane 5: Negative control; Lane 6: Mass Ruler DNA Ladder. Expected size is 6.4 kb; the size of pMIR vector.

After PCR, samples were digested by *DpnI* enzyme. By this digestion, parental methylated strand was digested. Remaining strand contained the non-methylated, mutation bearing sequence. Deletion was confirmed through DNA sequencing. Figure 3.21 shows the BLAST analysis of mutated construct, C1-MUT.

```

>lcl|3917
Length=485

Score = 845 bits (936), Expect = 0.0
Identities = 478/485 (98%), Gaps = 7/485 (1%)
Strand=Plus/Plus

Query 763 GAGCTCCATT CAGGTCCTGCTG TACTCTGGGGGCAGGGAGAGGCTAGAGGGGCAGGACAG 822
          |||
Sbjct 1 GAGCTCCATT CAGGTCCTGCTG TACTCTGGGGGCAGGGAGAGGCTAGAGGGGCAGGACAG 60

Query 823 ACAGCGTTGTCCAAT-----TGTCTGGAGAACTGGGTGGGGGTCTGTGGGTGTCCAG 875
          |||
Sbjct 61 ACAGCGTTGTCCAATCAGGGATTGCTCTGGAGAACTGGGTGGGGGTCTGTGGGTGTCCAG 120

Query 876 CTTCTCCAGGGTTCCCCAGCCACCTCCCAGCTCAGGGCACAGTGTATCGACAATCTGTC 935
          |||
Sbjct 121 CTTCTCCAGGGTTCCCCAGCCACCTCCCAGCTCAGGGCACAGTGTATCGACAATCTGTC 180

Query 936 AGCCGACGCAGGGCTGGAGGCCCTCCATTTCCCTCCCTTTTAAATTTATTTCCCTGACCC 995
          |||
Sbjct 181 AGCCGACGCAGGGCTGGAGGCCCTCCATTTCCCTCCCTTTTAAATTTATTTCCCTGACCC 240

Query 996 TGCCTTCTGCCATGACCCAGGGCCACTAGTCTCTTCCCCTGTTTTAAGTCCCATGTGG 1055
          |||
Sbjct 241 TGCCTTCTGCCATGACCCAGGGCCACTAGTCTCTTCCCCTGTTTTAAGTCCCATGTGG 300

Query 1056 GGCTGCCAGGAGCCAAGAGCATGCCCTTCATGCCCTTCTCTGCAGAGCATGGGATGGGGCC 1115
          |||
Sbjct 301 GGCTGCCAGGAGCCAAGAGCATGCCCTTCATGCCCTTCTCTGCAGAGCATGGGATGGGGCC 360

Query 1116 CTTCCAGCCCACTTTGCCTACTGTTAGGTTCTGGGGTACGGGTCCCTCAAACACAAGTC 1175
          |||
Sbjct 361 CTTCCAGCCCACTTTGCCTACTGTTAGGTTCTGGGGTACGGGTCCCTCAAACACAAGTC 420

Query 1176 TTGAATCAGTCCTCAGGGCCCCAGATCCCCCTTCTAACAGTCTGAAGGAAGAGGCTGTGA 1235
          |||
Sbjct 421 TTGAATCAGTCCTCAGGGCCCCAGATCCCCCTTCTAACAGTCTGAAGGAAGAGGCTGTGA 480

Query 1236 AGCTT 1240
          |||
Sbjct 481 AGCTT 485

```

Figure 3.21: BLAST analysis of sequencing result for C1-MUT construct. 5' – CAGGGAT – 3' sequence, 218th-224th nucleotides of *ARID3B* 3'UTR, was deleted from C1 construct.

Sequence confirmed MUT-C1 construct together with C1, pMIR and phRL-TK vectors were transiently transfected into MCF7-EV and MCF7-125b-1 cells. Normalization of the samples was done by co-transfecting all the constructs in pMIR with phRL-TK Renilla Luciferase vector. Transfection was done in 3:1 pMIR to phRL-TK ratio. 2 μ L Lipofectamine 2000, 600 ng pMIR vector; C1-MUT, C1 and empty pMIR, 200ng phRL-TK vector were diluted in Optimem in a final volume of 100 μ L. 48 hours after transfection, cells were lysed and dual-luciferase assay was performed. Figure 3.22 showed the results of dual-luciferase assay.

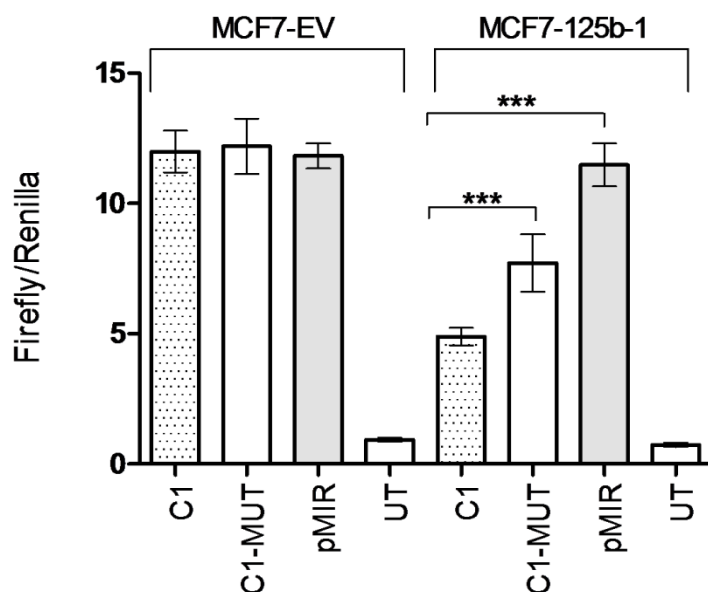


Figure 3.22: Interaction of miR-125b with *ARID3B* 3' UTR C1 and C1-MUT constructs. MCF7-EV and MCF7-125b-1 cells were co-transfected with pMIR (C1, C1-MUT constructs and empty pMIR) and phRL-TK vectors. 48 hours after transfection, luciferase activities were measured. UT stands for either untransfected MCF7-EV cells or untransfected MCF7-125b-1 cells. Transfection efficiencies were normalized by Renilla luciferase. Data shown is a result of two independent experiments with a total of 8 replicates. Data were analyzed by one way ANOVA followed by Tukey's multiple Comparison test. *** indicates statistical significance ($P < 0.0001$).

As can be seen from the Figure 3.22, there was an increase in C1-MUT compared to C1 construct in MCF7-125b-1 cells. ~30% recovery of the low luciferase activity of C1 construct was observed in C1-MUT construct compared to pMIR in MCF7-125b-1 cells. As expected, no significant difference was detected in MCF7-EV cells. These results indicated that the decrease in Luciferase activity directly was caused by miR-125b-1.

Having said that, luciferase activity was still lower in C1-MUT transfected cells compared to empty pMIR. This may be due to other miR-125b binding sites in the C1 construct of *ARID3B* 3' UTR. There were two poorly conserved miR-125b binding sites in C1 construct (295th-301st and 575th-581st). Conserved binding site

was selected for site directed mutagenesis as it had higher score compared to two poorly conserved sites according to TargetScan. Nevertheless, when results were considered, these sites may also have an effect on miRNA binding (according to results in Figure 3.23). These sites have more negative $\Delta \Delta G$ values compared to mutated site, according to PITA prediction program, indicating that these sites in target 3'UTR are more accessible to miRNA binding, although these prediction sites were not evolutionarily conserved.

CHAPTER 4

CONCLUSION

miRNAs are small non-coding RNA molecules that regulate gene expression post-transcriptionally. They have important roles in almost all aspects of cancer biology such as proliferation, apoptosis, invasion/metastasis, and angiogenesis. To identify the roles of miRNAs by confirming the interaction between miRNAs and tumor suppressors-oncogenes in cancer will elucidate cancer progression.

The objective of this study was to identify the roles of miR-125 in breast cancer tumorigenesis. For this purpose, miR-125 family members' expressions were investigated in 11 breast cancer cell lines. pre-miR-125b-1 levels were found to be low or absent in 7 of 11 breast cancer cell lines. miR-125b expression was restored in MCF7 cells and functional assays were performed to better understand the roles of miR-125b in breast cancer tumorigenesis. Ectopic expression of miR-125b in MCF7 cells caused 45% decrease in the proliferation rate at the 9th day. *In vitro* wound healing assay and transwell migration assay confirmed the decreased wound closure and migration capacities of MCF7 cells upon miR-125b expression. 3 fold decreased in migration capacities and 55% decreased in distance travelled by the cells upon wound introduction were observed. All these findings indicate that miR-125b acts as a tumor suppressor in breast cancer cell line.

To better understand the functions of miR-125b in cancer, targets of miR-125b were bioinformatically searched. One predicted target of miR-125b, *ARID3B*, was further investigated for the interaction between its 3'UTR and miR-125b. *ARID3B* was selected as it was predicted by four different predictions program with high scores. Furthermore, there were publications about *ARID3B* that the protein acts as an oncogene. Members of the ARID family have roles in cell cycle control,

embryonic patterning, cell lineage gene regulation, transcriptional regulation and possibly in chromatin structure modification. Moreover, *ARID3B* protein was shown to have homologous domains with two proteins that bind to the retinoblastoma gene product. It associates with the retinoblastoma gene product and was predicted to regulate retinoblastoma gene product negatively. *ARID3B* protein has roles in the development of embryonic mesenchymal cells. *ARID3B* also induces the malignant transformation of embryonic fibroblast cells and was associated with malignant neuroblastoma. Together with these findings and miRNA target predictions, *ARID3B* 3'UTR was partially cloned in 3 constructs for further investigation by dual luciferase assay to confirm the interaction between *ARID3B* and miR-125b. Dual luciferase assay confirmed the interaction between miR-125b and *ARID3B* 3'UTR in one of the construct, C1, by showing ~60% decrease in luciferase activity. To further confirm direct interaction, binding site in C1 construct was deleted by site directed mutagenesis. Mutagenesis resulted in ~30% recovery in luciferase activity indicating additional binding sites in C1 construct other than the deleted site.

Future studies are needed to understand the other targets of mir-125b and the roles of miR-125b in pathways that regulate cell proliferation, migration and others that may play roles during tumorigenesis. Mature miRNA levels will be screened with an increased number of breast cancer cell lines by quantitative real-time PCR (qRT-PCR). For morphological changes after stable miR-125b transfection, different functional assays will be performed such as hanging drop assay for determination of changes in aggregation properties, 3D on top assay to determine the changes in shape and structure of cells on 3D culture. For determination of miR-125b effect on *ARID3B*, protein levels of this gene will be screened in breast cancer cell lines. Moreover, to decide that the functional changes caused by miR-125 expression were related with decreased *ARID3B*, silencing of *ARID3B* will be done by short hairpin RNA (shRNA) and the functional assays will be repeated. Moreover, other predicted targets will be screened and will be tested by dual luciferase assay. One putative target to be checked is *HOXB7*, which is an oncogene overexpressed in breast cancer samples. Together with studies presented in this study and these planned future work, roles of miR-125b in breast cancer tumorigenesis will be more identified.

REFERENCES

1. Lee, R.C., R.L. Feinbaum, and V. Ambros, *The C. elegans heterochronic gene lin-4 encodes small RNAs with antisense complementarity to lin-14*. Cell, 1993. **75**(5): p. 843-54.
2. Lagos-Quintana, M., et al., *Identification of novel genes coding for small expressed RNAs*. Science, 2001. **294**(5543): p. 853-8.
3. Llave, C., et al., *Endogenous and silencing-associated small RNAs in plants*. Plant Cell, 2002. **14**(7): p. 1605-19.
4. Elbashir, S.M., W. Lendeckel, and T. Tuschl, *RNA interference is mediated by 21- and 22-nucleotide RNAs*. Genes Dev, 2001. **15**(2): p. 188-200.
5. Pfeffer, S., et al., *Identification of virus-encoded microRNAs*. Science, 2004. **304**(5671): p. 734-6.
6. Lagos-Quintana, M., et al., *New microRNAs from mouse and human*. RNA, 2003. **9**(2): p. 175-9.
7. Pasquinelli, A.E., et al., *Expression of the 22 nucleotide let-7 heterochronic RNA throughout the Metazoa: a role in life history evolution?* Evol Dev, 2003. **5**(4): p. 372-8.
8. Floyd, S.K. and J.L. Bowman, *Gene regulation: ancient microRNA target sequences in plants*. Nature, 2004. **428**(6982): p. 485-6.
9. Lee, Y., et al., *MicroRNA genes are transcribed by RNA polymerase II*. EMBO J, 2004. **23**(20): p. 4051-60.

10. Borchert, G.M., W. Lanier, and B.L. Davidson, *RNA polymerase III transcribes human microRNAs*. Nat Struct Mol Biol, 2006. **13**(12): p. 1097-101.
11. Lee, Y., et al., *The nuclear RNase III Drosha initiates microRNA processing*. Nature, 2003. **425**(6956): p. 415-9.
12. Gregory RI, Y.K., Amuthan G, Chendrimada T, Doratotaj B, Cooch N, Shiekhattar R., *The Microprocessor complex mediates the genesis of...* [Nature. 2004] - PubMed result. Nature, 2004. **11**(432): p. 235-40.
13. Kim, V.N., *MicroRNA biogenesis: coordinated cropping and dicing*. Nat Rev Mol Cell Biol, 2005. **6**(5): p. 376-85.
14. Lund, E., et al., *Nuclear export of microRNA precursors*. Science, 2004. **303**(5654): p. 95-8.
15. Hutvagner, G., et al., *A cellular function for the RNA-interference enzyme Dicer in the maturation of the let-7 small temporal RNA*. Science, 2001. **293**(5531): p. 834-8.
16. Cullen, B.R., *Transcription and processing of human microRNA precursors*. Mol Cell, 2004. **16**(6): p. 861-5.
17. Zhang, H., et al., *Single processing center models for human Dicer and bacterial RNase III*. Cell, 2004. **118**(1): p. 57-68.
18. Wiemer, E., *The role of microRNAs in cancer: no small matter*. Eur J Cancer, 2007. **43**(10): p. 1529-44.
19. Rana, T.M., *Illuminating the silence: understanding the structure and function of small RNAs*. Nat Rev Mol Cell Biol, 2007. **8**(1): p. 23-36.

20. Schwarz, D.S., et al., *Asymmetry in the assembly of the RNAi enzyme complex*. Cell, 2003. **115**(2): p. 199-208.
21. Matranga, C., et al., *Passenger-strand cleavage facilitates assembly of siRNA into Ago2-containing RNAi enzyme complexes*. Cell, 2005. **123**(4): p. 607-20.
22. Ro, S., et al., *Tissue-dependent paired expression of miRNAs*. Nucleic Acids Res, 2007. **35**(17): p. 5944-53.
23. He, L. and G.J. Hannon, *MicroRNAs: small RNAs with a big role in gene regulation*. Nat Rev Genet, 2004. **5**(7): p. 522-31.
24. Rodriguez, A., et al., *Identification of mammalian microRNA host genes and transcription units*. Genome Res, 2004. **14**(10A): p. 1902-10.
25. Lee, Y., et al., *MicroRNA maturation: stepwise processing and subcellular localization*. EMBO J, 2002. **21**(17): p. 4663-70.
26. Lin, S.L., J.D. Miller, and S.Y. Ying, *Intronic microRNA (miRNA)*. J Biomed Biotechnol, 2006. **2006**(4): p. 26818.
27. Ruby, J.G., C.H. Jan, and D.P. Bartel, *Intronic microRNA precursors that bypass Drosha processing*. Nature, 2007. **448**(7149): p. 83-86.
28. Bartel, D.P., *MicroRNAs: genomics, biogenesis, mechanism, and function*. Cell, 2004. **116**(2): p. 281-97.
29. Doench, J. and P. Sharp, *Specificity of microRNA target selection in translational repression*. Genes Dev, 2004. **18**(5): p. 504-11.
30. Lytle, J., T. Yario, and J. Steitz, *Target mRNAs are repressed as efficiently by microRNA-binding sites in the 5' UTR as in the 3' UTR*. Proc Natl Acad Sci U S A, 2007. **104**(23): p. 9667-72.

31. Millar, A.A. and P.M. Waterhouse, *Plant and animal microRNAs: similarities and differences*. *Funct Integr Genomics*, 2005. **5**(3): p. 129-35.
32. Yu, Z., T. Raabe, and N.B. Hecht, *MicroRNA Mirn122a reduces expression of the posttranscriptionally regulated germ cell transition protein 2 (Tnp2) messenger RNA (mRNA) by mRNA cleavage*. *Biol Reprod*, 2005. **73**(3): p. 427-33.
33. Moss, E.G., *MicroRNAs: hidden in the genome*. *Curr Biol*, 2002. **12**(4): p. R138-40.
34. Wu, L., J. Fan, and J.G. Belasco, *MicroRNAs direct rapid deadenylation of mRNA*. *Proc Natl Acad Sci U S A*, 2006. **103**(11): p. 4034-9.
35. Chen, C.-Y.A., et al., *Ago-TNRC6 triggers microRNA-mediated decay by promoting two deadenylation steps*. *Nat Struct Mol Biol*, 2009. **16**(11): p. 1160-1166.
36. Bartel, D.P., *MicroRNAs: target recognition and regulatory functions*. *Cell*, 2009. **136**(2): p. 215-33.
37. Grimson, A., et al., *MicroRNA targeting specificity in mammals: determinants beyond seed pairing*. *Mol Cell*, 2007. **27**(1): p. 91-105.
38. Nielsen, C.B., et al., *Determinants of targeting by endogenous and exogenous microRNAs and siRNAs*. *RNA*, 2007. **13**(11): p. 1894-910.
39. Lewis, B.P., C.B. Burge, and D.P. Bartel, *Conserved seed pairing, often flanked by adenosines, indicates that thousands of human genes are microRNA targets*. *Cell*, 2005. **120**(1): p. 15-20.
40. Friedman, R.C., et al., *Most mammalian mRNAs are conserved targets of microRNAs*. *Genome Res*, 2009. **19**(1): p. 92-105.

41. Betel, D., et al., *The microRNA.org resource: targets and expression*. Nucleic Acids Res, 2008. **36**(Database issue): p. D149-53.
42. Krek, A., et al., *Combinatorial microRNA target predictions*. Nat Genet, 2005. **37**(5): p. 495-500.
43. Kertesz, M., et al., *The role of site accessibility in microRNA target recognition*. Nat Genet, 2007. **39**(10): p. 1278-84.
44. Calin, G.A., et al., *Frequent deletions and down-regulation of micro- RNA genes miR15 and miR16 at 13q14 in chronic lymphocytic leukemia*. Proc Natl Acad Sci U S A, 2002. **99**(24): p. 15524-9.
45. Cimmino, A., et al., *miR-15 and miR-16 induce apoptosis by targeting BCL2*. Proc Natl Acad Sci U S A, 2005. **102**(39): p. 13944-9.
46. Calin, G.A., et al., *Human microRNA genes are frequently located at fragile sites and genomic regions involved in cancers*. Proc Natl Acad Sci U S A, 2004. **101**(9): p. 2999-3004.
47. Lagana, A., et al., *Variability in the incidence of miRNAs and genes in fragile sites and the role of repeats and CpG islands in the distribution of genetic material*. PLoS One, 2010. **5**(6): p. e11166.
48. Sempere, L., et al., *Expression profiling of mammalian microRNAs uncovers a subset of brain-expressed microRNAs with possible roles in murine and human neuronal differentiation*. Genome Biol, 2004. **5**(3): p. R13.
49. Ambros, V., *microRNAs: tiny regulators with great potential*. Cell, 2001. **107**(7): p. 823-6.
50. Lim, L.P., et al., *Vertebrate microRNA genes*. Science, 2003. **299**(5612): p. 1540.

51. Liu, C.G., et al., *An oligonucleotide microchip for genome-wide microRNA profiling in human and mouse tissues*. Proc Natl Acad Sci U S A, 2004. **101**(26): p. 9740-4.
52. Nelson, P.T., et al., *Microarray-based, high-throughput gene expression profiling of microRNAs*. Nat Methods, 2004. **1**(2): p. 155-61.
53. Babak, T., et al., *Probing microRNAs with microarrays: tissue specificity and functional inference*. RNA, 2004. **10**(11): p. 1813-9.
54. Lu, J., et al., *MicroRNA expression profiles classify human cancers*. Nature, 2005. **435**(7043): p. 834-8.
55. Jay, C., et al., *miRNA profiling for diagnosis and prognosis of human cancer*. DNA Cell Biol, 2007. **26**(5): p. 293-300.
56. Volinia, S., et al., *A microRNA expression signature of human solid tumors defines cancer gene targets*. Proc Natl Acad Sci U S A, 2006. **103**(7): p. 2257-61.
57. Iorio, M., et al., *MicroRNA gene expression deregulation in human breast cancer*. Cancer Res, 2005. **65**(16): p. 7065-70.
58. Yanaihara, N., et al., *Unique microRNA molecular profiles in lung cancer diagnosis and prognosis*. Cancer Cell, 2006. **9**(3): p. 189-98.
59. Iorio, M.V., et al., *MicroRNA signatures in human ovarian cancer*. Cancer Res, 2007. **67**(18): p. 8699-707.
60. Calin, G.A., et al., *A MicroRNA signature associated with prognosis and progression in chronic lymphocytic leukemia*. N Engl J Med, 2005. **353**(17): p. 1793-801.

61. Lee, Y.S. and A. Dutta, *MicroRNAs in cancer*. *Annu Rev Pathol*, 2009. **4**: p. 199-227.
62. Lehmann, U., et al., [*Epigenetic inactivation of microRNA genes in mammary carcinoma*]. *Verh Dtsch Ges Pathol*, 2007. **91**: p. 214-20.
63. Lehmann, U., et al., *Epigenetic inactivation of microRNA gene hsa-mir-9-1 in human breast cancer*. *J Pathol*, 2008. **214**(1): p. 17-24.
64. Lujambio, A. and M. Esteller, *CpG island hypermethylation of tumor suppressor microRNAs in human cancer*. *Cell Cycle*, 2007. **6**(12): p. 1455-9.
65. Scott, G.K., et al., *Rapid alteration of microRNA levels by histone deacetylase inhibition*. *Cancer Res*, 2006. **66**(3): p. 1277-81.
66. Bommer, G., et al., *p53-mediated activation of miRNA34 candidate tumor-suppressor genes*. *Curr Biol*, 2007. **17**(15): p. 1298-307.
67. Dews, M., et al., *Augmentation of tumor angiogenesis by a Myc-activated microRNA cluster*. *Nat Genet*, 2006. **38**(9): p. 1060-5.
68. Esquela-Kerscher, A. and F.J. Slack, *Oncomirs - microRNAs with a role in cancer*. *Nat Rev Cancer*, 2006. **6**(4): p. 259-69.
69. Johnson, S.M., et al., *RAS is regulated by the let-7 microRNA family*. *Cell*, 2005. **120**(5): p. 635-47.
70. Johnson, C., et al., *The let-7 microRNA represses cell proliferation pathways in human cells*. *Cancer Res*, 2007. **67**(16): p. 7713-22.
71. Shell, S., et al., *Let-7 expression defines two differentiation stages of cancer*. *Proc Natl Acad Sci U S A*, 2007. **104**(27): p. 11400-5.

72. Lee, Y.S. and A. Dutta, *The tumor suppressor microRNA let-7 represses the HMGA2 oncogene*. Genes Dev, 2007. **21**(9): p. 1025-30.
73. Shah, Y.M., et al., *Peroxisome proliferator-activated receptor alpha regulates a microRNA-mediated signaling cascade responsible for hepatocellular proliferation*. Mol Cell Biol, 2007. **27**(12): p. 4238-47.
74. Tian, S., et al., *MicroRNA-1285 inhibits the expression of p53 by directly targeting its 3' untranslated region*. Biochem Biophys Res Commun, 2010. **396**(2): p. 435-9.
75. Hu, W., et al., *Negative regulation of tumor suppressor p53 by microRNA miR-504*. Mol Cell, 2010. **38**(5): p. 689-99.
76. Le, M., et al., *MicroRNA-125b is a novel negative regulator of p53*. Genes Dev, 2009. **23**(7): p. 862-76.
77. Zhang, Y., et al., *MicroRNA 125a and its regulation of the p53 tumor suppressor gene*. FEBS Lett, 2009. **583**(22): p. 3725-30.
78. He, X., L. He, and G.J. Hannon, *The guardian's little helper: microRNAs in the p53 tumor suppressor network*. Cancer Res, 2007. **67**(23): p. 11099-101.
79. Merkel, O., et al., *Interdependent regulation of p53 and miR-34a in chronic lymphocytic leukemia*. Cell Cycle, 2010. **9**(14): p. 2764-8.
80. Luan, S., L. Sun, and F. Huang, *MicroRNA-34a: a novel tumor suppressor in p53-mutant glioma cell line U251*. Arch Med Res, 2010. **41**(2): p. 67-74.
81. Mattie, M.D., et al., *Optimized high-throughput microRNA expression profiling provides novel biomarker assessment of clinical prostate and breast cancer biopsies*. Mol Cancer, 2006. **5**: p. 24.

82. Klinge, C.M., *Estrogen Regulation of MicroRNA Expression*. Curr Genomics, 2009. **10**(3): p. 169-83.
83. Lowery, A.J., et al., *MicroRNA signatures predict oestrogen receptor, progesterone receptor and HER2/neu receptor status in breast cancer*. Breast Cancer Res, 2009. **11**(3): p. R27.
84. Selcuklu, S.D., M.T. Donoghue, and C. Spillane, *miR-21 as a key regulator of oncogenic processes*. Biochem Soc Trans, 2009. **37**(Pt 4): p. 918-25.
85. Si, M., et al., *miR-21-mediated tumor growth*. Oncogene, 2007. **26**(19): p. 2799-803.
86. Zhu, S., et al., *MicroRNA-21 targets tumor suppressor genes in invasion and metastasis*. Cell Res, 2008. **18**(3): p. 350-9.
87. Qian, B., et al., *High miR-21 expression in breast cancer associated with poor disease-free survival in early stage disease and high TGF-beta1*. Breast Cancer Res Treat, 2009. **117**(1): p. 131-40.
88. Meng, F., et al., *MicroRNA-21 regulates expression of the PTEN tumor suppressor gene in human hepatocellular cancer*. Gastroenterology, 2007. **133**(2): p. 647-58.
89. Asangani, I., et al., *MicroRNA-21 (miR-21) post-transcriptionally downregulates tumor suppressor Pcd4 and stimulates invasion, intravasation and metastasis in colorectal cancer*. Oncogene, 2008. **27**(15): p. 2128-36.
90. Löffler, D., et al., *Interleukin-6 dependent survival of multiple myeloma cells involves the Stat3-mediated induction of microRNA-21 through a highly conserved enhancer*. Blood, 2007. **110**(4): p. 1330-3.

91. Cheng, A., et al., *Antisense inhibition of human miRNAs and indications for an involvement of miRNA in cell growth and apoptosis*. *Nucleic Acids Res*, 2005. **33**(4): p. 1290-7.
92. Sathyan, P., H. Golden, and R. Miranda, *Competing interactions between micro-RNAs determine neural progenitor survival and proliferation after ethanol exposure: evidence from an ex vivo model of the fetal cerebral cortical neuroepithelium*. *J Neurosci*, 2007. **27**(32): p. 8546-57.
93. Chan, J.A., A.M. Krichevsky, and K.S. Kosik, *MicroRNA-21 is an antiapoptotic factor in human glioblastoma cells*. *Cancer Res*, 2005. **65**(14): p. 6029-33.
94. Zhao, Y., et al., *Let-7 family miRNAs regulate estrogen receptor alpha signaling in estrogen receptor positive breast cancer*. *Breast Cancer Res Treat*, 2010.
95. Ma, L., et al., *Therapeutic silencing of miR-10b inhibits metastasis in a mouse mammary tumor model*. *Nat Biotechnol*, 2010. **28**(4): p. 341-7.
96. Moriarty, C.H., B. Pursell, and A.M. Mercurio, *miR-10b targets Tiam1: implications for Rac activation and carcinoma migration*. *J Biol Chem*, 2010. **285**(27): p. 20541-6.
97. Zhang, X., et al., *Oncogenic Wip1 Phosphatase is Inhibited by miR-16 in the DNA Damage Signaling Pathway*. *Cancer Res*, 2010.
98. Li, H., et al., *miR-17-5p promotes human breast cancer cell migration and invasion through suppression of HBPI*. *Breast Cancer Res Treat*, 2010.
99. Yu, Z., et al., *microRNA 17/20 inhibits cellular invasion and tumor metastasis in breast cancer by heterotypic signaling*. *Proc Natl Acad Sci U S A*, 2010. **107**(18): p. 8231-6.

100. Cascio, S., et al., *miR-20b modulates VEGF expression by targeting HIF-1 alpha and STAT3 in MCF-7 breast cancer cells*. J Cell Physiol, 2010. **224**(1): p. 242-9.
101. Al-Nakhle, H., et al., *Estrogen receptor {beta}1 expression is regulated by miR-92 in breast cancer*. Cancer Res, 2010. **70**(11): p. 4778-84.
102. Kong, W., et al., *MicroRNA-155 regulates cell survival, growth, and chemosensitivity by targeting FOXO3a in breast cancer*. J Biol Chem, 2010. **285**(23): p. 17869-79.
103. Jiang, S., et al., *MicroRNA-155 functions as an OncomiR in breast cancer by targeting the suppressor of cytokine signaling 1 gene*. Cancer Res, 2010. **70**(8): p. 3119-27.
104. Imam, J.S., et al., *MicroRNA-185 suppresses tumor growth and progression by targeting the Six1 oncogene in human cancers*. Oncogene, 2010.
105. Uhlmann, S., et al., *miR-200bc/429 cluster targets PLCgamma1 and differentially regulates proliferation and EGF-driven invasion than miR-200a/141 in breast cancer*. Oncogene, 2010. **29**(30): p. 4297-306.
106. Zhao, J.J., et al., *MicroRNA-221/222 negatively regulates estrogen receptor alpha and is associated with tamoxifen resistance in breast cancer*. J Biol Chem, 2008. **283**(45): p. 31079-86.
107. Pan, Y.Z., M.E. Morris, and A.M. Yu, *MicroRNA-328 negatively regulates the expression of breast cancer resistance protein (BCRP/ABCG2) in human cancer cells*. Mol Pharmacol, 2009. **75**(6): p. 1374-9.
108. Cui, W., et al., *MiRNA-520b and miR-520e sensitize breast cancer cells to complement attack via directly targeting 3'UTR of CD46*. Cancer Biol Ther, 2010. **10**(3).

109. Vetter, G., et al., *miR-661 expression in SNAIL-induced epithelial to mesenchymal transition contributes to breast cancer cell invasion by targeting Nectin-1 and StarD10 messengers*. *Oncogene*, 2010. **29**(31): p. 4436-48.
110. Shen, C., et al., *Genome-wide search for loss of heterozygosity using laser capture microdissected tissue of breast carcinoma: an implication for mutator phenotype and breast cancer pathogenesis*. *Cancer Res*, 2000. **60**(14): p. 3884-92.
111. Ohgaki, K., et al., *Mapping of a new target region of allelic loss to a 6-cM interval at 21q21 in primary breast cancers*. *Genes Chromosomes Cancer*, 1998. **23**(3): p. 244-7.
112. Zhang, H., et al., *[Differential expression profiles of microRNAs between breast cancer cells and mammary epithelial cells]*. *Ai Zheng*, 2009. **28**(5): p. 493-9.
113. Yang, H., et al., *MicroRNA expression profiling in human ovarian cancer: miR-214 induces cell survival and cisplatin resistance by targeting PTEN*. *Cancer Res*, 2008. **68**(2): p. 425-33.
114. Jiang, L., et al., *Hsa-miR-125a-3p and hsa-miR-125a-5p are downregulated in non-small cell lung cancer and have inverse effects on invasion and migration of lung cancer cells*. *BMC Cancer*, 2010. **10**: p. 318.
115. Wong, T.S., et al., *Mature miR-184 as Potential Oncogenic microRNA of Squamous Cell Carcinoma of Tongue*. *Clin Cancer Res*, 2008. **14**(9): p. 2588-92.
116. Henson, B., et al., *Decreased expression of miR-125b and miR-100 in oral cancer cells contributes to malignancy*. *Genes Chromosomes Cancer*, 2009. **48**(7): p. 569-82.

117. Ozen, M., et al., *Widespread deregulation of microRNA expression in human prostate cancer*. *Oncogene*, 2008. **27**(12): p. 1788-93.
118. Chen, J.F., et al., *The role of microRNA-1 and microRNA-133 in skeletal muscle proliferation and differentiation*. *Nat Genet*, 2006. **38**(2): p. 228-33.
119. García, A.J., M.D. Vega, and D. Boettiger, *Modulation of Cell Proliferation and Differentiation through Substrate-dependent Changes in Fibronectin Conformation*. *Mol Biol Cell*, 1999. **10**(3): p. 785-98.
120. Mizuno, Y., et al., *miR-125b inhibits osteoblastic differentiation by down-regulation of cell proliferation*. *Biochem Biophys Res Commun*, 2008. **368**(2): p. 267-72.
121. Lee, Y., et al., *Depletion of human micro-RNA miR-125b reveals that it is critical for the proliferation of differentiated cells but not for the down-regulation of putative targets during differentiation*. *J Biol Chem*, 2005. **280**(17): p. 16635-41.
122. Shi, L., et al., *MiR-125b is critical for the suppression of human U251 glioma stem cell proliferation*. *Brain Res*, 2010. **1312**: p. 120-6.
123. Le, M., et al., *MicroRNA-125b promotes neuronal differentiation in human cells by repressing multiple targets*. *Mol Cell Biol*, 2009. **29**(19): p. 5290-305.
124. Gururajan, M., et al., *MicroRNA 125b inhibition of B cell differentiation in germinal centers*. *Int Immunol*, 2010. **22**(7): p. 583-92.
125. Scott, G., et al., *Coordinate suppression of ERBB2 and ERBB3 by enforced expression of micro-RNA miR-125a or miR-125b*. *J Biol Chem*, 2007. **282**(2): p. 1479-86.

126. Shi, X., et al., *An androgen-regulated miRNA suppresses Bak1 expression and induces androgen-independent growth of prostate cancer cells*. Proc Natl Acad Sci U S A, 2007. **104**(50): p. 19983-8.
127. Zhou, M., et al., *MicroRNA-125b confers the resistance of breast cancer cells to paclitaxel through suppression of pro-apoptotic Bcl-2 antagonist killer 1 (Bak1) expression*. J Biol Chem, 2010. **285**(28): p. 21496-507.
128. Mohri, T., et al., *MicroRNA regulates human vitamin D receptor*. Int J Cancer, 2009. **125**(6): p. 1328-33.
129. Komagata, S., et al., *Human CYP24 catalyzing the inactivation of calcitriol is post-transcriptionally regulated by miR-125b*. Mol Pharmacol, 2009. **76**(4): p. 702-9.
130. Chen, K. and H. DeLuca, *Cloning of the human 1 alpha,25-dihydroxyvitamin D-3 24-hydroxylase gene promoter and identification of two vitamin D-responsive elements*. Biochim Biophys Acta, 1995. **1263**(1): p. 1-9.
131. Guan, Y., et al., *MiR-125b targets BCL3 and suppresses ovarian cancer proliferation*. Int J Cancer, 2010.
132. Huang, L., et al., *MicroRNA-125b suppresses the development of bladder cancer by targeting E2F3*. Int J Cancer, 2010.
133. Guo X, W.Y., Hartley RS., *MicroRNA-125a represses cell growth by targeting H...* [RNA Biol. 2009 Nov-Dec] - PubMed result. RNA Biol., 2009. **6**(5): p. 575-83.
134. Rajabi, H., et al., *MUCIN 1 ONCOPROTEIN EXPRESSION IS SUPPRESSED BY THE miR-125b ONCOMIR*. Genes Cancer, 2010. **1**(1): p. 62-68.

135. Xia, H., et al., *MiR-125b expression affects the proliferation and apoptosis of human glioma cells by targeting Bmf*. *Cell Physiol Biochem*, 2009. **23**(4-6): p. 347-58.
136. Hofmann, M., et al., *A short hairpin DNA analogous to miR-125b inhibits C-Raf expression, proliferation, and survival of breast cancer cells*. *Mol Cancer Res*, 2009. **7**(10): p. 1635-44.
137. Le, M.T., et al., *MicroRNA-125b is a novel negative regulator of p53*. *Genes Dev*, 2009. **23**(7): p. 862-76.
138. Kobayashi, K., et al., *ARID3B induces malignant transformation of mouse embryonic fibroblasts and is strongly associated with malignant neuroblastoma*. *Cancer Res*, 2006. **66**(17): p. 8331-6.
139. Takebe, A., et al., *Microarray analysis of PDGFR alpha+ populations in ES cell differentiation culture identifies genes involved in differentiation of mesoderm and mesenchyme including ARID3B that is essential for development of embryonic mesenchymal cells*. *Dev Biol*, 2006. **293**(1): p. 25-37.
140. Alves, C.C., et al., *Role of the epithelial-mesenchymal transition regulator Slug in primary human cancers*. *Front Biosci*, 2009. **14**: p. 3035-50.
141. Cowden Dahl, K.D., et al., *The epidermal growth factor receptor responsive miR-125a represses mesenchymal morphology in ovarian cancer cells*. *Neoplasia*, 2009. **11**(11): p. 1208-15.
142. Erson, A., et al., *Overexpressed genes/ESTs and characterization of distinct amplicons on 17q23 in breast cancer cells*. *Neoplasia*, 2001. **3**(6): p. 521-6.
143. Sambrook J, R.D., *Molecular Cloning: A Laboratory Manual*. Third ed. 2001: Cold Spring Harbor Laboratory Press. 2,344.

144. Todaro, G., G. Lazar, and H. Green, *The initiation of cell division in a contact-inhibited mammalian cell line*. *J Cell Physiol*, 1965. **66**(3): p. 325-33.
145. LM, S., *Tumor Cell Invasion Assays*, in *Cell Migration: Developmental Methods and Protocols*, J.-L. Guan, Editor. 2004, Springer. p. 97-105.
146. Fisher, C.L. and G.K. Pei, *Modification of a PCR-based site-directed mutagenesis method*. *Biotechniques*, 1997. **23**(4): p. 570-1, 574.
147. Cline, J., J. Braman, and H. Hogrefe, *PCR fidelity of pfu DNA polymerase and other thermostable DNA polymerases*. *Nucleic Acids Res*, 1996. **24**(18): p. 3546-51.
148. Calin, G.A. and C.M. Croce, *MicroRNA signatures in human cancers*. *Nat Rev Cancer*, 2006. **6**(11): p. 857-66.
149. Vermeulen, A., et al., *The contributions of dsRNA structure to Dicer specificity and efficiency*. *RNA*, 2005. **11**(5): p. 674-82.
150. Miletti-González, K., et al., *The CD44 receptor interacts with P-glycoprotein to promote cell migration and invasion in cancer*. *Cancer Res*, 2005. **65**(15): p. 6660-7.
151. Hanahan, D. and R.A. Weinberg, *The hallmarks of cancer*. *Cell*, 2000. **100**(1): p. 57-70.
152. Wang, B., J.G. Doench, and C.D. Novina, *Analysis of microRNA effector functions in vitro*. *Methods*, 2007. **43**(2): p. 91-104.

APPENDIX A

MAMMALIAN CELL CULTURE PROPERTIES

Below table shows the basic properties of breast cancer cell lines that were used in this study. These properties include source of tumor, tumor type and tumor subtype and ER-PR-ERBB2 gene status.

Table A.1: Mammalian cell lines' properties.

Cell Lines	Subtype	ER Status	PR Status	ERBB2 Status	Source	Tumor Type
BT-474	Luminal	+	+	+	Primary Tumor	Invasive Ductal Carcinoma
Cal-51	Basal B subtype	-	NA	-	Pleural Effusion	Adenocarcinoma
Cal-85-1	NA	NA	NA	NA	NA	NA
EFM-19	Luminal	+	+	-	Pleural Effusion	Invasive Ductal Carcinoma
HCC-1143	Basal A subtype	-	-	-	Primary Tumor	Ductal Carcinoma
HCC-1937	Basal A subtype	-	-	-	Primary Tumor	Ductal Carcinoma
HDQ-P1	NA	NA	NA	NA	NA	NA
JIMT-1	NA	NA	NA	NA	NA	NA
MCF7	Luminal	+	+	-	Pleural Effusion	Metastatic Adenocarcinoma
MCF10A	Basal B subtype	-	-	-	Reduction Mammoplasty	Fibrocystic Disease
MDA-MB-231	Basal B subtype	-	-	-	Pleural Effusion	Metastatic Adenocarcinoma
T47D	Luminal	+	+	-	Pleural Effusion	Invasive Ductal Carcinoma

APPENDIX B

BACTERIAL CULTURE MEDIUM

LB

Yeast Extract	5g
Tryptone	10g
NaCl	10g
1N NaOH	1mL

All the components were mixed, pH was adjusted to 7.4 and the volume is completed to 1L with dH₂O.

LB Agar

Yeast Extract	5g
Tryptone	10g
NaCl	10g
1N NaOH	1mL
Agar	15g

All the components were mixed, pH was adjusted to 7.4 and the volume is completed to 1L with dH₂O.

APPENDIX C

PRIMERS AND DUPLEX PCR OPTIMIZATION CONDITIONS

Table C.1: List of primers used in PCR

Primer	Sequence	Expected size	Annealing Temperature
pre-miR-125a	Forward: 5'-TGCCAGTCTCTAGGTCCTG-3'	75bp	58°C
	Reverse: 5'-AGGCTCCCAAGAACCTCACC-3'		
pre-miR-125b-1	Forward: 5'-TGCGCTCCTCTCAGTCCCTGAG-3'	88bp	55°C
	Reverse: 5'-AGCACGACTCGCAGCTCCCAAG-3'		
pre-miR-125b-2	Forward: 5'-ACCAGACTTTTCTAGTCCC-3'	70bp	54°C
	Reverse: 5'-AAGAGCCTGACTTGTGATGT-3'		
GAPDH	Forward: 5'-TATGACAACGAATTGGCTAC-3'	115bp	56°C
	Reverse: 5'-TCTCTCTTCTTGTGCTCT-3'		
Cloned pre-miR-125b-1 (Short)	Forward: 5'-CAGTCCCTAGACCCTAA-3'	66bp	56°C
	Reverse: 5'-CAGCTCCCAAGAGCCTAA-3'		
ARID3B -C1	Forward: 5'-ATTGGCCAGACATTGAGAGCTCGGA-3'	472bp	59°C
	Reverse: 5'-CCCAAGCTTCACAGCCTCTTCTTCAGACTA-3'		
ARID3B -C2	Forward: 5'-TATGTGTGAGCTCACTTTTGTTTTTT-3'	422bp	60°C
	Reverse: 5'-CCCAAGCTTGGAGCTGTGGAGTTAAT-3'		
ARID3B -C3	Forward: 5'-ACACATACCCGAGCTCCCGAGGGCTG-3'	300bp	65°C
	Reverse: 5'-CCCAAGCTTAGGGCAGTGAGGGTCACTCCA-3'		
pSUPER	Forward: 5'-TGGCAACAAATTGATGAGCAATGC-3'	1405bp	56°C
	Reverse: 5'-TGGCAAGAAATTGAGCAAITA-3'		

Table C.2: Duplex PCR Optimization Conditions

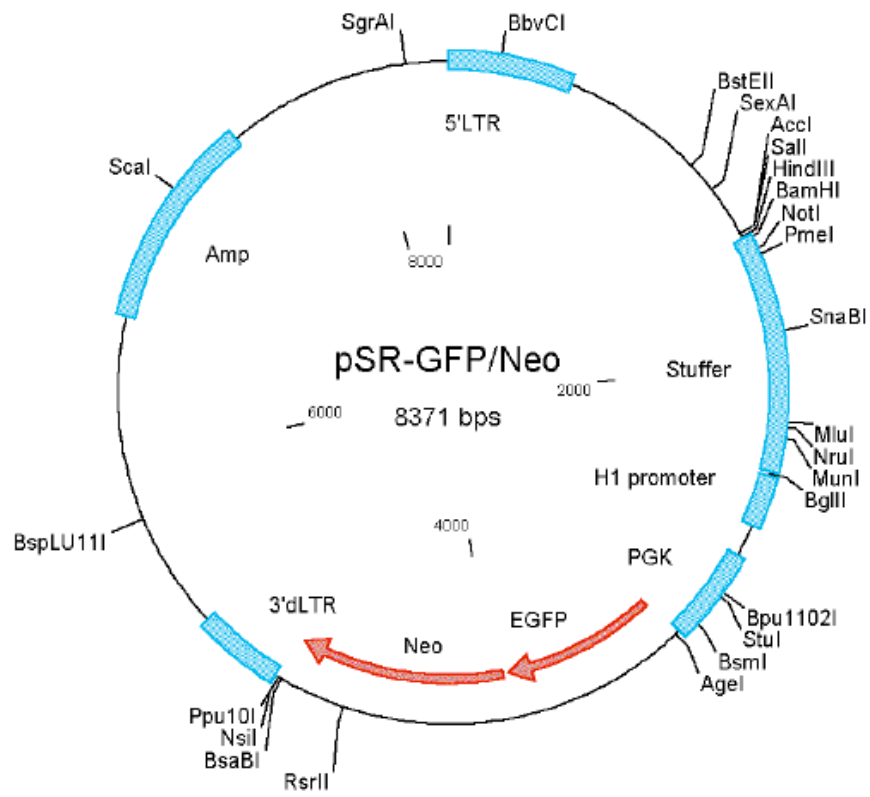
	GAPDH primer volume	miRNA primer volume	Additional Reagent
pre-miR-125a	1µL	3µL	None
pre-miR-125b-1	1.5µL	3µL	None
pre-miR-125b-2	3µL	3µL	10% DMSO

All primers have 5µM stock concentration. Apart from duplex RT-PCRs, 3µL primers were used in all reactions. All PCRs contain 35 cycles of melting, annealing and elongation.

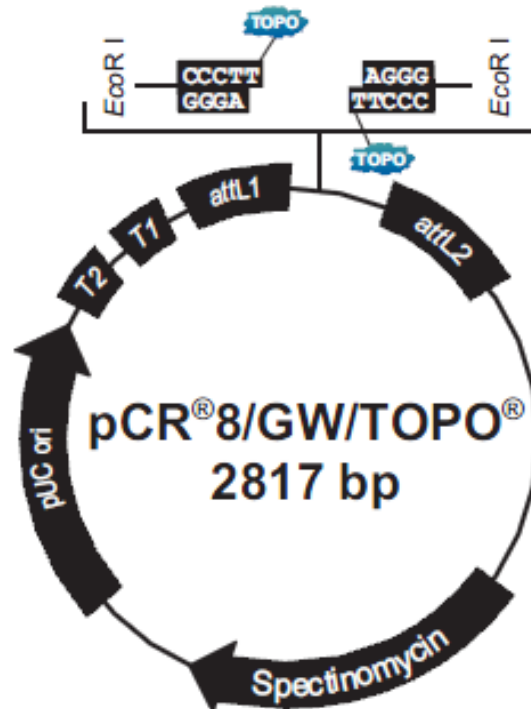
APPENDIX D

MAPS OF VECTORS

1) Map of pSUPER.retro.neo+GFP Vector (Invitrogen)



2) Map of pCR8/GW/TOPO vector (Invitrogen)



M13 forward (-20) priming site

501 TAACGCTAGC ATGGATGTTT TCCAGTCAC GACGTTGTA A ACGACGGCC AGTCTTAAGC TCGGGCCCCA AATAATGATT

attL1 GW1 priming site

581 TTATTTTGAC TGATAGTGAC CTGTTGTTG CAACAAATTG ATGAGCAATG CTTTTTTATA ATGCCAACT TTG TAC AAA
AAC ATG TTT
Leu Tyr Lys

EcoRI EcoRI

659 AAA GCA GGC TCC GAA TTC GCC CTT PCR product AAG GGC GAA TTC GAC CCA GCT TTC TTG TAC
TTT CGT CCG AGG CTT AAG CGG GAA TTC CCG CTT AAG CTG GGT CGA AAG AAC ATG
Lys Ala Gly Ser Glu Phe Gly Leu Lys Gly Glu Phe Asp Pro Ala Phe Leu Tyr

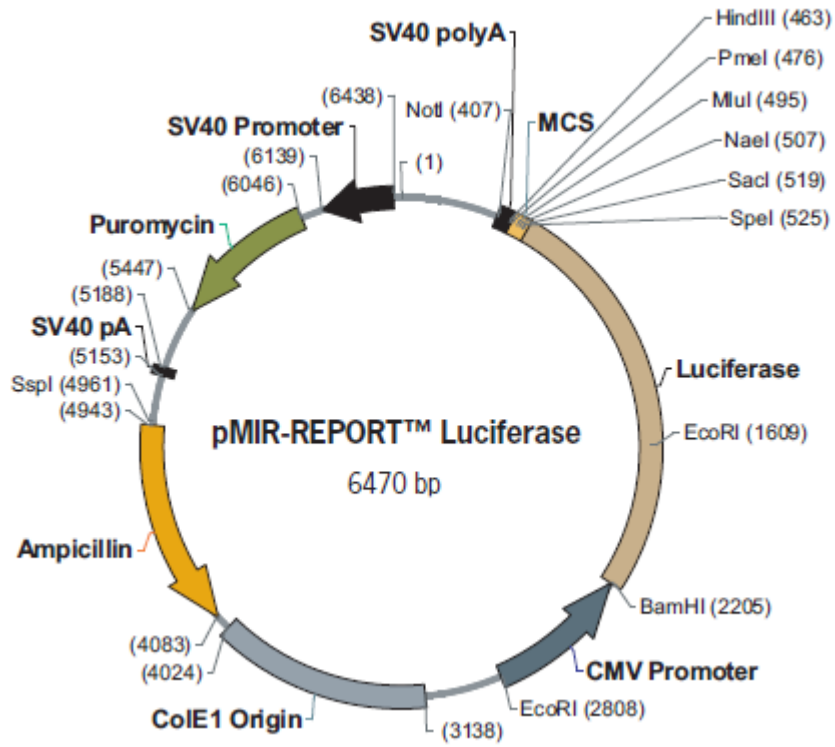
attL2 GW2 priming site

713 AAAGTTGG CATTATAAAA AATAATTGCT CATCAATTG TTGCAACGAA CAGGTCAC TA CAGTCAAAA TAAATCATT

M13 reverse priming site

791 ATTTGCCATC CAGCTGATAT CCCCTATAGT GAGTCGTATT ACATGGTCAT AGCTGTTTCC TGGCAGCTCT

3) Map of pMIR-REPORT Luciferase vector (Ambion)



4) Map of phRL-TK vector (Promega)

